UNIVERSIDADE FEDERAL DE SANTA CATARINA
CENTRO TECNOLÓGICO - CTC
PROGRAMA DE PÓS-GRADUAÇÃO EM ENGENHARIA QUÍMICA

THAIANE ANDRADE CRUZ

Evaluation of Thermal and Catalytic Pyrolysis of Hardwood and Softwood Kraft Lignin

Florianópolis
2023

Thaiane Andrade Cruz

Evaluation of Thermal and Catalytic Pyrolysis of Hardwood and Softwood Kraft Lignin

Dissertação submetida ao Programa de Pós-Graduação em Engenharia Química da Universidade Federal de Santa Catarina como requisito parcial para a obtenção do título de Mestra em Engenharia Química.

Orientador: Prof. Bruno Francisco Oechsler, Dr.
Coorientadora: Prof.(a) Regina de Fátima Peralta Muniz Moreira, Dra.

Florianópolis
2023

Ficha de identificação da obra elaborada pelo autor, através do Programa de Geração Automática da Biblioteca Universitária da UFSC.

Cruz, Thaiane Andrade
Evaluation of Thermal and Catalytic Pyrolysis of Hardwood and Softwood Kraft Lignin / Thaiane Andrade Cruz ; orientador, Bruno Francisco Oechsler, coorientador, Regina de Fátima Pereira Muniz Moreira , 2023.
143 p.

Dissertação (mestrado) - Universidade Federal de Santa Catarina, Centro Tecnológico, Programa de Pós-Graduação em Engenharia Química, Florianópolis, 2023.

Inclui referências.

1. Engenharia Química. 2. Kraft Lignin. 3. Lignin source. 4. Pyrolysis. 5. ZSM-5. I. Oechsler, Bruno Francisco . II. Moreira , Regina de Fátima Pereira Muniz. III. Universidade Federal de Santa Catarina. Programa de Pós-Graduação em Engenharia Química. IV. Título.

Thaiane Andrade Cruz

Evaluation of Thermal and Catalytic Pyrolysis of Hardwood and Softwood Kraft Lignin

O presente trabalho em nível de Mestrado foi avaliado e aprovado, em 21 de setembro de 2023 pela banca examinadora composta pelos seguintes membros:

Prof.(a) Suelen Maria de Amorim Dr.(a)
Instituição Universidade Federal do Sul e Sudeste do Pará

Prof.(a) Cíntia Marangoni, Dr.(a)
Instituição Universidade Federal de Santa Catarina

Certificamos que esta é a versão original e final do trabalho de conclusão que foi julgado adequado para obtenção do título de Mestra em Engenharia Química.

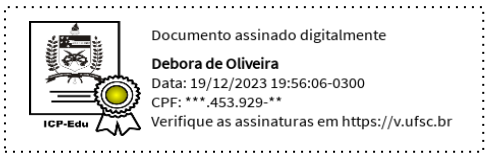

Coordenação do Programa de Pós-Graduação

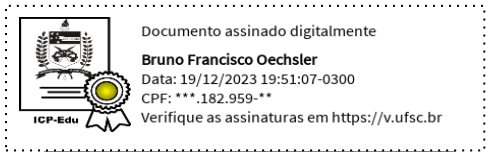

Prof. Bruno Francisco Oechsler, Dr.
Orientador

Florianópolis, 2023.

Este trabalho é dedicado minha família.

AGRADECIMENTOS

Durante a minha jornada no mestrado tive a oportunidade de compartilhar e vivenciar diversas experiências com tantas pessoas especiais. Quero deixar aqui meus agradecimentos a todos que me acompanhar e me ajudaram nessa conquista.

Primeiramente agradeço aos meus pais, Adalberto e Eugênia Cruz, a minha irmã, Thaise Cruz, minha segunda mãe Eufrânia de Andrade, e meu sobrinho Davi Cruz por sempre se fazerem presentes mesmo a distância, por me apoiarem e embarcarem comigo em todas as minhas aventuras, amo muito vocês. Obrigada por acreditarem em mim nos momentos em que nem eu conseguia acreditar.

Ao Professor Doutor Bruno Francisco Oechsler, meu orientador, pelo apoio incondicional, disponibilidade, compreensão e aconselhamento, que muito contribuíram para esta pesquisa.

À Professora Doutora Regina de Fátima Pereira Muniz Moreira e o Professor Doutor Ricardo Antônio Francisco Machado, por todas as orientações, conselhos e apoio no decorrer de toda a pesquisa.

À minha parceira de laboratório e amiga querida, Jaqueline de Oliveira Brotto, sou grata por ter tido a oportunidade de trabalhar contigo. Obrigada por sua constante disponibilidade, seja para discutir resultados, desenvolver experimentos ou apenas conversamos.

Às minhas amigas Joice Costa, Larissa Lins, Larissa Morais e Thaís Kelly por todo o apoio e suporte no momento bons e ruins. Sou grata também a Andrea Melga, Eliana Weiss e Vanessa Lima por toda a leveza, companheirismo e momentos especiais da minha passagem por Florianópolis. Obrigada a todas por me ajudar a diminuir a saudade de casa.

Aos companheiros do LCP e LEMA pelo suporte e ajuda para concretização deste trabalho.

Agradeço ao PósENQ pela oportunidade de desenvolvimento profissional e a CNPq e a FAPESC, pelo suporte financeiro.

Por fim, agradeço a todos que contribuíram de forma direta e indireta para o desenvolvimento deste trabalho. Muito obrigada a todos.

RESUMO

Esta pesquisa explora o papel dos processos de degradação térmica e catalítica na valorização da lignina como uma alternativa sustentável para substituir recursos fósseis no setor energético e na produção de produtos químicos de valor agregado. A lignina é um polímero aromático complexo que oferece caminhos promissores para a geração de compostos aromáticos e aromáticos oxigenados. No entanto, sua diversa composição estrutural pode influenciar significativamente a composição dos produtos. A pirólise térmica de dois tipos distintos de lignina Kraft, derivados do *Eucalyptus spp* e do Pinheiro, conhecidas como madeira dura e madeira mole, respectivamente, foi realizada em três temperaturas (500, 600 e 700 °C) usando um reator de leito fixo. Foi empregada uma análise abrangente, incluindo análises imediatas e elementar, FT-IR, TGA/DTG com deconvolução, ss-NMR e GC-MS para caracterizar as propriedades físicas e químicas das ligninas e avaliar a distribuição dos produtos no bio-óleo e biocarvão. Os resultados destacaram o papel crítico da metoxila (-OCH_3) na pirólise da lignina e a predominância da decomposição do guaiacol como uma via proeminente para a geração de hidrocarbonetos aromáticos e aromáticos oxigenados, com a madeira dura favorecendo a produção de siringol. O teor de grupo metoxila afetou os rendimentos dos produtos: a lignina de madeira mole apresentou um rendimento de biocarvão mais elevado (14 – 18% m/m), enquanto a lignina de madeira dura exibiu um rendimento de gás mais elevado (13 – 22% m/m). A produção de bio-óleo também foi afetada pela temperatura, sendo responsável por converter fenóis do tipo S em fenóis do tipo G, monofenol ou catechol em temperaturas mais elevadas. Sendo o maior rendimento do bio-óleo da lignina de madeira dura há 700 °C (14,74% m/m) e da lignina de madeira mole há 500 °C (14,59% m/m). O estudo também investigou a conversão termoquímica catalítica da lignina utilizando um catalisador comercial, como a ZSM-5. Dada sua complexidade estrutural, a fonte de lignina torna-se um fator crucial na composição do produto. Para avaliar as propriedades do catalisador, foram realizadas análises BET e BJH, análises DRX e FT-IR de piridina, seguidas de TGA/DTG acopladas à deconvolução para avaliação da degradação catalítica. Uma análise de covariância também foi empregada para avaliar as dependências funcionais entre vários fatores que afetam os rendimentos dos produtos. Na pirólise térmica o bio-óleo da lignina de madeira mole apresentou maiores quantidades de compostos do tipo guaiacol, juntamente com certos hidrocarbonetos aromáticos e aromáticos policíclicos. Por outro lado, a lignina de madeira dura produziu maiores quantidades de compostos do tipo siringol. Em ambos os casos, as temperaturas elevadas resultaram no aumento da produção de cetonas, sendo este o componente predominante do bio-óleo. As principais descobertas revelaram o potencial da ZSM-5 na redução do teor de oxigênio na composição do bio-óleo. No entanto, a fonte de lignina emergiu como fator predominante na formação de componentes não oxigenados, principalmente aromáticos (BTX). No geral, os compostos oxigenados no bio-óleo da lignina de madeira dura diminuíram apenas 3,7%, enquanto os compostos não oxigenados aumentaram cerca de 1%. Em contraste, os compostos oxigenados diminuíram cerca de 52% e os compostos não oxigenados aumentaram 41,6% no bio-óleo da lignina de madeira mole. Portanto, a ZSM-5 exibiu uma maior afinidade pela madeira mole do que pela madeira dura. Este trabalho destacou a lignina como uma promissora fonte renovável para aplicações energéticas e químicas, oferecendo informações valiosas para a otimização do processo e seleção do catalisador, visando soluções sustentáveis.

Palavras-chaves: Lignina Kraft, Madeira dura, Madeira dura, Pirólise, ZSM-5, análise estatística.

ABSTRACT

This research explores the role of thermal and catalytic degradation processes of lignin valorization as a sustainable alternative to replace fossil resources in the energy sector and value-added chemicals production. Lignin, a complex aromatic polymer comprising guaiacyl, syringyl, and p-hydroxyphenyl units, offers promising pathways for generating oxygenated aromatic and aromatic compounds. However, its diverse structural composition can significantly influence the composition of end products. Thermal pyrolysis of two distinct Kraft lignin samples, derived from *Eucalyptus spp* and Pine Tree, as hardwood and softwood, respectively, was conducted at three temperatures (500, 600, and 700 °C) using a fixed-bed reactor. A comprehensive analysis including proximate and ultimate analyses, FT-IR, TGA/DTG with deconvolution, ss-NMR, and GC-MS was employed to characterize the physical and chemical properties of the lignins and evaluate product distribution in bio-oil and biochar. Results highlighted the critical role of methoxyl group (-OCH_3) content in lignin pyrolysis and the prevalence of guaiacol decomposition as a prominent pathway for generating aromatic hydrocarbons and oxygenated aromatics, with hardwood lignin favoring syringol production. Methoxy group content affected the product yields: softwood lignin presented a higher biochar yield (14-18 wt.%), while hardwood lignin exhibited a higher gas yield (13-22 wt%). Bio-oil production was also affected by temperature, which is responsible for converting S-type phenols into G-types, monophenol, or catechol at higher temperatures. This conversion enhances bio-oil production, explaining the higher yield of hardwood lignin at 700°C (14.74 wt.%) and softwood lignin at 500°C (14.59 wt.%). The study also investigated the catalytic thermochemical conversion of lignin using a commercial catalyst, such as ZSM-5. Given its structural complexity, the source of lignin becomes a crucial factor in product composition. To evaluate the catalyst properties, BET and BJH analysis, X, and pyridine FT-IR analyses were conducted, followed by TGA/DTG coupled with deconvolution for catalytic degradation evaluation. An analysis of covariance was also employed to evaluate functional dependencies among several factors, which affect the product yields. Thermal pyrolysis reveals that softwood lignin bio-oil exhibited higher amounts of guaiacol-type compounds, along with certain aromatic hydrocarbons and polycyclic aromatics. Conversely, hardwood lignin yielded higher amounts of syringol-type compounds. In both cases, elevated temperatures result in increased ketone production, constituting the predominant component of the liquid product. Key findings have revealed the potential of ZSM-5 in the reduction of oxygen content in bio-oil composition. However, the source of lignin emerged as the predominant factor shaping non-oxygenated components, particularly aromatics (BTX). For instance, softwood/ZSM-5 bio-oil contained higher amounts of aromatics due to guaiacol decomposition, while hardwood bio-oil exhibited an increase in oxygenated aromatics. Overall, oxygenated compounds in hardwood bio-oil decreased by only 3.7% while the non-oxygenated compounds increased by 1%. In contrast, oxygenated compounds decreased by about 52% and non-oxygenated compounds increased by 41.6% in softwood lignin bio-oil. Therefore, ZSM-5 exhibited a higher affinity for softwood lignin than for hardwood lignin. This work underscored lignin as a promising renewable resource for energy and chemical applications, offering valuable insights for process optimization and catalyst selection, aiming at lignin-based sustainable solutions.

Keywords: Kraft Lignin, Hardwood, Softwood, Pyrolysis, ZSM-5, Renewable resources

RESUMO EXPANDIDO

INTRODUÇÃO

O crescimento econômico e os avanços tecnológicos nas últimas décadas impulsionaram o consumo de recursos fósseis finitos. À medida que o mundo enfrenta o esgotamento desses recursos finitos e suas consequências adversas, a busca por matérias-primas alternativas torna-se cada vez mais urgente. Nesse contexto, a biomassa tem surgido como uma fonte renovável promissora para substituir recursos fósseis em uma ampla gama de aplicações e a indústria de papel e celulose, que é responsável pela produção de grandes quantidades de resíduos lignocelulósicos, se tornou uma fonte abundante de biomassa.

A lignina é um dos três principais componentes da biomassa, consistindo em polímero amorfo, de natureza aromática e altamente complexa, formada pela combinação de três tipos de monolignóides primários por meio de reações de acoplamento fenólico oxidativo. Na indústria de papel e celulose, a lignina é encontrada como resíduo do processo de polpação (licor negro). O conceito de integração de biorrefinarias de lignina a uma planta de papel e celulose pode se tornar uma via promissora para reduzir custos de transporte de matérias-primas e obter combustíveis, produtos químicos e novas fontes de energia. Neste contexto, os processos de conversão termoquímica surgem como alternativa para a valorização da lignina como matéria-prima em rotas de reciclagem química.

Entre os processos de conversão termoquímica, a pirólise é um processo de degradação térmica conduzido sob atmosfera inerte e altas temperaturas, possibilitando a obtenção de três subprodutos: bio-óleo, gases e biocarvão. Em particular, o bio-óleo destaca-se como alternativa primária aos combustíveis tradicionais e matéria-prima valiosa para a indústria de polímeros. No entanto, devido ao seu alto teor de oxigênio, o bio-óleo derivado da pirólise da lignina possui baixa densidade de energia e estabilidade química. Sendo assim, para aprimorar sua produção, é essencial empregar catalisadores, como a zeólita ZSM-5, que facilitam a despolimerização da lignina, melhorando sua qualidade e estabilidade por meio de reações de desoxigenação.

As dificuldades na valorização da lignina são atribuídas principalmente à sua estrutura complexa e recalcitrante, bem como à alta reatividade de suas frações degradadas, que são propensas a reações de condensação. No entanto, estas reações podem ser úteis na preparação de vários materiais poliméricos, compósitos, hidrogéis etc.

Neste contexto, este trabalho teve como ênfase a elucidação dos mecanismos de pirólise térmica e catalítica por meio da aplicação de métodos estatísticos, utilizando especificamente matrizes de correlação e Análise de Componentes Principais (PCA). O objetivo é diferenciar os padrões espectrais distintivos apresentados pelos subprodutos gerados a partir da pirólise da lignina de diferentes fontes. Através dessa análise, busca-se aprimorar a compreensão das rotas envolvidas na pirólise da lignina. Em particular, a pirólise de duas variedades de lignina Kraft, provenientes de madeira macia e madeira dura, foi investigada a altas temperaturas (500, 600 e 700 °C). Além disso, avaliou-se a influência da introdução do catalisador ZSM-5 na composição dos produtos líquidos resultantes do processo de pirólise.

OBJETIVOS

O objetivo geral do trabalho consiste em avaliar as propriedades físicas, químicas e térmicas de duas amostras distintas de lignina Kraft e analisar o efeito da fonte de lignina (madeira dura e madeira macia) no comportamento da degradação térmica durante o processo de pirólise. Além disso, este estudo também visa investigar o comportamento de um catalisador comercial (como a ZSM-5) na degradação térmica da lignina Kraft proveniente de fontes diferentes, bem como avaliar as rotas envolvidas na formação dos componentes do bio-óleo.

METODOLOGIA

A metodologia desenvolvida envolveu a avaliação da degradação térmica de duas amostras de lignina Kraft: lignina de Eucalipto (Lignina A), doada pela Internacional Papear, e lignina de Pinheiro (Lignina B) (CAS# 8068-05-1, 471003), adquirida pela Sigma-Aldrich. Essas amostras podem ser classificadas como lignina de madeira dura (Lignina A) e madeira mole (Lignina B), respectivamente. O catalisador utilizado nos testes de pirólise catalítica, ZSM-5 (SM27), foi doado pelo CENPES/PETROBRÁS. Inicialmente, as amostras foram caracterizadas com o intuito de avaliar suas características físico-químicas por meio das análises elementar e imediata, da espectroscopia no infravermelho com transformada de Fourier (FT-IR), da ressonância magnética nuclear (ss-RMN) e do poder calorífico (HHV e LHV). O catalisador foi caracterizado por meio dos métodos de difração de raios X (DRX), análise piridina/FT-IR, Brunauer, Emmett e Taller (BET) e Barrett, Jouner e Halenda (BJH) com base nos resultados de fisiossorção em nitrogênio.

A análise termogravimétrica (TGA/DTG) acoplada ao método de deconvolução foi utilizada para avaliar a decomposição térmica e catalítica das amostras de lignina. Os ensaios termogravimétricos foram realizados em diferentes taxas de aquecimento (5, 10, 15 e 20 °C/min) sob atmosfera inerte (N_2) até atingir 900 °C. No caso da degradação catalítica, a proporção entre o catalisador e a lignina foi 1:1.

Os ensaios de pirólise das amostras de lignina foram realizados em um reator tubular de leito fixo composto por um cilindro concêntrico de quartzo nas temperaturas de 500, 600 e 700 °C. O tempo de residência foi mantido em 10 s, e os ensaios foram realizados em atmosfera inerte, com uma taxa de aquecimento de 20 °C/min. Esses parâmetros foram escolhidos de acordo com os resultados da análise de TGA e da literatura. Utilizou-se aproximadamente 0,5 a 0,6 g de amostra para a pirólise térmica, enquanto uma mistura de lignina com catalisador na proporção de 1:1 (totalizando 1 g) foi empregada no ensaio de pirólise catalítica. Após a pirólise, os produtos foram recuperados, pesados e caracterizados. O biocarvão foi caracterizado pelos métodos de FT-IR e ss-RMN, enquanto o bio-óleo foi caracterizado por meio de cromatografia gasosa acoplada à espectroscopia de massa (GC-MS). O rendimento dos produtos foi determinado por meio de análise gravimétrica das amostras de biocarvão e bio-óleo, enquanto os rendimentos dos gases foram determinados pelo balanço de massa da reação.

As matrizes de covariância e a Análise em Componentes Principais (PCA) foram os métodos estatísticos utilizados para estabelecer o grau de dependência entre as variáveis do processo de pirólise, incluindo as temperaturas, tipo de lignina, rendimento dos produtos, presença do catalisador e composição do bio-óleo.

RESULTADOS E DISCUSSÕES

Os resultados das técnicas de caracterização ilustram as diferenças nas propriedades físico-químicas e na composição química das duas amostras de lignina Kraft. Essas variações estão atribuídas à fonte de lignina e sua estrutura química. A lignina A apresentou maior quantidade de grupos metoxila quando comparada à lignina B, enquanto a lignina B apresentou uma maior razão de H/C_{eff}. A ZSM-5 possui uma típica estrutura morfológica de cristais MFI exibindo a forma de prisma pentagonal uniforme. Os resultados de FT-IR e RMN demonstraram que a lignina A indicou sinais mais específicos de siringuila, enquanto a lignina B apresentou sinais de guaiacila.

A avaliação térmica das amostras demonstrou que a decomposição dos monômeros foi afetada de maneira diferente durante o processo de pirólise, e a quantidade de $-OCH_3$ foi o

principal fator durante a reação, pois pela lignina A possui uma maior quantidade de -OCH_3 ela produziu menos biocarvão do que a lignina B. Na presença da ZSM-5, a degradação das ligninas apresentou comportamento similar à pirólise térmica, entretanto houve um aumento na perda de massa, que pode ser atribuído às reações de desidratação, rearranjo e craqueamento.

Os resultados das matrizes de correlação e da técnica de PCA determinaram que o tipo lignina é o principal fator responsável pela composição do bio-óleo e o rendimento de compostos aromáticos. A análise estatística demonstrou que o guaiacol e o siringol são os principais precursores para a formação de aromáticos oxigenados (AO), aromáticos e cetonas durante a pirólise térmica. O bio-óleo da lignina A apresentou maior composição em compostos oxigenados, com a presença de compostos aromáticos apenas em 700 °C. Em contrapartida, o bio-óleo da lignina B apresentou composição mais rica em aromáticos, apesar da presença de maior quantidade de compostos oxigenados. Neste tipo de lignina, o siringol foi produzido nas temperaturas de 600 e 700 °C, e está relacionado à produção de aromáticos apenas na temperatura mais alta.

Na pirólise catalítica, o rendimento em bio-óleo aumentou em ambas as amostras. No entanto, a composição do bio-óleo de cada lignina foi bem diferente. O bio-óleo proveniente da lignina B apresentou maior diversidade de compostos e maior rendimento de compostos aromáticos em comparação com a lignina A.

Por último, realizou-se uma comparação entre a composição do bio-óleo produzido pela pirólise térmica e catalítica, considerando os compostos oxigenados e não oxigenados. O bio-óleo da lignina A apresentou um decaimento de oxigenados entre 500 e 600 °C, com novo aumento em 700 °C, enquanto os compostos não-oxigenados aumentaram cerca de 3% com o aumento da temperatura. O que pode indicar que o uso de temperaturas mais altas pode proporcionar a formação de coque nos sítios ácidos da ZSM-5 a partir da decomposição das espécies carbonáceas provenientes do siringol, causando a desativação do catalisador e evitando a degradação dos compostos oxigenados aromáticos em outros componentes.

Já a lignina B, na presença do catalisador, apresentou uma redução significativa de oxigenados, cerca de 52 %, com o aumento da temperatura, produzindo cerca de 41,6 % de compostos não-oxigenados, entre eles aromáticos e hidrocarbonetos. Portanto, a lignina de madeira mole (lignina B) apresentou maior afinidade com a ZSM-5 em comparação com a lignina de madeira dura (Lignina A).

CONCLUSÕES

As principais unidades repetitivas das amostras de lignina foram o guaiacol e siringol, sendo a degradação destes compostos responsável pela formação dos componentes aromáticos e aromáticos oxigenados nas amostras de bio-óleo. A presença do grupo metoxila (-OCH_3) desempenha um papel significativo tanto na pirólise primária quanto na secundária, especialmente na amostra de eucalipto (Lignina A), que apresenta rendimento de biocarvão reduzido com o aumento da temperatura devido ao alto teor de –OCH_3.

Entre os três produtos da pirólise, os gases e o biocarvão apresentaram maior rendimento tanto na pirólise térmica quanto na catalítica, observando-se apenas uma ligeira diminuição em seus rendimentos com a presença do catalisador. No entanto, o rendimento do bio-óleo aumentou com a presença do catalisador. Com o auxílio das análises estatísticas, observou-se que o tipo de lignina é o fator mais importante quanto à produção de compostos aromáticos e oxigenados. Por exemplo, a pirólise da lignina B apresentou, um aumento nos rendimentos de compostos oxigenados (14%) e não oxigenados (2%), em comparação com a lignina A durante a pirólise térmica. Na pirólise catalítica, o bio-óleo da lignina B demonstrou maior diversidade de compostos não-oxigenados (41,6%) e um rendimento de aromáticos 25,4% superior em relação à lignina A. Adicionalmente, o bio-óleo da lignina A apresentou uma diminuição de apenas 3,7% em compostos oxigenados e um aumento de 1% em compostos não oxigenados.

Os resultados das matrizes de correlação indicaram que o alto teor de grupos -OCH_3 na lignina A pode dificultar a conversão de componentes com alta massa molar devido ao tamanho molecular maior do que a abertura de poro da zeólita ZSM-5, podendo causar sua desativação. Logo, o aumento da produção de compostos aromáticos a partir da lignina de madeira dura requer a modificação das características de acidez e porosidade da zeólita para aprimorar as reações de desoxigenação do bio-óleo.

Por fim, esta pesquisa determinou os mecanismos de formação dos produtos da pirólise e os efeitos da zeólita ZSM-5 durante a pirólise de diferentes fontes de lignina. Os resultados obtidos proporcionam importantes percepções para estudos futuros que visem a produção de compostos específicos ou produtos de alto valor agregado a partir da pirólise de lignina Kraft.

Palavras-chaves: Lignina Kraft, Madeira dura, Madeira dura, Pirólise, ZSM-5, análise estatística.

LIST OF FIGURES

LIST OF TABLES

SUMMARY

CHAPTER 1

In this chapter, the motivations and objective of this work are presented.

.

1 INTRODUCTION

Economic growth and technological advancements have increased over the last few decades, leading to progress that has driven the high consumption of finite fossil feedstocks. Consequently, the growing consumption of non-renewable resources has been responsible by several environmental impacts. As the world faces the depletion of these finite resources and its adverse consequences, the search for alternative raw materials becomes increasingly urgent. The use of fuels derived from renewable resources, such as biomass, which offer low or neutral carbon emissions, has been gaining prominence as a strategy to replace conventional fossil fuels in several applications. Therefore, the use of renewable resources can reduce the energetic dependence on finite fossil fuels and mitigate the negative impact of its use on the environment. (COLLARD; BLIN, 2014; WANG *et al.*, 2017).

Biomass refers to any organic material that can be replenished or regenerated over time. Composed mainly of carbon and sharing many similarities with fossil raw materials, biomass has emerged as a promising renewable source to replace fossil resources in a wide range of applications. According to the International Energy Agency, modern bioenergy is currently the largest source of renewable energy globally, accounting for 55% of renewable energy and over 6% of global energy supply (IEA, 2021). With its significant potential for scaling up in the upcoming decades, biomass is poised to play an even greater role in meeting the energy requirements on a sustainably way (KANG; ASMELASH, 2021).

Lignocellulosic biomass is an abundant renewable material, that serves as the primary raw material for the pulp and paper industry since is cost-effective, sustainable, and promotes efficient resource use in the industry. Lignin, a constituent found in almost all dry-land plant cell walls, is second only to cellulose in terms of natural abundance (EUGENIO *et al.*, 2019; HEITNER; DIMMEL; SCHMIDT, 2010). Lignin is one of the three main components of lignocellulosic biomass and acts as a resin that holds the lignocellulosic matrix together. It consists of an amorphous polymer of an aromatic nature with a highly complex structure formed by different units of phenylpropanoids and methoxylated compounds, depending on the plant source. (DEMUNER *et al.*, 2019; LI *et al.*, 2015; SALIBA *et al.*, 2001).

In various industries, two main types of pulp are used: hardwood and softwood. Each type has distinct properties that make it suitable for specific applications. Softwood pulp, which is known for its high strength and durability, is often used in producing newsprint,

magazine papers, and high-quality printing paper. On the other hand, hardwood pulp, which has strong bonding properties, is commonly used for manufacturing tissues and packaging materials (CNBM, 2020, p.3).

In the pulp and paper industry, traditional pulping processes, such as soda, Kraft, and sulfite, generally produce the high-quality cellulose fiber. The presence of lignin in cellulose separated from wood makes it more susceptible to oxidation by oxygen in air compared to cellulose. Papers with higher lignin and hemicellulose content are generally more vulnerable to oxidation, which can negatively affect their durability (CUI *et al.*, 2022; LI *et al.*, 2014; MAŁACHOWSKA *et al.*, 2020). Approximately 50 million tons of lignin are produced annually worldwide as a by-product of the pulp and paper industry, of which 98 – 99% of the industrial lignin is incinerated to produce steam and energy. Lignin is mostly used in low-value commercial applications, as a low-grade fuel for heat and power generation applications, or as a concrete additive. (DEMUNER *et al.*, 2019; LI *et al.*, 2015).

The lignin fraction in lignocellulosic resources is normally influenced by both the extraction technique and the biomass source. Lignin content can fluctuate significantly among different biomass sources and even within distinct parts of plant structure. For instance, softwood typically contains 25-35% lignin as a proportion of the total plant mass, whereas hardwood and grasses typically have lignin content in the range of 20-25% and 10-15%, respectively (DEMUNER *et al.*, 2019; WANG *et al.*, 2017).

The study of lignin biomass and its conversion processes presents a compelling motivation for further research and exploration. In the Kraft process, biomass undergoes conversion into cellulose and black liquor. The black liquor, primarily composed of lignin, holds immense potential as a valuable resource for biorefineries from its chemical recycling. Currently, the burning of black liquor in recovery boilers allows for the recycling of chemical reagents and the generation of electricity and steam. However, this stage remains a barrier to increasing production capacity within the paper industry (NALI; RIBEIRO; HORA, 2016).

An intriguing solution lies in the extraction of lignin from black liquor. By removing lignin from the black liquor, the volume destined for recovery boilers can be reduced, thereby enabling an increase in cellulosic fiber production capacity without hindering the recovery of white liquor. Some research works has extensively explored the extraction of lignin for use as fuel in the lime kiln at the white liquor preparation plant. However, major companies in the sector have expressed reservations about direct lignin burning due to investment justifications (MONICA EK, GÖRAN GELLERSTEDT, 1993; NALI; RIBEIRO; HORA, 2016).

Nevertheless, the integration of a lignin biorefinery with a pulp and paper plant offers a promising avenue to reduce transportation costs for raw materials and obtain value-added chemical platforms, fuels, and renewable energy sources. Thermochemical conversion processes emerge as a notable alternative for the recovery of lignin as a raw material in chemical recycling routes. By delving into these areas of study, researchers can contribute to the development of sustainable and economically viable solutions that harness the full potential of lignocellulosic biomass (NALI; RIBEIRO; HORA, 2016).

To obtain renewable biofuels and chemicals from Kraft lignin, it is crucial understand how this macromolecule with high molar mass, crosslinked structure and heterogeneous nature undergoes thermal degradation processes (DEMUNER *et al.*, 2019; RAGAUSKAS *et al.*, 2014). Among the thermochemical conversion processes, pyrolysis stands out for its distinct advantage, allowing the production of three by-products: bio-oil, gases, and biochar. In particular, bio-oil stands out as a primary alternative to traditional fuels and a valuable raw material for the polymer industry. However, due to its high oxygen content, bio-oil derived from lignin pyrolysis has low energy density and chemical stability. To enhance the bio-oil production, it is essential to employ catalysts that facilitate the depolymerization of lignin to improve oil quality and stability through deoxygenation reactions. This can be achieved alongside the use of high temperatures and shorter residence times to efficiently transform lignin or selectively convert it into target products (BRIDGWATER, 2012; LU; GU, 2022).

The difficulties in lignin valorization are mainly attributed to its complex and recalcitrant structure, as well as the high reactivity of its degraded fractions, which are prone to condensation reactions. However, these condensation reactions may be useful in the preparation of various polymeric materials, composites, hydrogels, etc (HÁZ *et al.*, 2019).

In this context, this work focused on elucidating the mechanisms behind thermal and catalytic pyrolysis through the application of statistical methods, specifically employing correlation matrices and Principal Component Analysis (PCA). The objective is to differentiate the distinctive spectral patterns exhibited by by-products yielded from lignin pyrolysis from different sources. Through this analysis, the aim is to enhance the understanding of the pathways involved in lignin pyrolysis. The research focused on the pyrolysis of two varieties of Kraft lignin, sourced from softwood and hardwood at high temperatures (500, 600, and 700 °C). Additionally, the influence of introducing a ZSM-5 catalyst on the composition of the resulting liquid products was explored.

The present work was divided into 5 chapters. The first chapter presents the motivation and objective for the work (Chapter 1), followed by the literature review (Chapter 2). Subsequently, the results of thermal (Chapter 3) and catalytic pyrolysis (Chapter 4) were addressed, to describe the physical and chemical characteristics of by-products and mechanism for each lignin pyrolysis. Chapters 3 and 4 also present the results of the correlation matrices and PCA analyses for the by-products yields and bio-oil composition from thermal and catalytic pyrolysis, while comparing all the results. The main conclusions and highlights can be found in chapter 5. Ultimately, this research aims to identify which lignin presents ideal performance, both in the presence and absence of catalyst, based on the operational parameters outlined in the study.

1.1 GENERAL OBJETIVES

The general objective of this study is to assess the physical, chemical, and thermal properties of two distinct Kraft lignin samples and analyze the effect of lignin source (hardwood and softwood) in the thermal degradation behavior. Besides, this study also aims to investigate the behavior of a commercial catalyst (such as ZSM-5) in the thermal degradation of Kraft lignin derived from different sources, as well evaluate the pathways involved in the formation of bio-oil components.

1.2 SPECIFIC OBJETIVES

One may cite among the specific objectives of this work:

- To investigate the behavior of the thermal and catalytic degradation of Kraft lignin from hardwood and softwood;
- To investigate the effect of a commercial catalyst (such as ZSM-5) in the pyrolysis of Kraft lignin from hardwood and softwood sources;
- To compare the thermal and catalytic degradation of the Kraft lignin in different temperatures, and evaluate its effect on by-products distribution;
- To analyze and compare the components present in the bio-oil;
- To investigate the pathways for the formation of aromatic compounds in the bio-oil;
- To compare the by-products yields and bio-oil composition from pyrolysis of each type of lignin;
- To apply statistical methods, such as covariance matrices and Principal Component Analysis (PCA), to improve the understanding of the mechanisms followed for the by-product formation.

CHAPTER 2

This chapter presents the theoretical foundation of the research with a focus on lignin origin, composition, application, and thermochemical conversion processes.

2 LITERATURE REVIEW

Abstract: This chapter presents the state of the art regarding the thermal and catalytic pyrolysis of lignin in the last years. Special focus is given to lignin and its extraction processes in pulp and paper plants, aiming at its use as a raw material in thermal conversion processes of biomass into value-added products. In this chapter, the processes of thermal and catalytic pyrolysis of lignin are also highlighted with emphasis on the effect of main process variables (such as temperature, residence time, and use of zeolite as catalysts) in the yields of the main products (biochar, bio-oil, and gases) and distribution of value-added products (such as aromatic hydrocarbons and phenolic compounds).

2.1 LIGNIN

The pulp and paper sector produces streams with large amounts of lignocellulose, an abundant form of biomass with numerous possibilities as raw materials for the energy sector and the chemical industry due to its composition and availability. This type of biomass consists of three main components: hemicellulose (20 – 30%), cellulose (40 – 50%), and lignin (10 – 35 %) (LI *et al.*, 2015).

Lignin is a three-dimensional amorphous polymer consisting of methoxylated phenylpropane structures, that is responsible for the transport of water, nutrients, and metabolites of plants, and its presence increases the mechanical resistance in vegetables. In addition, lignin also protects issues against the attack of microorganisms, being found filling the spaces between cellulose and hemicellulose in the plant cell walls, acting like a resin that holds the lignocellulose matrix together (Figure 1) (CHAKAR; RAGAUSKAS, 2004; SALIBA *et al.*, 2001; ZAKZESKI *et al.*, 2010).

Recently, lignin has been viewed as a significant source of aromatic renewable resources because it represents an excellent alternative feedstock in the production of chemicals, polymers, and value-added chemicals. Therefore, lignin is a promising raw material because it is readily available in large amounts, accumulates high levels of energy, represents a potential energy supply, and is a direct source of several types of phenolic and aromatic compounds. The aromatic compounds derived from lignin can be used to produce several basic chemical building blocks (HÁZ *et al.*, 2019; HITA *et al.*, 2018).

In the pulping industry, lignin is considered a by-product. The most common industrial application involves its use as fuel for heat generation. However, numerous potential applications of technical lignin have been considered, and it is worth mentioning its use as a

dispersant, protective UV-absorbents, nanoparticles (in systems of drug delivery and heavy metal absorption), and in the production of biodegradable polymers and phenolic resins (CHIO; SAIN; QIN, 2019). Thus, a deep knowledge of lignin phenolic structure is important to allow its chemical recycling to produce value-added chemicals. In plant cell walls, lignin is associated with hemicellulose and cellulose, forming ether or ester linkages. Therefore, the chemical bonds between these natural polymers build a complex chemical structure and valuable lignocellulose polymer. Each type of biomass has a distinct molecular structure, and the composition of the major components changes according to the kind of plant. Hardwood (including species of Angiosperms, such as Eucalyptus) contains 40 – 55 % of cellulose, 24 – 40 % of hemicellulose, and 18 – 25 % of lignin, while softwood (including species of Gymnosperms, such as Pinus, for example) contains 45 – 50 % of cellulose, 25 – 35 % of hemicellulose and 25 – 35 % of lignin (CHIO; SAIN; QIN, 2019; HÁZ *et al.*, 2019)

Figure 1: Lignocellulose biomass and its composition.

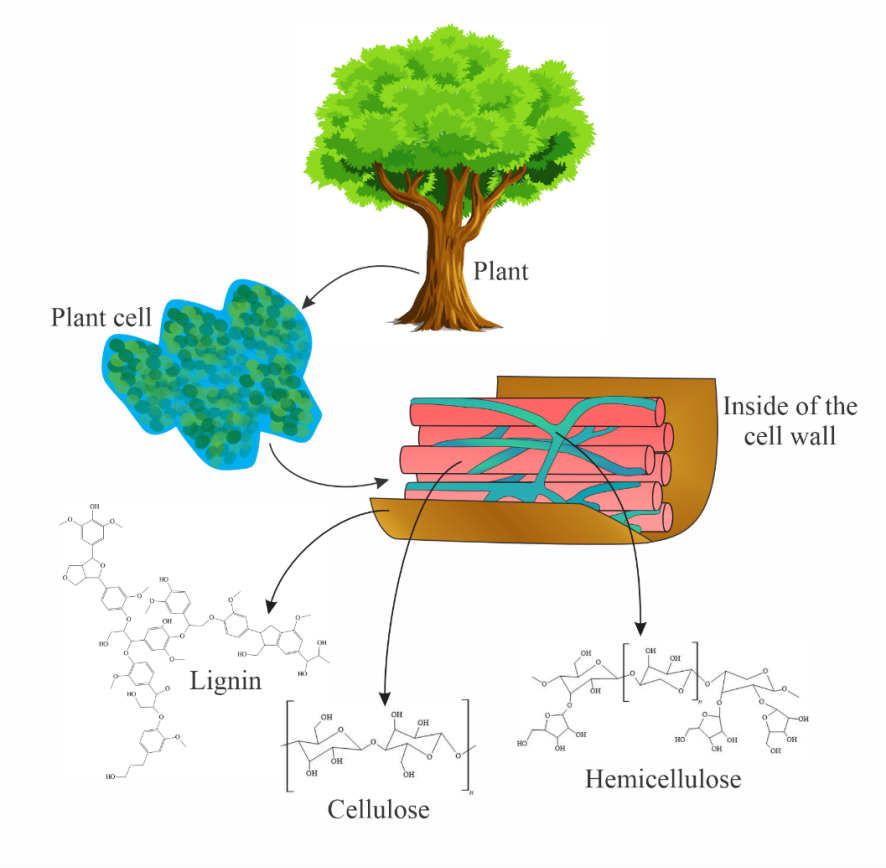

Source: Adapted from Kuthi; Norzali; Badri (2016); and Zakzeski *et al.* (2010).

The cross-linked structure of lignin contains several functional groups within the macromolecule, including aliphatic hydroxyl, phenolic hydroxyl, and methoxyl groups. These groups are responsible for the reactivity and chemical properties of lignin, but the ratios between the hydroxyl groups change according to different sources of biomass. The lignin structure depends on the kind of plant (softwood, hardwood, or grass), and consists of three main precursors also referred to as monolignols which are p-coumaryl alcohol, coniferyl alcohol, and sinapyl alcohol (Figure 2). These precursors are also known as lignin repeating units: siringyl (S), guaiacyl (G), and p-hydoxyphenyl (H), which are linked to each other by different ether and carbon-carbon bonds, forming a three-dimensional network (CHAKAR; RAGAUSKAS, 2004; CHIO; SAIN; QIN, 2019).

Figure 2: Lignin structure and main repeating units.

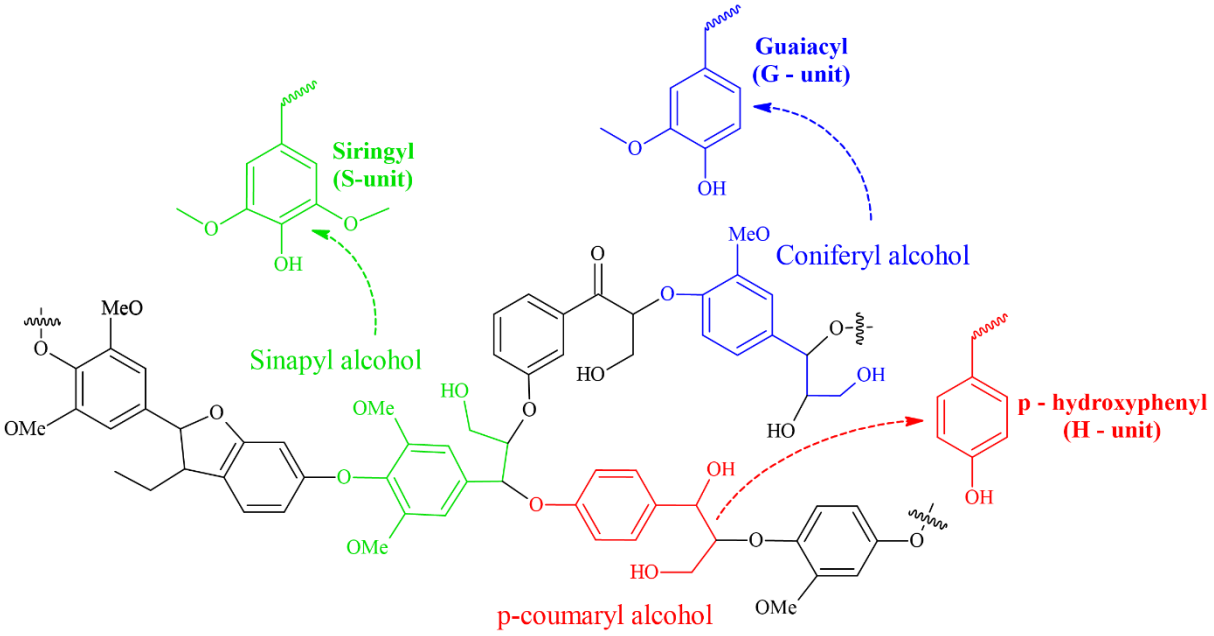

Source: From the author.

The main difference in the repeating units is in the number of methoxyl groups attached to an aromatic ring since the H/G/S units in lignin depend specifically on the biomass source. Softwood lignin mainly contains coniferyl alcohol, around 90-95%, while hardwood usually contains coniferyl and sinapyl alcohols, around 25-50%, and 50-70%, respectively, and the grass typically contains all three repeating units (WANG *et al.*, 2017).

The main linkages between these repeating units, as presented in Figure 3, are the carbon–carbon linkages (β-5 and β-5), also known as condensed linkages, and the ether

linkages (β-O-4, α-O-4, 5-O-4). Different types of lignin have different ratios of repeating units, which influences the linkages ratios. Ether bonds (β-O-4) are the most common linkages in lignin, representing around 43 –50% in softwoods, and 50 – 65% in hardwoods. Moreover, softwood contains more carbon-carbon linkages (β-5 and β-1) due to higher contents of G-units. Consequently, softwood presents a higher condensation degree than hardwood, which contains less carbon-carbon linkages (CHIO; SAIN; QIN, 2019; WANG *et al.*, 2017)

Figure 3: Typical linkages within the lignin macromolecule

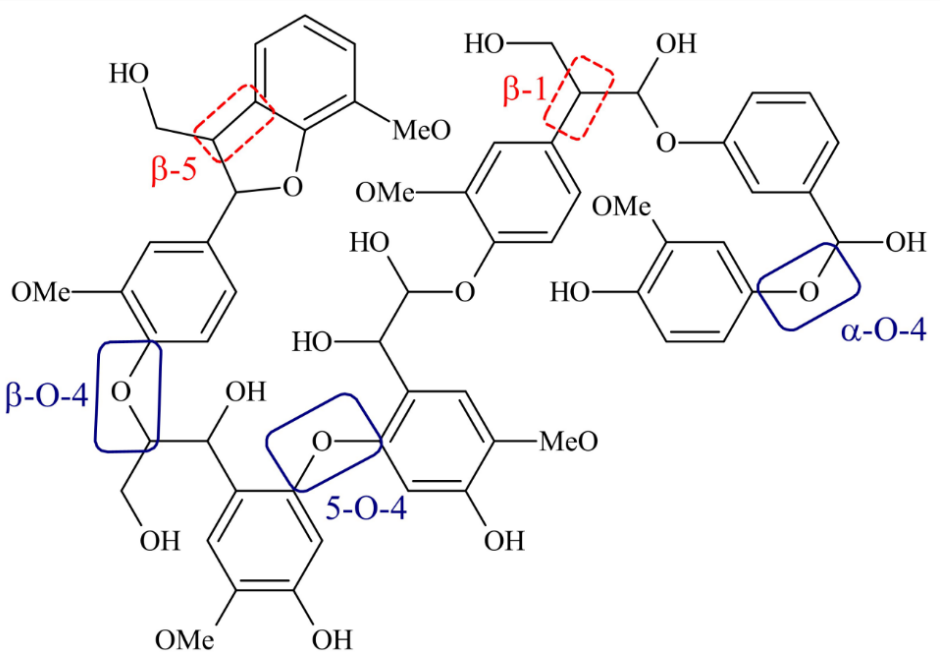

Source: From author.

2.1.1 Lignin sources

Lignin is usually mentioned as native lignin or modified lignin. Unfortunately, the first does not find practical application, because it refers to the original lignin structure in the lignocellulose biomass without any modification. As it is necessary to extract the lignin from the plant through chemical or biochemical processes, only the second form attracts industrial interest. Thus, modified lignin refers to the lignin extracted directly from biomass or recovered from waste streams as a by-product, as observed in industrial sites of cellulosic pulp production (CHIO; SAIN; QIN, 2019). In typical industrial operation of biorefineries, the first step is the pretreatment of lignocellulosic biomass, which consists of the separation of

its main components, by depolymerization process in its smaller compounds. Depending on the pretreatment method, the depolymerization processes can involve chemical transformation (by the use of sulfur compounds) or biochemical reactions (as seen in fermentative or enzymatic processes) (ZAKZESKI *et al.*, 2010).

The extraction method plays an important role in determining the nature and structure of lignin because each separation method modifies the chemical structure of the lignin naturally occurring in the cell wall. Lignin is normally named according to the separation method. The chemical methods of lignin isolation can be divided into two categories. The first one includes methods involving the dissolution and removal of lignin, leaving cellulose and hemicelluloses as insoluble residues. The alkaline lignin, lignosulfonates, and lignin organosolv from the pulp and paper industries fall into this category. In the second category, the hydrolysis processes of biomass by acids leave lignin as an insoluble residue, while cellulose and hemicellulose are converted into fermentable sugars. Klason lignin and hydrolytic lignin are the most common examples in this category (JIANG; NOWAKOWSKI; BRIDGWATER, 2010b; PANDEY; KIM, 2011).

Among the alkaline pulping processes, it is worth highlighting the Kraft lignin process, which uses strong alkalis to cleave the ester bonds between hemicellulose and lignin macromolecules. Lignin remains soluble in the alkalis after the treatment process. The Kraft process is the most traditional pulping and paper production method, representing almost 80% of chemical pulp production. In this process, wood is treated with the solution of sodium hydroxide (NaOH) and sodium hydrosulphide (NaHS) under a temperature range of 150 – 170 °C at elevated pressure to break the ester bonds with the polysaccharides (hemicellulose), and the lignin fragments dissolve in the solvent, forming black liquor (CHIO; SAIN; QIN, 2019; JIANG; NOWAKOWSKI; BRIDGWATER, 2010b; LI *et al.*, 2015).

Lignosulfonates are obtained as a product of the sulfite pulping treatment and are also relatively common in the pulp and paper industry. This process is conducted between pH 2 – 12, at elevated pressure and temperature, using sulfite with either calcium or magnesium as the counterion. In addition, an aqueous solution containing sulfur dioxide and salt of sulfurous acid is used to break the linkages with polysaccharides, and the lignin fragments dissolve in the solvent forming brown liquor. After separation, lignosulfonates are typically soluble in water and some highly polar organics and amine (JIANG; NOWAKOWSKI; BRIDGWATER, 2010b; NIAOUNAKIS, 2015; ZAKZESKI *et al.*, 2010).

The organosolv process can produce high-purity lignin using biomass sourced from wood or bagasse, as well as the fibrous residue left over after plant material is crushed to extract the juice. This method uses a variety of organic solvents, such as methanol or ethanol, and a suitable catalyst (such as HCl) to break the bounds with the polysaccharides, and the lignin fragments are soluble in the solvent. Furthermore, this method has the advantage of preventing the pollution brought on by sulfur-containing inorganic compounds and separates the cellulose and hemicelluloses from the lignin streams, allowing the recovery of all components of lignocellulose biomass (CHIO; SAIN; QIN, 2019; JIANG; NOWAKOWSKI; BRIDGWATER, 2010b; ZAKHAROV *et al.*, 2021).

Since hardwood lignin can partially dissolve during acid hydrolysis, the Klason technique is better suited for the extraction of softwood lignin because it uses a strong mineral to achieve a high lignin yield. The majority of the polysaccharides are hydrolyzed in this procedure using 72% sulphuric acid, which leaves lignin as a solid residue (LI *et al.*, 2015; PANDEY; KIM, 2011).

In ethanol production by enzymatic hydrolysis, lignin is formed like a solid by-product because the cellulose in the lignocellulose is fermented to bioethanol using different types of enzymes. However, the lignin in the lignocellulose forms a complex “shield” that blocks the interaction between the enzyme and cellulose, decreasing the yield of bioethanol production. Therefore, the lignin that cannot react with the enzyme appears as a by-product of enzymatic hydrolysis. This lignin is sulfur-free, has a low phenolic ratio and its structure is similar to the native lignin (CHIO; SAIN; QIN, 2019).

2.1.1.1 Kraft lignin

Kraft pulping is a widespread worldwide process, intending to remove the lignin from cellulose fibers and produce cellulose pulp for paper production, among other products. This process is the basis for several processes of lignin modification and employs an aqueous solution of sodium hydroxide and sodium sulfide (also known as white liquor), which reacts with wood chips at high pressures (7 to 10 bar) inside a digester at high pH and temperatures between 150 – 170 °C, lasting 2 hours. The main point of this process is the disruption of the bonds due to the chemical attack by the alkaline solutes, increasing the hydroxyl group amounts in the lignin structure (CHAKAR; RAGAUSKAS, 2004; VICTOR, 2014)

The advantages of this method include the low requirement on the quality of raw material, a fast cooking time, heat generation for boilers from the lignin combustion, and finally, the production of cellulose pulp of great quality and strength. However, this method has several drawbacks, including an unpleasant odor (related primarily to sulfur compounds), a poor pulp yield of 45 to 55%, and a high cost for plant installation. A small portion of the lignin extracted during the Kraft process is recovered and sold as a powder, while the majority is burned to provide energy (VICTOR, 2014).

The development of large-scale chemical products and processes derived from Kraft lignin requires knowledge of the structural characteristics, reactivity, and thermal properties of these materials. For example, softwood Kraft lignin has a higher condensation degree which contributes to a greater char yield compared to hardwood lignin (GELLERSTEDT, 2015; WANG *et al.*, 2017)

2.1.1.2 Lignin recovery

In the Kraft process, the biomass is converted into cellulose and black liquor. The latter consists mainly of lignin, which is an immediate candidate for conversion into value-added products in biorefineries. Although the burning of black liquor in the recovery boilers enables the recycling of chemical reagents (white liquor) to the extraction step of cellulose pulp, as well as the generation of electricity and steam (both for the process and sale), this stage is still a bottleneck in increasing production capacity of the industries in this sector. Therefore, the simple removal of lignin from the black liquor reduces the volume destined for the recovery boilers, making it possible to increase the production capacity of cellulosic fibers, without the bottlenecks in the recovery of white liquor (NALI; RIBEIRO; HORA, 2016).

The extraction of lignin from black liquor for use as fuel in the lime kiln at the white liquor preparation plant has been widely investigated. In this step, the washed lime mud is dried and endothermically decomposed into calcium oxide and carbon dioxide (MONICA EK, GÖRAN GELLERSTEDT, 1993). However, the positioning of the main companies in the sector is that the extraction of lignin for direct burning does not justify the investments. Therefore, the integration between a lignin biorefinery and a pulp and paper plant make it possible to reduce the costs of transporting raw materials (biomass), as well as obtaining value-added chemical platforms (building blocks), fuels, and energy from renewable sources.

In this sense, thermochemical conversion processes are a promising alternative for lignin recovery as a raw material in chemical recycling routes (NALI; RIBEIRO; HORA, 2016).

The first step to covert the pulp mill into a biorefinery is extracting a renewable raw material such as lignin from black liquor, improving the yield of the mill and reducing production costs. Lignin is the major constituent among the different organic components in black liquor and has a higher heating value when compared to carbohydrates. As the high heating value of black liquor is attributed to lignin, its extraction has the advantage of providing a decrease in the heat load of the recovery boiler. Therefore, a capacity increase in the chemical recovery plant is observed, which can be used as an off-load to the recovery boiler or to avoid expansion when pulp production is increased (TOMANI, 2010; ZHU; WESTMAN; THELIANDER, 2014)

In the Kraft process, lignin is extracted using the Lignoboost process, which allows for the commercial production of lignin with high dry and low ash contents. This method involves the physical and chemical steps of lignin precipitation, filtering, and re-slurring of the lignin cake, followed by a second filtration, and final washing. The main factors influencing filtration properties are related to precipitation temperature, pH, and chemical composition of black liquor (ZHU; WESTMAN; THELIANDER, 2014)

The Lignoboost process consists of a stream of black liquor taken from the black liquor evaporation plant, followed by lignin precipitation by acidification with CO_2 and filtration. In the next step, the filter cake is re-dispersed and acidified, resulting in the slurry that is filtered and washed. This process has the advantage of having a lower investment cost because the filter area and the volume of acidic washing water can be kept at lower values. Also, the yield of lignin is higher, with a lower ash and carbohydrate content (TOMANI, 2010).

2.2 THERMOCHEMICAL CONVERSION PROCESSES

Biomass can be converted into three types of primary fuels, which can be liquid fuels (represented by ethanol, biodiesel, and pyrolysis oil), gaseous fuels (such as biogas), and solid fuels (such as charcoal, torrefied biomass, and biochar). Biomass conversion into value-added products and energy can be achieved through different routes, including thermal, biological, mechanical, and physical processes. Thermochemical conversion processes stand out by allowing the production of multiple products in short reaction times. Depending on the thermochemical route, biomass can be converted into gases that can be used in the synthesis

of chemical products or used directly as fuel in combustion processes. Among the thermochemical processes of biomass conversion, it is worth mentioning torrefaction, pyrolysis, and gasification (BASU, 2013).

The torrefaction process occurs at moderate temperatures between 200 – 300 °C, with residence time ranging from several minutes up to hours under an inert or limited oxygen atmosphere. The main products of torrefaction are solids with improved physicochemical properties and energy density because the carbon content increases and oxygen content decreases. Particularly, the energy density increases due to a change in the lignocellulose structures caused by temperature, which favors the elimination of CO and CO_2 by decarboxylation of hemicellulose and cellulose. In this process, the hemicellulose is preferably decomposed, while the cellulose is weakly decomposed, and the lignin remains in waste biomass due to its complex chemical structure (DA SILVA *et al.*, 2020).

Pyrolysis is a thermal degradation process widely applied to decompose organic products into smaller units by use of heat in the absence of air. As pyrolytic reactions are highly endothermic, macromolecules are broken down into products of low molar mass. In addition, due to the limited oxygen available for the reaction, there is no further combustion of carbon dioxide released on reactions (PANDEY; KIM, 2011). The nature of final products obtained in this process depends mainly on the temperature and residence times: charcoal is favored at lower temperatures and longer residence times, however, liquid compounds are produced at moderate temperatures and short residence times, while gaseous products are obtained at high temperatures and longer residence times (BRIDGWATER, 2012).

By eliminating oxygen from the fuel to increase its energy density, gasification is a process that turns biomass fuel into gases with usable heating value, such as hydrogen, carbon monoxide, and methane. Several exothermic and endothermic reactions occur throughout the gasification process. Therefore, the proper selection of process variables in gasification is a common strategy to produce syngas (which can be manufactured into value-added chemicals) or fuel gas that can be used to produce energy (BASU, 2013; KUMAR, 2009).

2.2.1 Thermal pyrolysis

Pyrolysis is the decomposition of organic components in biomass with temperatures starting at 350 – 550 °C and reaching 700 – 800 °C in the absence of oxygen. Through the heating, vapor and gaseous species are released, while the solid non-volatile is collected as

biochar. The steam portion in the gas phase is further condensed into a black, viscous fluid, known as bio-oil. Pyrolysis reactions are classified depending on operation conditions (mainly heating rate and residence time). Slow pyrolysis involves low heating rates (in the range of 0.1-1 °C/s), and a longer residence time between minutes to hours, producing similar yields of biochar, biogas, and bio-oil. On the other hand, fast pyrolysis involves a high yield of bio-oil achieved through high heating rates of 10 °C/s until values above 1000 °C/s and short residence times (until 2 s). Other process parameters important to consider are the reactor configuration, pressure, temperature, presence of a reduction agent (such as hydrogen), biomass average particle size, and feedstock composition (BASU, 2013; DICKERSON; SORIA, 2013; JAHIRUL *et al.*, 2012; LI *et al.*, 2015).

The main advantage of fast pyrolysis is related to its high yield of liquid, which is produced from the rapid decomposition of biomass that generates condensable gases that, when cooled, form a homogeneous dark brown liquid. However, this process requires careful control of pyrolysis reaction temperature around 500 °C (to maximize the bio-oil yield), the fast removal of product char to minimize cracking of vapors, and the fast cooling of pyrolysis vapors to give the bio-oil product (BRIDGWATER, 2012). On the other hand, operation conditions of slow pyrolysis (temperature, heating rate, and residence time) can be adjusted to maximize the biochar yield. However, bio-oil and gas are also produced during this process. Therefore, the operational parameters used in slow pyrolysis can be adjusted to optimize the production of the products of interest (SETTER *et al.*, 2020)

Pyrolysis reactions are complex and not fully understood due to the complexity of biomass composition. However, these reactions can be generally classified as a mix of dehydration, depolymerization, re-polymerization, fragmentation, rearrangement, and condensation, as presented in Figure 4. Particularly, the bio-oil from the pyrolysis process contains over 300 individual compounds (DICKERSON; SORIA, 2013).

Figure 4: Representation of pyrolysis reactions

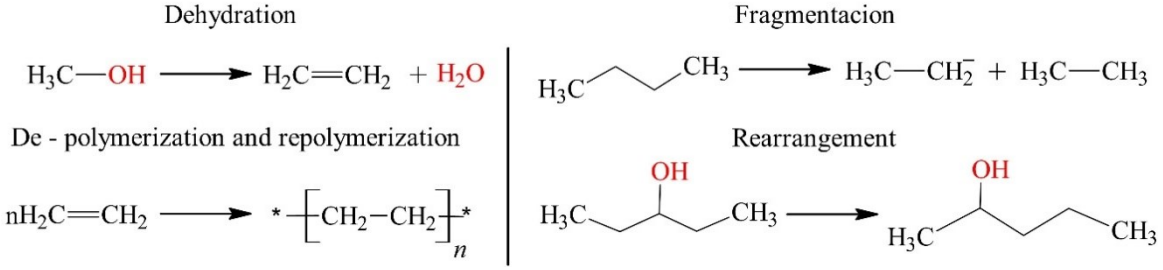

Source: Adapted from Dickerson; Soria (2013).

The pyrolysis process can be represented by two main steps: the primary decomposition reactions that occur at low pyrolysis temperatures (250 – 300 °C), where the release of volatile happens at a rate 10 times faster than the second step of the process. The second step involves the cracking and condensation reactions, followed by the formation of char, gas, and bio-oil (JAHIRUL *et al.*, 2012).

The representation of these pathways is seen in Figure 5, where primary mechanisms follow three main processes depending on the type of break of the chemical bond. Char formation is favored by intra- and intermolecular rearrangement reactions, which result in a solid residue with higher thermal stability. Depolymerization breaks the bonds between the repeating units of the macromolecules, producing condensable molecules at ambient temperature. These molecules are frequently found in the liquid fraction (bio-oil) in the form of dimer or trimer and compounds derived from repeating units. Lastly, fragmentation is the linkage of many covalent bonds of the macromolecula, and also of repeating units, resulting in the formation of non-condensable gas and a diversity of small chains of organic compounds condensable at ambient temperature (COLLARD; BLIN, 2014).

Figure 5: Representation of reaction paths for biomass pyrolysis.

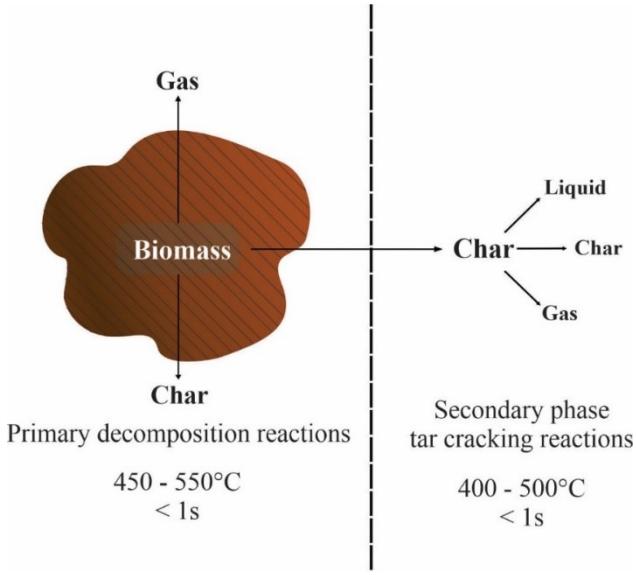

Source: Adapted from Basu, 2013; Jahirul *et al.* (2012).

Secondary mechanisms occur when the released volatile compounds are not stable under the reactor temperature conditions, leading to a secondary reaction such as cracking and recombination. The first one consists of breaking chemical bonds within the volatile compounds, resulting in the formation of lower molar mass molecules. Recombination is the

combination of volatile compounds to give a higher molar mass molecule, leading to the formation of a secondary char. These reactions can be catalyzed at the surface of the char, of the reactor, or eventually by added catalysts (COLLARD; BLIN, 2014).

Lignin pyrolysis produces monoxide and dioxide carbon (by the conversion of carbonyl and carboxyl functional groups), H_2O, gaseous hydrocarbons (methane, ethane, ethylene, propylene, etc.), volatile liquids (benzene and alkyl substituted derivatives, methanol, acetone, and acetaldehyde), monolignols, monophenols (such as phenol, syringol, guaiacol, and catechol), and other polysubstituted phenols, as well as coke and char. The condensable volatile products present a large fraction of methoxyl phenols, like syringol and guaiacol, because methoxyl groups are more resistant than the ether linkages in thermal degradation. At low temperatures, ether bond and hydroxyl groups attached to β and γ carbons are cleaved to form condensable volatile products and water, however, the C – C bonds are only broken at very high temperatures (LI *et al.*, 2015).

As pointed out in some works published in the open literature, lignin pyrolysis occurs over a wide temperature range (44 – 824 °C). The mechanism of lignin pyrolysis involves a network of complex reactions, such as the breakage of weakly linked functional groups (at 44 – 194 °C, providing the melting of lignin), followed by the massive degradation of lignin through the breakage of ether bonds (at 194 – 604 °C), and cleavage of various bond types (at 604 – 824 °C) (CHEN *et al.*, 2019). By using TG, FT-IR, and GC/MS results, Yang *et al.* (2020) studied the mechanism of lignin pyrolysis. Particularly, these authors suggested four possible pathways to obtain the gaseous, liquid, and solid products of lignin (Figure 6). Repeating units of lignin include p-hydroxyphenyl, guaiacol, and syringyl groups, linked together by ether (β-O-4) and C-C (β-1, β-5) bonds through polymerization reactions, forming a complex polymer structure. During thermal pyrolysis, these structures can be cleaved, producing many phenols, aromatic hydrocarbons, and different functional groups, such as carboxyl, carbonyl, and methoxy, released from benzene rings to form light gases (CH_4, CO_2) by cracking repolymerization, and aromatization reactions. The last pathway generates the lignin biochar with abundant functional groups through carbonization or repolymerization. The first route involves the cracking of functional groups with the temperature increase, releasing light gases. In the second route, active aromatic species in bio-oil can be converted into biochar (LU; GU, 2022).

Figure 6: Synthesis pathways of the main products from lignin pyrolysis.

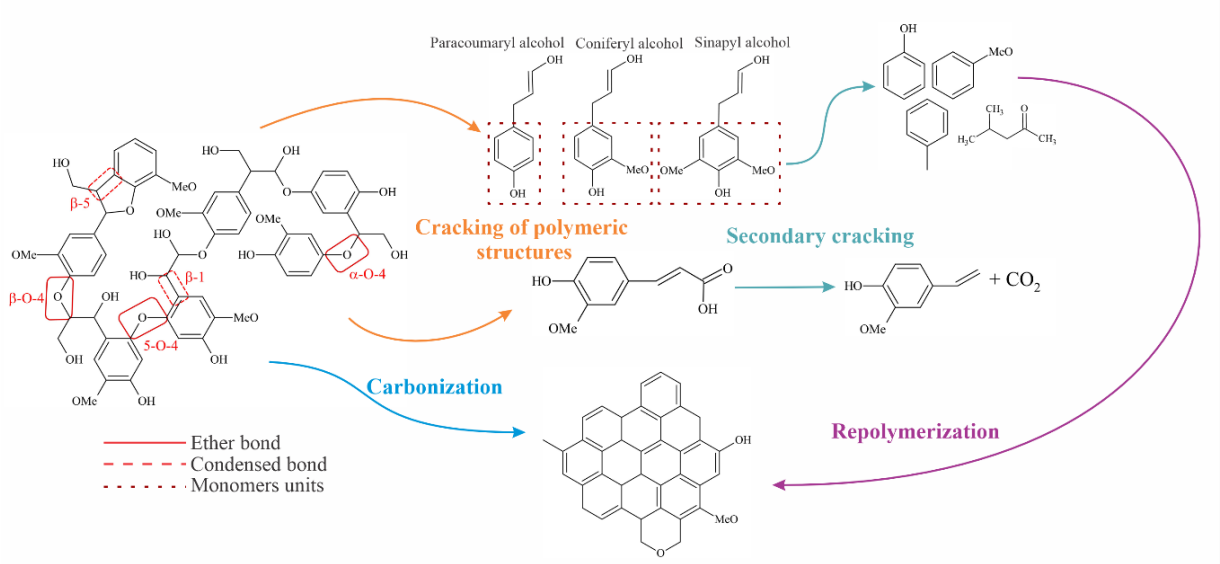

Source: Adapted from YANG *et al.* (2020).

Bio-oil can be a substitute for fuel oil in various applications, such as burning in boilers and furnaces, however, this liquid gradually degrades when exposed to light, O_2, or heat at temperatures above 80 °C, leading to storage issues. In addition, bio-oil pH is relatively low due to the presence of organic acids, increasing the corrosion issues. So, to overcome these problems, it is necessary to modify the bio-oil chemically (through upgrading), mainly by remotion of unwanted oxygenated compounds. For the achievement of these results, bio-oil can be re-volatilized in a catalytic environment (typically referred to as catalytic upgrading) or the lignin can be pyrolyzed in the presence of catalysts, allowing the desired changes before the initial condensation, as seen in catalytic fast pyrolysis (DICKERSON; SORIA, 2013).

2.2.2 Catalytic pyrolysis

Catalytic pyrolysis is defined as the conversion of the pyrolysis primary products (mainly oxygenated species) in the vapor phase into thermally stable products through a series of catalyzed reactions such as deoxygenation, decarbonylation, and oligomerization to the final aromatic products. In this process, oxygen is mainly removed as CO, CO_2, and water, and the yield of the deoxygenated compounds can be increased. However, the inclusion of a catalyst requires operation at a specific temperature, and a sufficient quantity of catalyst

should be added to ensure proper conversion and product selectivity in pyrolysis reactions, resulting in less flexibility in operational conditions (BRIDGWATER, 2012).

Catalytic pyrolysis can be classified into two groups according to the contact mode between the catalyst and the biomass. For *in situ* catalytic pyrolysis, the catalysts are mixed with biomass to provide the decomposition of compounds of higher molar mass and reduce the secondary char formation. The shorter residence time of pyrolysis vapors requires a large catalyst-to-biomass ratio to ensure a higher degree of upgrading and yield of hydrocarbon products. The main disadvantage of this process is the use of the same temperature for cracking and upgrading reactions. In addition, the deactivation of the catalyst by coke formation is typically fast and requires the continuous regeneration of the catalysts through reactors with a configuration of FCC (Fluid Catalytic Cracking) type (WAN; WANG, 2014).

For *ex-situ* catalytic pyrolysis, as the catalyst is placed separately from biomass in the reactor, the operation of catalytic upgrading/cracking can be flexibly performed under different conditions of reaction temperature and residence time, targeting the desired products. In addition, biochar can be easily separated and collected as a potentially valuable solid product. Another advantage is the flexibility of the *ex-situ* configuration, allowing the integration of different catalytic beds arranged in series. As pointed out by these authors, it is hard to justify a choice for in-situ or ex-situ catalytic pyrolysis because the performance depends on the reactor system, catalyst, and other operational conditions such as catalyst/biomass ratio, temperature, and kind of feedstock (WAN; WANG, 2014).

From a biorefinery point of view, catalytic fast pyrolysis is a promising way to improve the liquid composition. The main challenge involves the development of catalysts with proper activity, selectivity, and stability. In this case, catalysts are a key point for biorefineries to become cost-competitive with current infrastructure, allowing the progress of biomass utilization (DICKERSON; SORIA, 2013). Catalytic cracking involves the deoxygenation through simultaneous dehydration, decarboxylation, and decarbonylation reactions in the presence of catalysts, where catalysts have the purpose of altering the product yields and selectivity, thus affecting the composition of bio-oil and its chemical and physical properties (FRENCH; CZERNIK, 2010; ILIOPOULOU *et al.*, 2012a).

As shown in Figure 7, the properties of bio-oil are improved by catalytic upgrading through of conversion of oxygenated compounds into hydrocarbons of lower molar mass with the simultaneous releasing of H_2O, CO, and CO_2. Although the addition of a catalyst can improves the product distribution into valuable hydrocarbon compounds, catalysts must be

highly active, selective to desirable products and reactions, resistant to deactivation, readily recycled by regeneration, and cheap. Nearly all catalysts used in the upgrading of bio-oil are supported, meaning that a metallic active phase is typically dispersed in a cheaper and thermal-resistant material such as carbon, silica, or alumina (DICKERSON; SORIA, 2013; LI *et al.*, 2015).

Figure 7: Catalytic pyrolysis reaction for bio-oil upgrading.

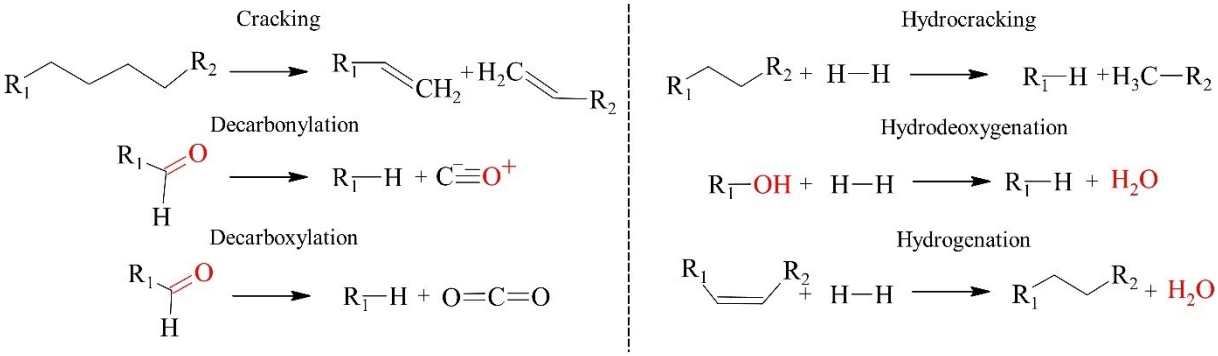

Source: Adapted from Dickerson; Soria (2013).

Zeolites are the most important commercial catalysts used in the cracking processes, consisting of a microcrystalline aluminosilicate. Silicon and aluminum atoms are connected to each bond with the oxygen atom, forming bridges of type Si-O-Al, arranged in a well-defined tridimensional structure of SiO_4 and AlO_4 tetrahedrons. In consequence, zeolites present high catalytic activity due to high specific area and porosity, and low dispersion of pore size distribution that allows better access of desired molecules to active sites. These catalysts are well known to promote cracking reactions during pyrolysis, leading to highly deoxygenated and hydrocarbon-rich compounds, like aromatic hydrocarbons (ESPINDOLA, 2014; YANG *et al.*, 2018). The zeolite is also known to be a molecular sieve with high selectivity, whose mechanism performs like molecular tweezers, immobilizing each substrate molecule in the appropriate position to break only the necessary chemical bond to form the expected product (LUNA; SCHUCHARDT, 2001).

Therefore, the zeolite efficiency is related to: (i) high physisorption rates due to the high specific area; (ii) high chemisorption rates provided when its structure is modified by adding active sites, such as acid sites (whose strength and concentration can be controlled according to the application), and (iii) high selectivity due the presence of a complex network of channels and cavities with size compatible with most raw material molecules in the

industry (which provides transition state selectivity for both reactants and products) (LUNA; SCHUCHARDT, 2001)

Zeolites of medium and high-size pores (such as ZSM5 and Y) are commonly used in catalytic cracking processes. As reported in the literature, zeolites play two roles in the lignin pyrolysis process. Firstly, the zeolite acid site catalyzes the depolymerization of lignin into desirable and thermally stable products. Secondly, the small volume pore can avoid polymerization and coke formation reactions. Therefore, selectivity to the desired products and yield of bio-oil can be changed, tuning the acidity and pore size of zeolites. However, the main disadvantage of catalytic pyrolysis is related to the formation of coke/char that can cause the catalyst deactivation upon both pore blockage and active site poisoning (LI *et al.*, 2015).

The recycling of non-condensable gases such as hydrogen and carbon dioxide can increase the bio-oil yield (due to the occurrence of hydrocracking reactions in the presence of hydrogen) and decrease the yield of char/coke (due to the occurrence of Bourdoard reaction in the presence of carbon dioxide). Therefore, the recycling of carbon dioxide can be an interesting strategy to improve the coke resistance of catalysts used in the pyrolysis process (MANTE *et al.*, 2012).

Figure 8 shows a comparison between thermal pyrolysis and the roles of zeolites in the lignin pyrolysis reaction. In the thermal pyrolysis route without catalysts, the intermediate radicals are firstly generated by depolymerization through a free radical mechanism. Next, the active primary products are polymerized to produce char and coke or stabilized to form low molar mass aromatics. In the ZSM-5 without treatment to provide acid sites, the intermediate products of depolymerization are selectively adsorbed in the pores, decreasing the biochar/coke yield, and increasing the bio-oil yield. For H-ZSM-5, the addition of strong acid sites promotes the cleavage of C–O, and C–C bonds, inducing decarboxylation, dehydration, dealkylation, cracking, and oligomerization reactions. All these processes release gases consisting of CO_2, CO, and CH_4 which probably are generated from the cracking of different side-chain structures and methoxy groups on the aromatic ring. This generation occurs through a direct hydrogen-transfer mechanism, for example (LI *et al.*, 2015).

Figure 8: Lignin fast pyrolysis pathway with and without catalyst

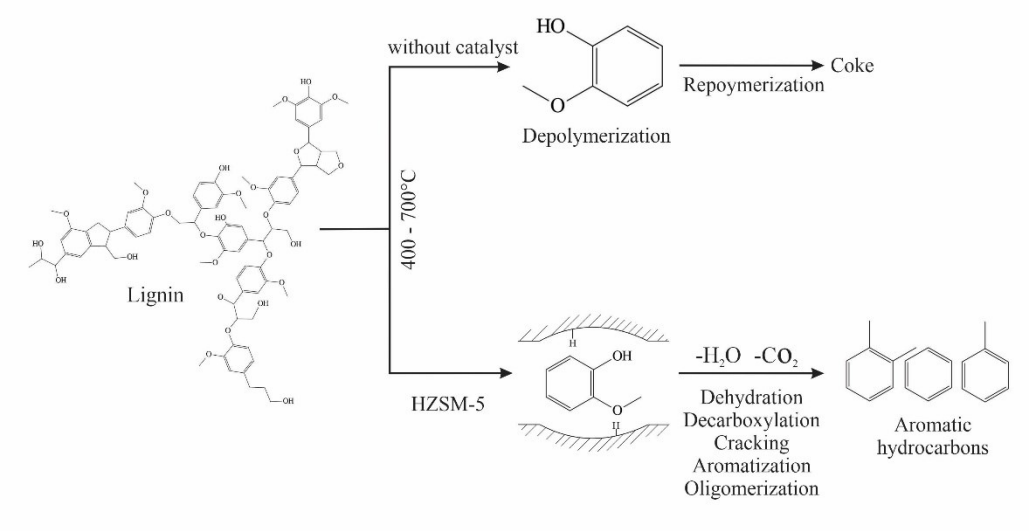

Source: Adapted from LI *et al.* (2015).

The ZSM-5 presents a suitable shape selectivity for aromatics and olefin formation due to channels and pores with uniform diameters. This type of zeolite can improve the quality of bio-oil in terms of its viscosity and heating values. Providing a sufficient surface area, the ZSM-5 allows the transfer of matter through intracrystalline space and determines its capacity to catalyze some reactions, which occurs over restricted pores. Therefore, the product distribution in catalytic pyrolysis is highly influenced by the pore size, shape selectivity, and acidity of the catalyst (NISHU *et al.*, 2020).

It is possible to classify ZSM-5 as a zeolite with medium-sized pores with straight and sinusoidal channels, that have distinct pore openings by a cross-section of 10 member rings of 0.54 – 0.57 nm and sinusoidal channels by elliptic pores of 0.51 – 0.54 nm in cross-section. The pore size influences the reaction activity by affecting the mass transfer of reactants and products (HERNÁNDEZ *et al.*, 2018; NISHU *et al.*, 2020). Although pyrolysis catalyzed by zeolites presents high aromatic production attributed to the pore structure, acidity, and excellent hydrothermal stability, certain intermediate molecules are constrained by diffusion into micropores, thereby promoting coke formation. Therefore, enhancing the accessibility of ZSM-5 to larger compounds, as observed in the synthesis of hierarchical zeolites, may be necessary (NISHU *et al.*, 2020).

Shape selectivity is the ability of the catalyst to only convert reactants and produce products that fit its active sites. Since zeolites are known as mesoporous materials with very specific pore sizes, reactants that are larger than the pores of the ZSM-5 cannot diffuse into its pore structure where most active sites are located, excluding them from the chemical reaction.

The product shape selectivity determines that reaction products of a particular shape and size form within zeolite pores are unable to diffuse out of the pores due to incompatibilities. The product shape selectivity in Figure 9, shows an example of how the product shape selectivity works through ZSM-5 catalyst. Nonetheless, the product molecule that is less mired possesses the capability to diffuse out of zeolite micropores. Then again, larger-size products either do not form or diffuse very slowly or are converted into undesired products, resulting in blockage of the pores and consequently a catalyst deactivation (KIM *et al.*, 2015; NISHU *et al.*, 2020; PATTIYA, 2018; RAHMAN; LIU; CAI, 2018).

Figure 9: ZSM-5 product shape selectivity.

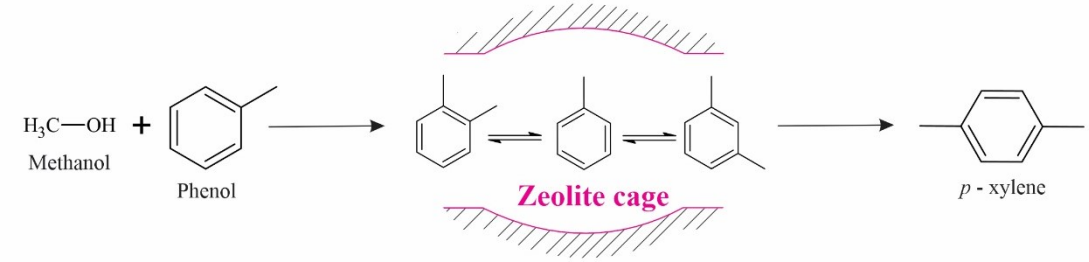

Source: Adapted from Nishu *et al.* (2020)

The zeolite acidity presents an impact in catalytic reactions such as cracking, deoxygenation, oligomerization, and polymerization, through the carbonium ion mechanism forming carbocation intermediate in the active Brønsted acid sites. The acid sites are present on the outer surface of ZSM-5, being responsible for the cracking of high molar mass oxygenate compounds while the conversion of lower molar mass compounds into aromatics occurs on the acid sites inside the pores. This acidity is responsible for the formation of aromatic compounds from pyrolytic vapors, and by increasing the acidity of the catalyst, it is possible to enhance the selectivity of aromatic compounds (NISHU *et al.*, 2020).

2.3 LIGNIN PYROLYSIS PRODUCTS

2.3.1 Biochar

The pyrolysis of lignocellulosic biomass primarily yields a solid product called biochar, which is a carbonaceous material containing approximately 65 to 90% carbon. The physical and chemical properties of biochar, such as porosity and shape, depend on the

specific feedstock and the pyrolysis operation conditions. Lignin, known for its strucutre rich in aromatic groups, is recognized as a biochar precursor. Particularly, biochar derived from lignin present high fixed carbon content, high specific area, and structure rich in aromatic groups. The maximum production of biochar occurs during slow pyrolysis (<500 °C), with simultaneous reduction of bio-oil yield (LI *et al.*, 2020b; YOGALAKSHMI *et al.*, 2022).

Biochar has the capacity to filter and adsorb toxic pollutants owing to its microporous nature, high specific surface area, and cation exchange capacity. Additionally, it can be used as a catalyst, catalyst support, and for electrochemical energy storage. In addition, biochar present high nutrient retention, providing a symbiotic environment for microorganisms growth, which becomes biochar a promising organic fertilizer (YOGALAKSHMI *et al.*, 2022).

2.3.2 Bio-oil

The liquid product generated through pyrolysis, commonly referred to as bio-oil, is a dark brown liquid consisting of a complex mixture of oxygenated compounds such as phenols and aromatic oligomers. Bio-oil can be used as both fuel and chemical feedstock. The yield of bio-oil depends on factors such as the type of biomass, temperature, residence time, char separation, and biomass ash content. To maximize bio-oil yield, a fast/flash pyrolysis process with short residence times of 1-10 s can be employed (BRIDGWATER, 2012; COLLARD; BLIN, 2014; YOGALAKSHMI *et al.*, 2022).

The bio-oil use as a substitute for conventional liquid fuel requires its upgrade by reduction of oxygen content. Bio-oil upgrade is required, because thermal pyrolysis reaction present low-selectivity regarding deoxygenation reactions, restricting its use in specific applications. Techniques like catalytic cracking can be employed to convert bio-oil into liquid fuel for transportation. Additionally, these techniques can be used to produce chemicals like phenols, additives for the fertilizer and pharmaceutical industries, as well as various other specialty chemicals (CHIO; SAIN; QIN, 2019; COLLARD; BLIN, 2014; YOGALAKSHMI *et al.*, 2022).

2.3.3 Gases

When lignin is gasified at high temperatures, a range of gases known as pyrolytic gases are released. These gases include hydrogen, carbon dioxide, carbon monoxide, methane, hydrocarbon gases (C1–C2), and H_2S. To be used to produce syngas for various applications, further processing of these gases requires elevated temperatures, the addition of catalysts, and a prolonged residence time (CHIO; SAIN; QIN, 2019; YOGALAKSHMI *et al.*, 2022).

2.3.4 Effects of operating variable on products.

It is well known that the operation parameters of pyrolysis are the main variables that affects product yields and composition (BRIDGWATER, 2012; BRIDGWATER; CZERNIK; PISKORZ, 2008; CHIO; SAIN; QIN, 2019; LU; GU, 2022). Table 1 presents a detailed description regarding the several by-products obtained from different types of lignin sources with and without a catalyst presence, as well as the operation conditions applied in pyrolysis reactions.

Farag *et al.*, (2016) conducted a study comparing the outcomes of microwave heating and conventional heating ovens for thermal pyrolysis of softwood lignin. The aim was to prevent temperature gradients both inside and outside the heated material and to avoid char layer formation. As electromagnetic waves have a selective interaction with certain materials, this process reduces the amount of heat required to achieve a specific by-product type. The study found that microwave heating did not significantly affect the yield of the liquid product compared to conventional pyrolysis, but it did increase the yield of oxygenated and non-oxygenated compounds. Moreover, Py-Microwave reduced the water content in bio-oil by preserving aliphatic hydroxyl group structures. Supriyanto *et al.*, (2020), used a micro-pyrolyzer coupled with CG-MS-FID aiming to analyze the volatile product. This study showed that proper control of temperature and residence time of pyrolysis could decrease the secondary reaction, and the decomposition pathway for alkaline lignin involves depolymerization, dehydration, demethylation, and demethoxylation reaction from guaiacyl units.

Using a fluidized bed, Diehl *et al.*, (2013), studied the thermal degradation of two different lignin types on biochar formation. For this research, ^{13}C CP-MAS NMR spectroscopy, FT-IR, and Raman spectroscopy were used to characterize the chemical

evolution of refined lignins through different operation conditions. The main findings were related to lignin structure since hardwood lignin is mostly formed by syringyl units and softwood for guaiacyl units. Therefore, hardwood tends to pyrolyze at lower temperatures due to the lack of condensed moieties and 5-5 linkages in its structure.

Yu *et al.*, (2012) and Santana; Carvalho; and Ataíde, (2018) compared both thermal and catalytic fast pyrolysis of hardwood lignin (py-CG/MS) using ZSM-5 in different catalyst-to-lignin ratios. The focus was on analyzing volatile compounds. The results showed that increasing the ZSM-5 proportion also increased the percentage of hydrocarbons. Additionally, SiO_2/Al_2O_3 ratios are associated to the conversion of lignin-derived oxygenates into aromatics due to the concentration of Brønsted acid sites. Therefore, if SiO_2/Al_2O3 increases, acidity decreases, and oxygenates are not converted into aromatics.

To focus on solid, liquid, and gas yields, Lazaridis *et al.*, (2018) used a py-GC-MS, catalytic fast pyrolysis, and a fixed bed reactor. The study demonstrated that the presence of ZSM-5 reduces bio-oil yield while enhancing its composition by promoting the formation of aromatics, including mono-aromatics and naphthalenes. The yield and composition of gases also increased with the catalyst presence, while biochar experiences a slight increase. The results determine those higher temperatures together with a high catalyst-to-lignin ratio favored mono-aromatic, naphthalene, and alkyl-phenols formation.

Below, a summary of the key findings about thermal and catalytic pyrolysis reactions is presented, which can have significant impacts on the composition and properties of the by-products:

- Methoxyl linkages in lignin can be cleaved through depolymerization and condensation reactions at temperatures between 250 and 350 °C;
- At higher temperatures (450 – 650 °C), guaiacyl-type compounds can be converted into alkyl phenols through demethylation, demethoxylation, and dehydrogenation reactions;
- Longer residence time and very high temperature can improve the occurrence of a secondary reaction, reducing phenolic products from Kraft lignin pyrolysis;
- Increasing heating rate and/or residence time can produce radical aromatic rings that may be converted to polycyclic aromatic hydrocarbons;
- The type of lignin can affect the composition of the products produced, particularly; softwood tends to produce more biochar than hardwood due to the predominance of S-units;

- Thermal pyrolysis of lignin typically results in the production of phenolic compounds such as phenol, alkyl phenol, and alkoxy phenol;
- The presence of ZSM-5 provides the reduction of oxygen compounds in the liquid products, as the primary vapors diffuse into the pores of the catalyst. Therefore, catalytic cleavage of C-O and C-C bonds occurs, leading to the formation of intermediates on active sites that ultimately are converted into small molecules and aromatic hydrocarbons;
- High molar mass monolignols derived from syringyl may not be effectively converted by ZSM-5 due to size exclusion or pore blockage;
- To enhance the selectivity of deoxygenation, increase the formation of aromatic hydrocarbons, and the overall quality of bio-oil, modifications to shape selectivity and acidity are commonly required to ZSM-5.

Table 1: By-products obtained from Kraft lignin pyrolysis of different sources and operation conditions.

Lignin Type	Pyrolysis type	Reactor type	Operation Conditions	Products yields	Products distribution and composition	Reference
Softwood	Thermal	Quartz semi-batch reactor	**Microwave and conventional pyrolysis:** For py-Microwave, the lignin was mixed with 30% of char. Temperature: 800 °C Heating rate: 50 °C/min Residence time: 10 min. Sample weight: 50 g	**Microwave:** Biochar: 40 wt.%, Bio-oil: 38 wt.%, Gases: 22 wt.% **Conventional:** Biochar: 46 wt. %, Bio-oil: 35 wt.%, Gases: 19 wt.%	**Bio-oil composition:** **Microwave:** Guaiacol[1], catechol, phenol[1], and benzene. Water composition: 11 wt.% **Conventional:** Guaiacol[1], catechol, phenol, and benzene. Water composition: 16 wt.%	(FARAG *et al.*, 2016)
Softwood	Thermal	Py/GC-MS-FID: Micro-pyrolyzer (fast pyrolysis)	Temperatures: 400, 500, 600 °C Residence times: 0.5, 1, 2, and 5 s. Sample weight: 500 µg	Only volatile products were analyzed	**Main volatile compounds:** 4-ethyl-2-methoxyphenol, vanillin, 2-methoxyphenol, 2-methoxy-4-vynilphenol, acetaldehyde, and 2-methoxy-methyl-phenol.	(SUPRIYANTO *et al.*, 2020)
Softwood and Hardwood	Thermal	Fluidized bed	Temperature: 250 to 900 °C. Heating rate: 20 °C/min Residence time: 5min Sample weight: 1.5g	Only biochar was analyzed. Hardwood started to lose significant weight at 400 °C, while softwood started at 500 °C. Softwood had a higher char yield.	Biochar composition: Hardwood had more methoxyl groups and was mostly formed syringyl units. Softwood had more carbon-carbon linkages and high content of guaiacyl repeating units.	(DIEHL *et al.*, 2013)

[1] Main component; [2] Higher % GC-MS peak area. Source: From author.

Lignin Type	Pyrolysis type	Reactor type	Operation Conditions	Products yields	Products distribution and composition		Reference
Hardwood	Thermal and Catalytic	Micro-pyrolyzer coupled to a GC/MS	ZSM-5 catalyst: 1:1, 1:5 and 1:10 Temperatures: 450, 550 and 650 °C Heating rate: 20 °C/ms Residence time: 10 s	Only volatile products were analyzed	**Thermal:** The main compounds formed were syringol and guaiacol. **Catalytic:** The main hydrocarbon compounds were o-xylene, toluene, 1,2,3-trimethyl-benzene, and naphthalene.		(SANTANA; CARVALHO; ATAÍDE, 2018)
Softwood	Thermal (T) and Catalytic (C)	Py/GC-MS (fast pyrolysis) and Fixed bed reactor	**Py/GC-MS:** Temperature: 400, 500, 600 °C, Residence time: 12 s. ZSM-5 (40) catalyst: 1:4 mg **Fixed bed:** Temperature: 600 °C Residence time: 20 min. ZSM-5 (40): 1:1 - 0,5g	**Py/GC-MS:** Biochar: **T:** 54.5 wt.%, 43.3 wt.%; 34.5 wt.%. **C:** 39.9 wt. %, 28.1 wt. % **Fixed bed:** **T:** Bio-oil: 30.6 wt. %. Biochar: 42.2 wt.%. Gases: 14 wt.% **C:** Bio-oil: 16.2 wt.%; Biochar: 47.9 wt. %; Gases: 22 wt.%	**Py/GC-MS:** bio-oil [1]: **T:** Most G-type. **C:** mono-aromatics and naphthalenes. **Fixed bed:** Bio-oil: **T:** Oxygenated phenols[2], Phenols, and Ketones.	**Fixed bed:** **C:** Aromatics[2], Phenol, Naphthalene. Biochar: Sulfur content Gases: CO_2, CO, CH_4 **T:** 6.4, 4.1, 3.2 wt% **C:** 8.9, 8.0, 3.6 wt%.	(LAZARIDIS *et al.*, 2018a)
Hardwood	Thermal and Catalytic	Py/GC-MS (Fast pyrolysis)	Temperature: 650 °C Heating rate: 20 °C/ms Residence time: 10 – 120 s C/L: 20:1 (ZSM-5, mordenite, beta, and Y zeolites)	Only volatile compounds were analyzed	**Thermal:** Oxygenated compounds were predominant (syringol). **Catalytic:** Production of monocyclic and polycyclic aromatics increases.		(YU *et al.*, 2012)

[1] Main component; [2] Higher % GC-MS peak area. Source: From author.

2.4 CONCLUDING REMARKS

This chapter introduces lignin as a promising source of renewable resources to produce chemicals, polymers, and aromatic compounds. Pyrolysis technology is regarded as one of the most promising methods for converting lignin into value-added products. Several studies have been conducted for a better understanding of the lignin pyrolysis mechanism. However, there are still a lot of challenges to be overcome, since the complexity of lignin structure always leads to complex phenolics products after pyrolysis reactions.

Different pyrolysis conditions have been employed to analyze the by-products, including adjustments to reactor configuration, heating sources, heat/condensation methods, residence time, and catalyst presence, among other factors. The most common method for analyzing condensed vapors is pyrolysis coupled with a CG/MS spectrometer at high temperatures (400 – 800 °C) and short residence times (seconds), which provides detailed information about the components present at each temperature and allows a better understanding of the pyrolysis mechanism. To analyze the yield and content of all products, fixed bed, and fluidized bed reactors can be used, enabling the extraction of the three products using similar conditions to those used in py-GC/MS.

ZSM-5 is a widely studied and commonly used zeolite, whose shape selectivity is largely dependent on structure, size of pores channels, particle composition (Si/Al ratio), number of acid sites, and total acidity. Most of the research on ZSM-5 has focused on its use in softwood Kraft lignin and the various methods for modifying ZSM-5 to enhance its shape selectivity to upgrade bio-oil quality.

The knowledge of lignin structure and pyrolytic mechanisms can be a useful pathway to remove methoxyl compounds from the liquid product. The pyrolysis mechanism for softwood lignin is well established in the literature. In contrast, hardwood lignin and its pyrolysis products have received relatively less attention in published works in open literature. Additionally, the literature also lacks a clear understanding regarding the use of catalysts in pyrolysis of hardwood lignin, and how syringyl types behave in their presence.

CHAPTER 3

This chapter presents the results obtained by the thermal pyrolysis and provides lignin and products characterizations. An article based on Chapter 3 will be submitted to a scientific journal.

Graphical Abstract

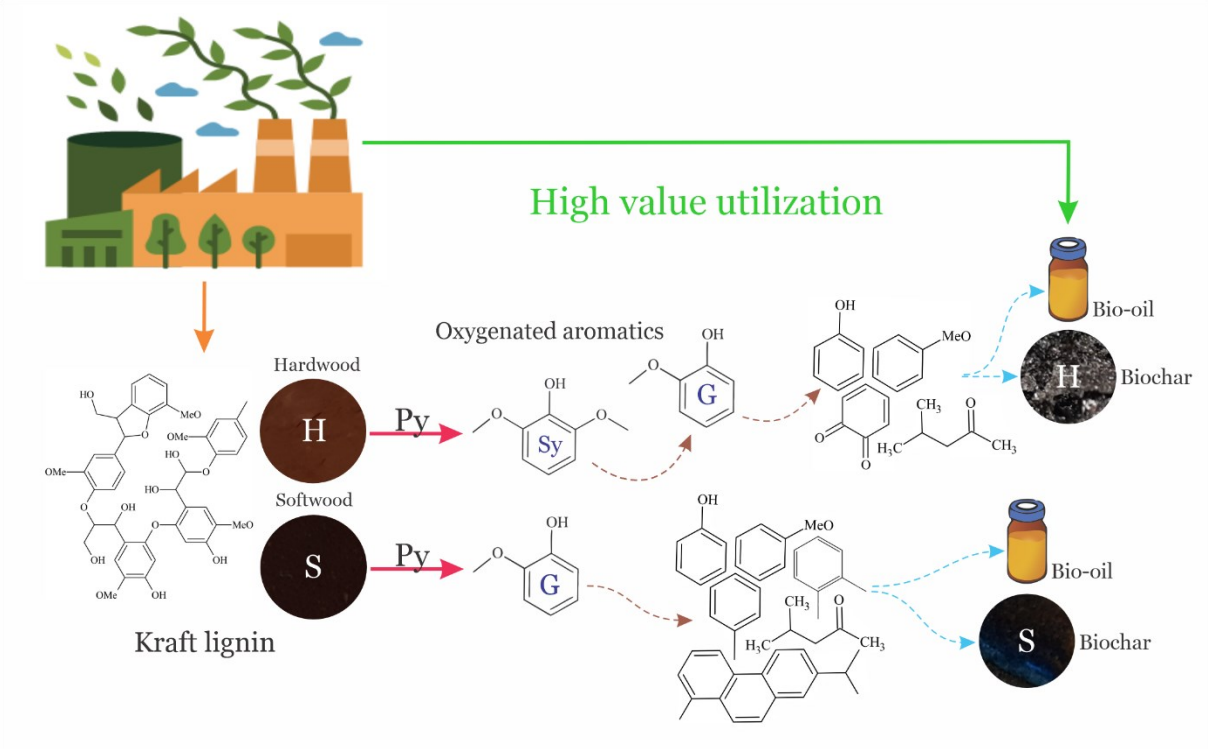

3 EVALUATION OF THERMAL DEGRADATION MECHANISMS OF SOFTWOOD AND HARDWOOD KRAFT LIGNIN THROUGH STATISTICAL ANALYSIS.

Abstract: Thermal pyrolysis is a prominent technology to convert biomass into products that could be used in energy and chemical applications. So, the purpose of this research is to study the thermochemical conversion of lignin as a potential pathway to replace fossil resources in different applications due to its structure composed of repeating units of guaiacyl, syringyl, and p-hydroxyphenyl, whose decomposition yields oxygenated aromatic compounds. Because of its complex structure, the type of lignin can influence the composition of the final products. In this study, thermal pyrolysis of two Kraft lignin samples (*Eucalyptus spp* and Pine Tree) was evaluated in a fixed-bed reactor at different temperatures (500, 600, and 700 °C). The physical and chemical properties of each lignin were measured by proximate analysis, ultimate analyses, FT-IR, TGA/DTG coupled with a deconvolution method, and ss-NMR. Product distribution in bio-oil was analyzed by GC-MS, while the biochar composition was analyzed by FT-IR and ss-NMR. Moreover, an analysis of covariance was performed to assess the degree of functional dependence between the different variables, including the yields of products in bio-oil, the type of lignin sample, and temperature. The results showed that the methoxyl group content was the most important factor in the lignin pyrolysis, since a higher amount of -OCH_3 can directly affect the composition and yield of the products. Moreover, guaiacol decomposition was the most common pathway to produce aromatic hydrocarbons and aromatics oxygenated (OA). However, as hardwood lignin presented more ether bonds than softwood lignin, syringol was preferentially produced and its decomposition was the main pathway to produce aromatics and OA.

Keywords: lignin; softwood; hardwood; pyrolysis; thermal conversion.

3.1 INTRODUCTION

Lignin is an abundant natural phenolic polymer, belonging to a group of macromolecules that account for the lignocellulosic biomass. In nature, lignin is usually found in ether or ester linkages with hemicellulose and cellulose, thus constructing a complicated and valuable lignocellulose polymer. Lignin content varies in different species of biomass. Hardwood stems, for instance, usually contain 18 – 25 % of lignin, while softwood stems contain 25 – 35 % (CHIO; SAIN; QIN, 2019; LU; GU, 2022; WANG *et al.*, 2017).

The use of lignin in biorefineries involves its extraction directly from the plant or its recovery from industrial by-products (CHIO; SAIN; QIN, 2019). In biorefinery operation, the

first step is the pretreatment of lignocellulosic biomass, providing the fractionating of the main components of biomass and related material. In this step, the degradation of biomass into macromolecules (as lignin) occurs through chemical transformations, such as the incorporation of sulfur, depending on the pretreatment method (ZAKZESKI *et al.*, 2010). The pretreatment method has an important role in determining the nature and structure of lignin because each separation method modifies the chemical structure of the naturally occurring lignin (PANDEY; KIM, 2011).

The pulp and paper sector produces streams with large amounts of lignocellulose, which consists of an abundant form of biomass with numerous possibilities as raw materials for the energy sector and the chemical industry due to its composition and availability. In industrial sites, lignin can be extracted from black liquor, a by-product of the cooking step, which is typically burned at recovery boilers. As well known, lignin presents an abundant natural phenolic structure and can be considered a renewable feedstock of phenolic and aromatic resources (basic building blocks of the chemical industry). In Kraft pulping processes, lignin is readily available in large amounts, and its extraction from black liquor can reduce the bottlenecks associated with scale-up in recovery boilers (CHIO; SAIN; QIN, 2019; HÁZ *et al.*, 2019; HITA *et al.*, 2018).

The Kraft lignin process uses strong alkalis to cleave the ester bonds between hemicellulose and lignin macromolecules, also known as alkali-soluble lignin. This process is the most traditional pulping and paper production method, representing almost 80% of chemical pulp production. The Kraft process involves the wood treatment with a solution of sodium hydroxide (NaOH) and sodium hydrosulphide (NaHS) under a temperature range of 150-170°C and high pressure, to break the linkages with polysaccharide. Thus, lignin fragments dissolve in the solvent, forming black liquor (CHIO; SAIN; QIN, 2019; JIANG; NOWAKOWSKI; BRIDGWATER, 2010a; LI *et al.*, 2015).

Lignin is extracted from black liquor using the Lignoboost ^{TM} method, which allows for the commercial production of lignin with a high dry and low ash content. This method involves the physical and chemical steps of lignin precipitation, filtering, re-slurring of the lignin cake, a second filtration, and final washing. The main factors influencing filtration properties are related to precipitation temperature, pH, and chemical composition of black liquor (ZHU; WESTMAN; THELIANDER, 2014).

Lignin is an amorphous tridimensional polymer, composed of three major precursors, such as p-coumaryl, coniferyl, and sinapyl alcohols, also known as p-hydroxyphenyl (H),

guaiacyl (G), and syringyl (S) units, respectively. These precursors are joined together by ether (C-O-C) and carbon – carbon (C-C) bonds (SUPRIYANTO *et al.*, 2020). The main difference in these units is the number of methoxyl groups attached to an aromatic ring, and the proportion of H/G/S units in lignin depends specifically on the biomass source (WANG *et al.*, 2017). According to the abundance of these units, softwood lignin contains around 90 – 95% of G-units, while hardwood lignin contains around 25 – 50% of G and S-units (CHIO; SAIN; QIN, 2019).

The linkages between monomers are complex and known as condensed linkages (C-C) and ether linkages. The most common linkages are the ether bonds, such as aryl ether (β-O-4, α-O-4, γ-O-4) which represent around 50% in softwood and 60% in hardwood. Moreover, softwood contains more carbon-carbon linkages (β-5 and 5 – 5) due to higher contents of G-units. Consequently, softwood presents a higher condensation degree than hardwood, which contains less carbon–carbon linkages. Also, the C-C condensation degree is highly dependent on lignin isolation process (CHIO; SAIN; QIN, 2019; WANG *et al.*, 2017).

Thermochemical processes are used to perform the degradation and conversion of lignin into diverse chemical compounds. Even though, lignin depolymerization to aromatic compounds is challenging due to its complex structure and heterogeneity of chemical bonds. Pyrolysis is considered a promising thermochemical process for the conversion of lignin to biochar, bio-oil, and gases, where the proportion of each product depends on the temperature, heating rate, and type of reactor (PANDEY; KIM, 2011; SUPRIYANTO *et al.*, 2020; YOGALAKSHMI *et al.*, 2022).

Pyrolysis consists of heating an organic substance in the absence of air, breaking down the molecular structure into smaller units. Also, there is no combustion of carbon dioxide in pyrolysis due to the limited available oxygen (PANDEY; KIM, 2011). The products yields obtained in this process depend on the temperature and residence times. Charcoal is typically favored in lower temperatures and longer residence times, while the liquid fraction yields increases in moderate temperatures and short residence times. High temperatures and longer residence times are employed to increase biomass conversion to gas (BRIDGWATER, 2012).

Biochar is a porous solid with a high carbon content, ranging from 65 – 90%. The physicochemical properties of biochar depend mainly on the type of raw material and the pyrolysis conditions. Biochar yield can be improved and reach its maximum value with the simultaneous decrease of the bio-oil yield during slow pyrolysis (at temperatures below 500

°C), due to the rich structure of lignin in the aromatic rings. Biochar is widely used in the filtration and adsorption processes of toxic pollutants because of its microporous internal structure, cation exchange capacity, and high specific surface area (LI *et al.*, 2020b). Bio-oil is a dark brown liquid comprised of several oxygenated compounds that can be used to produce fuels or chemicals. Bio-oil yield is generally improved by flash pyrolysis. However, the physicochemical properties of bio-oil should be improved to replace conventional fuels, as well as raw materials in chemical production like the manufacture of resins, and add-ons in the pharmaceutical industry (YOGALAKSHMI *et al.*, 2022).

Pyrolytic gases are produced in conditions of high temperatures, the presence of selective catalysts, and slow residence time, leading to degradation of carbonyl and carboxyl functional groups and depolymerization of aromatic moieties. Notably, biogas is composed of a mixture of H_2, light hydrocarbons (C1 – C4), CO_2, CO, CH_4, and H_2S, and it is widely used for the generation of heat, electricity, and liquid biofuel synthesis (YOGALAKSHMI *et al.*, 2022). Among some works published in the open literature, Chen *et al.*, (2019) reported the occurrence of lignin pyrolysis over a wide temperature range (44 – 824 °C). The mechanism of lignin pyrolysis involves a network of complex reactions, such as the breakage of weakly linked functional groups (at 44 – 194 °C, providing the melting of lignin), followed by the massive degradation of lignin through the breakage of ether bonds (at 194 – 604 °C), and cleavage of various bond types (at 604 – 824 °C).

Similarly, Yang *et al.* (2020) studied the mechanism of lignin pyrolysis, based on TG, FT-IR, and GC/MS results. Particularly, these authors pointed out four possible pathways to obtain the gaseous, liquid, and solid products of lignin (Figure 10). Repeating units of lignin include p-hydroxyphenyl, guaiacol, and syringyl groups, linked together by ether (β-O-4) and C-C (β-1, β-5) bonds through polymerization reactions, forming a complex polymer structure. During thermal pyrolysis, these structures can be cleaved, producing many phenols, aromatic hydrocarbons, and different functional groups, such as carboxyl, carbonyl, and methoxy, released from benzene rings to form light gases (CH_4, CO_2) by cracking repolymerization, and aromatization reactions. The last pathway generates the lignin biochar with abundant functional groups through carbonization or repolymerization. The first route involves the cracking of functional groups with the temperature increase, releasing light gases. In the second route, active aromatic species in bio-oil can be converted into biochar (LU; GU, 2022).

Figure 10: Synthesis pathways of the main products of lignin pyrolysis.

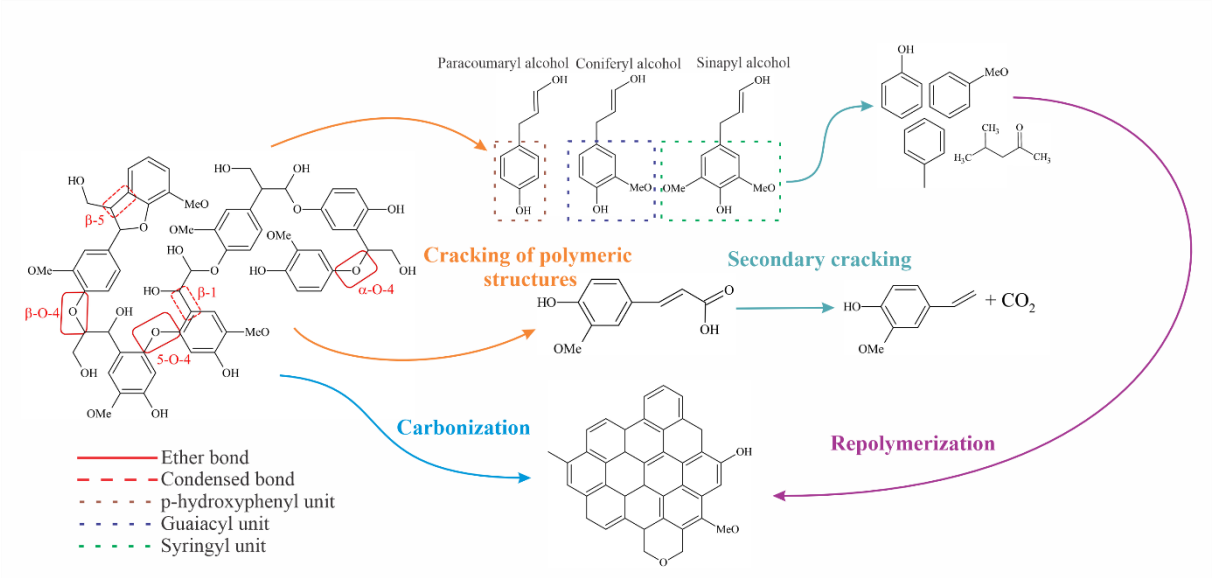

Source: Adapted from YANG *et al.*. (2020).

Usually, the set of reactions comprising lignin pyrolysis can be classified into primary and secondary reactions. Primary reactions or first pyrolysis involve reactions occurring at temperatures lower than 600 °C, while secondary reactions occur from the primary products released in the gas phase (SUPRIYANTO *et al.*, 2020). Specifically, Ben and Ragauskas, (2011) studied pyrolysis of softwood Kraft lignin at 400 – 700 °C using a quartz tube heated within a furnace and characterized the bio-oil with GPC and NMR analyses. Among their main results, cleavage of the ether bonds occurred during the primary decomposition, and components such as catechol and p-hydroxy-phenyl hydroxyl were released at higher temperatures along with oxygenated aromatics and hydrocarbons.

Zhou *et al.*, (2013b) performed pyrolysis tests using a fluidized bed reactor at 400, 500, and 550 °C, as well as residence times between 0 and 15s. In their tests, the thermal degradation rate increased with temperature and residence time. Interestingly, the effect of residence time was more pronounced at higher temperatures. The secondary reaction can decrease the yield of methoxylated phenol and phenolic compounds (ZHOU *et al.*, 2013a). Product distribution from lignin pyrolysis depends upon the pyrolysis temperature. Bio-oil yield is maximum between 450 and 600 °C, while demethylation, demethoxylation, decarboxylation, and alkylation occur at higher temperatures (CHOI; MEIER, 2013; JIANG; NOWAKOWSKI; BRIDGWATER, 2010b).

As the properties of lignin are contingent upon the lignocellulose source, the age, and the environment of the plant, as well as the extraction process, it is arduous to ascertain the

composition and structure of lignin, limiting the technological development of conversion routes to quality and high-value chemical products (SIMMONS; LOQUE; RALPH, 2010). Thermogravimetric analysis (TGA) coupled to a CG-MS or FT-IR are common methods to characterize products through pyrolysis. NARON *et al.*, (2017) used similar methods to determine the H:G:S composition of different lignin types, resulting in a Kraft softwood with a low content of S units, and a predominance of G-units, while Kraft hardwood had more S-units presence.

The Py-CG/MS method was investigated by ZHANG *et al.*, (2012) in Aspen (organosolv process) and Kraft lignin. In particular, guaiacol-substituted products were predominant, with Aspen lignin (hardwood) producing high amounts of all three monomers-substituted, with a predominance of G-type > S-type > H-type. While Kraft lignin (softwood) produced lower amounts of H:G:S and a small amount of S-type products. Similar results regarding the type of lignin were found by Borella *et al.*, (2022b), Diehl *et al.*, (2013), Fodil Cherif *et al.*, (2020), and Ház *et al.*, (2019).

Nevertheless, it was noticeable the lack of research that investigated the full mechanisms of pathways for liquid and solid products, and how G/S-units influence the process, especially for hardwood lignin. Therefore, the focus of this study is to evaluate the physical, chemical, and thermal characteristics of two different Kraft lignin samples and characterize the pyrolysis products. A covariance matrix coupled with a Principal Component Analysis (PCA) was used as a statistical method to differentiate the spectra pattern exhibited by the different lignins to improve the understanding of the mechanisms followed for the formation of products.

3.2 MATERIAL AND METHODS

3.2.1 Biomass selection and preparation

In this study, two different Kraft lignins were selected: *Eucalyptus spp* lignin (referred to as Lignin A), which was donated by International Paper, and Pine Tree lignin (referred to as Lignin B) (CAS# 8068-05-1, catalog number 471003), which was purchased from Sigma-Aldrich. These samples can be classified as hardwood (*Eucalyptus spp* lignin, Lignin A) and softwood (Pine Tree lignin, Lignin B), respectively.

3.2.2 Characterization

The ultimate analysis aimed to measure the carbon, hydrogen, nitrogen, sulfur, and oxygen content of the lignin samples, as well as their moisture and ash content. The analysis was performed using a 2400 Series II CHNS/O analyzer from Perkin Elmer, USA. The specific method followed for the analysis was ASTM D5373-08 (ASTM, 2016a).

The hydrogen-to-carbon effective (H/Ceff) ratio, as presented in Eq (1), serves as an indicator of the relative hydrogen content in different feedstocks based on the number of moles of oxygen (O), carbon (C), and hydrogen (H) present in the feed. A higher ratio suggests an increase in the amount of aromatic hydrocarbons in the bioproduct (LEE et al., 2018; ZHANG et al., 2011)

$$H/C_{eff} = \frac{H - 2O}{C} \quad (1)$$

Methoxyl groups (-OCH_3) of the samples were obtained based on the hydrogen and oxygen contents, as presented in Eq. (2) (JABLONSKY; BOTKOVA; ADAMOVSKA, 2015):

$$OCH_3(wt\,\%) = -18.57690 + 4.06580H + 0.34543O \quad (2)$$

where OCH_3 is the content of methoxyl groups in lignin, H and O are the hydrogen and oxygen contents (w/w%) (measured by the ultimate analysis).

The higher heating value (HHV) defines the energy content of the fuel and can be computed using the correlation described by Eq. (3), where C, H, O, N, S, and A represent the mass fractions (on a dry basis) of carbon, hydrogen, oxygen, nitrogen, sulfur, and ash, respectively. The low heating value (LHV) was calculated by subtracting the latent heat of vaporization of water from the HHV equation, as presented in Eq. (4) (OLIVEIRA *et al.*, 2023).

$$HHV\ (MJ.kg^{-1}) = 0.3491C + 1.1783H + 0.1005S - 0.1034O - 0.0151N - 0.0211A \quad (3)$$

$$LHV(MJ.kg^{-1}) = HHV\ (MJ.kg^{-1}) - 0.2183H(\%) \quad (4)$$

The approximate analysis allowed measuring the moisture (M), volatile material (VM), ash (A) and fixed carbon (FC) contents in the samples. This analysis was performed

following the modified ASTM E-1131-08 standard, using a DTG-60 thermogravimetric analyzer (Shimadzu, Japan). Approximately 40 mg of sample was heated at 100 °C/min, with gas flow rate of 100 mL/min (ASTM, 2014; OLIVEIRA *et al.*, 2023; PACIONI, 2006). The volatile material (VM) and ash (A) contents were measured on a dry basis, while the fixed carbon (FC) content was determined by difference, as indicated in Eq. (5).

$$FC(wt\,\%) = 100 - VM(wt\,\%) - A(wt\,\%) \quad (5)$$

The FT-IR analysis was conducted using a Spectrum 100 spectrophotometer from PerkinElmer, USA. The scanning range for the analysis was between 4000 and 400 cm^{-1}. For this procedure, the samples were dried and pressed with potassium bromide powder (KBr) at a ratio of 1:100, following the guidelines outlined in ASTM D2702-05 (ASTM, 2016b)

The solid-state nuclear magnetic resonance (ss-NMR) measurements were performed using a Bruker Avance-III spectrometer. The spectrometer was equipped with a 14.1 T narrow bore magnet and operated at a Larmor frequency of 150.91 and 600.09 MHz for ^{13}C and ^{1}H, respectively. The powder samples were packed into 4.0 mm ZrO_2 rotors and rotated at a magic angle spinning (MAS) rate of 10 kHz at room temperature. In the cross-polarization and magic angle spinning (^{13}C CP-MAS) experiments, a 5 s pulse delay was followed by a proton preparation pulse of 3.8 μs duration. The contact time was set to 2 ms, and the acquisition time was set to 45 ms. Glycine was employed as an external reference for the ^{13}C spectra and to establish the Hartmann-Hahn matching condition in the cross-polarization (CP) experiments in ^{13}C spectra. During acquisition, the SPINAL64 sequence was used for heteronuclear decoupling, and transients were averaged over 10k transients for CP experiments (MELKIOR *et al.*, 2012).

3.2.3 Kraft lignin thermal decomposition

The thermal stability and mass loss profiles of the lignin samples were investigated using a thermogravimetric analyzer DTG-60 (Shimadzu, Japan) through differential thermogravimetric analysis (DTG/TGA). For each experimental test, the initial sample mass (approximately 10 mg) was heated from room temperature to 900°C using four different heating rates (5, 10, 15, and 20 °C/min) under a constant flow rate (100 mL/min) of high purity nitrogen (99.997%) (DA SILVA *et al.*, 2020; SAHOO *et al.*, 2021). The deconvolution

method was applied to the DTG curves using OriginLab® software to investigate the reactions that occurred during the pyrolysis of each lignin.

3.2.4 Pyrolysis runs

Pyrolysis runs were carried out on bench scale. The experimental unit scheme is shown in Figure 11, consisting of a quartz fixed-bed tubular reactor (with an external diameter of 2.5 cm, internal diameter of 1.7 cm, and length of 53.5 cm) with a heat source provided by an electric furnace (MOD DI-600RP DIST, São Paulo, Brazil). The sample was placed inside the internal cylinder, and its temperature was measured by a type K thermocouple (Ecil) coupled to a digital dual K/J thermometer (Minipa MT-455A model). At the reactor outlet, there is a liquid nitrogen trap used for cooling and condensing the pyrolysis vapors and collecting the formed bio-oil. The volatile released from the biomass during the reaction passes through a condenser under a liquid nitrogen-cooled bath. To create and maintain an inert environment during pyrolysis, the reactor was purged for 15 min with nitrogen gas (400 mL/min) at room temperature (DA SILVA *et al.*, 2020; MUMBACH *et al.*, 2019; OLIVEIRA *et al.*, 2023).

Figure 11: Scheme of experimental setup for pyrolysis runs.

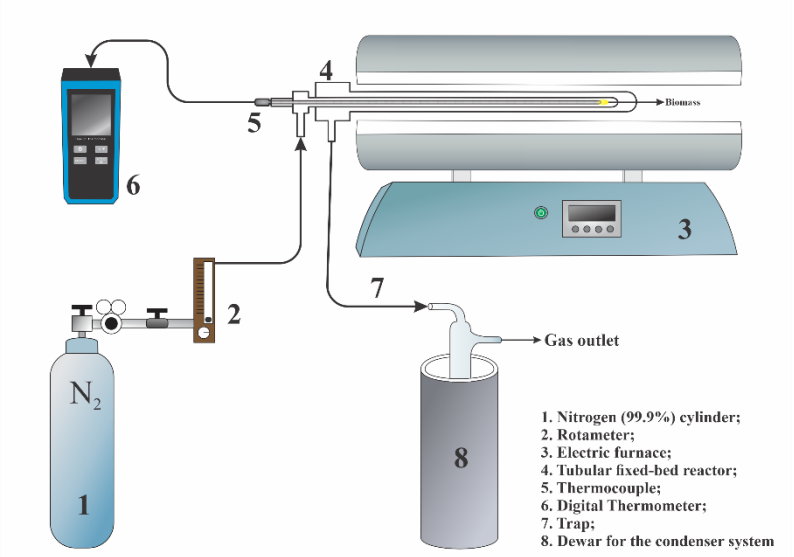

Source: From author.

The experiments were initiated by measuring the mass and dehumidifying the lignin samples at 105 °C using a moisture analyzer (MX-50, A&D Company). The mass of the samples changed between 0.5 and 0.6 g, depending on the type of lignin after dehumidification. Then, the sample was placed inside the internal tube of the reactor (indicated in Figure 11), followed by the assembly of the reactor components, and the attachment of the gas inlet and outlet pipes. Next, a purge stage was carried out, and the oven was preheated to the desired reaction temperatures (500, 600, and 700 °C) at a heating rate of 20 °C/min. The mass of the condensable trap was measured on an analytical balance (Mark, 205A), and the mass of condensed vapors produced by reaction was weighed at the end of the experiment. Then, the trap was placed inside the Dewar, followed by the addition of liquid nitrogen as a cold bath. With the oven heated, the reactor was carefully added inside the oven. The sample temperature was careful monitored by a K-type thermocouple (inserted inside the quartz reactor). The sample was held for 10s after reaching the desired temperature, and at the end of the reaction, the reactor was removed and cooled to room temperature, in an inert environment.

After the reactor cooling, the solid fraction was removed, weighed, and stored for subsequent analysis. The condensed bio-oil was removed from the trap after reaching room temperature, and its corresponding fraction was determined based on the mass collected in the trap. The bio-oil was recovered by its dissolution in dichloromethane (99.8%, CAS number 75-09-2, Sigma Aldrich, Darmstadt, Germany). The mixture was stored in amber vials at -22 °C for further composition analysis using gas chromatography coupled with mass spectrometry, GC-MS (Agilent 7890A GC System and 5975C inert MSD with Triple Axis Detector, USA). The pyrolysis runs were performed in triplicate.

The mass balance was applied to calculate the accumulated mass of gas (m_{gas}) in the pyrolysis experiments, as shown in Eq. (6).

$$m_{biomass} = m_{biochar} + m_{bio-oil} + m_{gas} \quad (6)$$

where $m_{biomass}$ is the mass of lignin on dry basis at start of reaction, while $m_{biochar}$ corresponds to the sample mass contained in the thermogravimetric analysis to minimize errors, and $m_{bio-oil}$ is the accumulated mass of condensed vapors in contact with liquid nitrogen in the trap. The yield of the i-th product (Y_i) is calculated by the following equation:

$$Y_i(wt\%) = \left(\frac{m_i}{m_{biomass}}\right) \times 100 \quad (7)$$

where m_i is the mass (g) of biochar, bio-oil, or biogas.

3.2.5 Analysis of pyrolysis product

3.2.5.1 Solid fraction

The chemical composition of biochar was characterized using FT-IR and ^{13}C-NMR, employing the same protocol used for the characterization of lignin.

3.2.5.2 Liquid fraction

The chemical composition of bio-oil was measured through a gas chromatography coupled to a mass spectrometry (GC-MS) system (Agilent 7890A GC System and a 5975C inert MSD with Triple Axis Detector, both from the USA), equipped with a capillary column HP-5MS (Agilent Technologies, USA). A volume of 1 µL was injected with the injector temperature kept at 250 °C, using a constant carrier gas flow rate of 1.00 mL/min of helium (He, 99.999%), and a 10:1 split ratio. The mass spectrophotometer (MS) was operated with an interface temperature maintained at 250 ºC, an ionizing energy of 70 eV, and in SCAN mode within the m/z range of 30-450. The oven was programmed to initiate the analysis at 30 °C for 5 min, followed by a temperature increase up to 180 °C at a rate of 2.5 °C/min, with a hold time of 1 min. Lastly, the temperature was raised to 300 °C at a heating rate of 15 °C/min, with a hold time of 5 min (DA SILVA *et al.*, 2020). The NIST05 Mass Spectral Library and the data compiled by Adams (2017) were used to identify the compounds present in the bio-oil, while the relative area was used for qualitative evaluation following the steps outlined by Bizzo et al. (2020).

3.2.6 Statistical analysis

Analysis of covariance was performed to assess the degree of functional dependence existing between different variables, including temperature, lignin type, product yields, and bio-oil composition (MIRANDA, 2016). Using the *Statistica*® software, it was possible to obtain a correlation matrix between the dependent and independent variables involved in the thermal pyrolysis process. If the absolute correlation values are close to zero (maximum of

0.25), the correlation between the analyzed data is low, indicating no significant dependence between the variables. However, a correlation index closes to zero does not only imply independence between variables. As the correlation index is a measure of linear dependence, a very low index can also indicate non-linear dependence between variables. In addition, when the correlation values are positive, it indicates a direct dependence between the variables. This means that the variables tend to fluctuate in the same direction. On the other hand, negative correlation values indicate a reverse dependence, where the variables tend to fluctuate in opposite directions (SCHAWAAB; PINTO, 2007). Besides, Principal Component Analysis (PCA), Appendix A - Principal Component Analysis (PCA) of covariance matrices was performed to evaluate whether experimental fluctuation of components contents in bio-oil is controlled by common sources of errors. PCA was performed in the software *Statistica*® with the experimental data of bio-oil product distribution in different temperatures.

Experimental errors were computed as

$$\boldsymbol{\sigma_{ij}^2 = \frac{\sum_{k=1}^{NE}\left(z_{ij}^k - \bar{z}_{ij}\right)^2}{NE-1}} \tag{8}$$

$$\boldsymbol{\xi_j^{im} = \frac{\sum_{k=1}^{NE}\left(z_{ij}^k - \bar{z}_{ij}\right)\left(z_{mj}^k - \bar{z}_{mj}\right)}{NE-1}} \tag{9}$$

$$\boldsymbol{\rho_j^{im} = \frac{\xi_j^{im}}{\sigma_{ij}\sigma_{mj}}} \tag{10}$$

Where σ_{ij}^2 is the variance of variable i at reaction condition j, ξ_j^{im} the covariance between variable i and m at reaction condition j, and ρ_j^{im} is the correlation coefficient between variables i and m at reaction condition j. z_{ij}^k is the kth evaluation of variable i at condition j and $\bar{z}_{ij}$ is the average of the measurements of variable i at condition j (LARENTIS *et al.*, 2003).

3.3 RESULTS AND DISCUSSION

3.3.1 Characterization

The observed differences in the physicochemical properties and elemental compositions of the two Kraft Lignin samples, as presented in Table 2, indicated variations in their chemical compositions. These variations can be attributed to the source of the lignin and its inherent chemical structure. Compared to lignin B (Pine sample), lignin A (Eucalyptus sample) has a higher quantity of methoxyl groups, as indicated by its higher carbon (C), hydrogen (H), sulfur (S), and oxygen (O) contents, along with a smaller nitrogen (N) content. The high content of methoxyl groups can indicate a negative effect on the yield of aromatic hydrocarbons (WANG *et al.*, 2017).

Table 2: Lignin physicochemical characterization.

Sample	**Ultimate Analysis (wt %)**						**Proximate Analysis (wt %)**			
	C [b]	H [b]	N [b]	S [b]	O [b, c]	Ash [b]	M [b]	V [b]	FC [b]	Ash [b]
Lignin A	56.4	5.91	0.18	3.3	32.87	1.34	2.29	66.80	29.10	1.81
Lignin B	49.36	4.82	0.23	0.67	24.69	20.23	3.78	63.91	21.90	10.40
Sample	**Calorific Value ($MJ.kg^{-1}$)**						**Molar ratio**		**Methoxyl groups**	
	HHV				LHV		H/C_{eff}		OCH_3 (wt %)	
Lignin A	23.56				22.27		0.38		16.81	
Lignin B	20.00				18.95		0.42		9.55	

[a] – As received basis; [b] – Dry basis; [c] – Calculated by difference. Source: From author.

The higher S content (as seen in Lignin A) also indicates a negative effect on the yield of aromatic compounds. During the lignin conversion, compounds containing sulfur, such as thiophenes and sulfides, can be produced. Typically, these compounds could increase the amount of CO_2 formed at high pyrolytic temperatures (>200 °C), and inhibit the depolymerization reactions (LU; GU, 2022). However, lignin B has a higher H/C_{eff} ratio, indicating an easier sample conversion into hydrocarbons (LEE; CHA; PARK, 2018; ZHANG *et al.*, 2012). The lower OCH_3 content in lignin B also indicates a liquid fraction with less acidity and a solid fraction with higher stability. Particularly, methoxy groups can be converted into acidic compounds, such as methanol and acetic acid, through hydrolyze reactions under certain conditions (KABIR; HAMEED, 2017; LU; GU, 2022). Lignin samples also presented similar values of HHV and LLV in comparison to other biomasses,

illustrating their potential as fuel in combustion processes (LI *et al.*, 2012; SANTANA JÚNIOR, 2018; ZHANG *et al.*, 2012).

The samples have a similar amount of moisture, volatile, and fixed carbon. However, the ash content in lignin B (10.40 w/w %) is higher than lignin A (1.81 w/w %), indicating the presence of inorganic elements that can influence both thermal decomposition and product formation (SANTANA JUNIOR; MENEZES; ATAÍDE, 2019). In particular, inorganic elements can perform as catalysts in thermal decomposition, promoting or inhibiting specific reactions (COLLARD; BLIN, 2014; SANTANA JUNIOR; MENEZES; ATAÍDE, 2019). The physicochemical characterization shows that the results are similar to the findings of Li *et al.*, (2012); Ohra-aho and Linnekoski, (2015); Santana Junior, Menezes, and Ataíde, (2019), and Zhang *et al.*, (2012).

The FT-IR spectra of the lignin samples are presented in Figure 12. Both samples exhibited strong absorbance peaks at 3450 cm^{-1} and 3410 cm^{-1} (1), assigned to -OH stretching vibrations caused by the presence of alcoholic and phenolic hydroxyl groups involved in hydrogen bonds. Peaks at 2939 and 2841cm^{-1} (2) are assigned to the C-H vibration of alkyls inside chains. Only lignin A presented a C=O stretching of carbonyl and carboxyl (ester) groups absorptive in 1703 cm^{-1} (3). Particularly, that functional group can explain the formation of ketones, aldehydes, and ester compounds along lignin thermal decomposition.

Figure 12: FTIR spectra of the Kraft lignin samples.

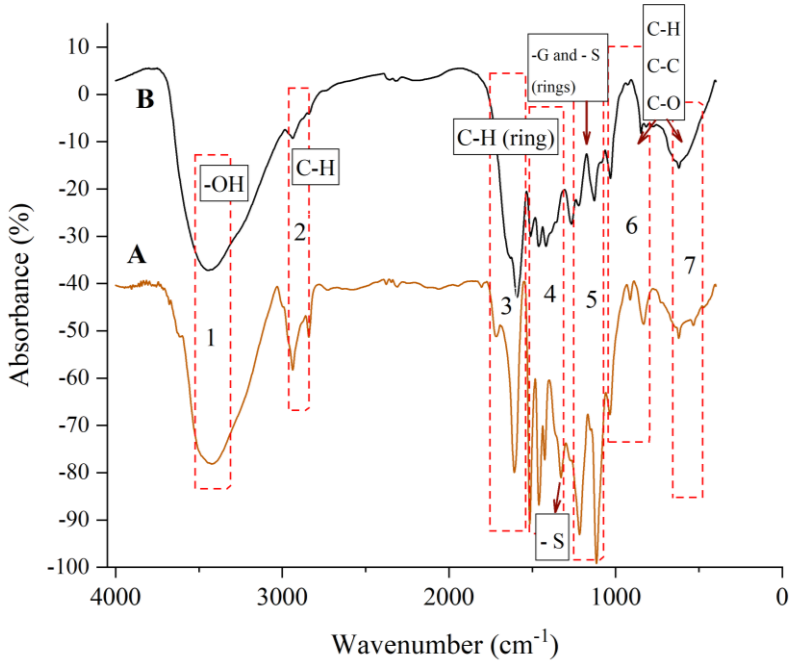

Source: From author.

The peaks between 1605 – 1595 cm^{-1} (3) and 1516, 1510, 1460, 1425, and 1416 cm^{-1} (4) are related to vibrations of aromatic rings, as expected in lignin samples. Lignin A has a characteristic hardwood vibration of syringyl rings and stretching vibrations of C-O bonds at 1330 cm^{-1} (4), and a guaiacyl ring vibration at 1217 cm^{-1} (5), while lignin B has a characteristic softwood vibration of guaiacyl rings and stretching vibrations of C-O bonds at 1263 and 1220 cm^{-1} (5) with a syringyl rings vibration at 1125 cm^{-1} (5) (BORELLA *et al.*, 2022b; MA *et al.*, 2019; MINU; JIBY; KISHORE, 2012).

The strong peak at 1032 cm^{-1} (6) corresponds to the aromatic C-H out of plain deformation (G > S units), while the many peaks in the range of 1300 – 1000 cm^{-1} (5 – 6) are due to C-C and C-O stretching coupled in different structure units. The region below 1000 cm^{-1} (6 – 7) corresponds to C-H and -OH bonds associated with aromatic rings, while the peak at 620 cm^{-1} (7) indicated a presence of sulfonic groups (S-C) that remained in lignin samples after the Kraft pulping process. The assignment of the peaks is consistent with those reported from Kraft lignin in previous report work (BORELLA *et al.*, 2022b; LAZARIDIS *et al.*, 2018b; MINU; JIBY; KISHORE, 2012; YANG *et al.*, 2016; ZHANG *et al.*, 2012).

Figure 13 presents the main peaks of the lignin ^{13}C NMR spectrum. According to the literature, the carbon structure could be divided into carbonyl (220 – 185 ppm), carboxylic (200 – 185 ppm), aryl (185 – 95 ppm), O – alkyl (90 – 45 ppm), and alkyl (45 – 0 ppm) groups (HILL; GRIGSBY; HALL, 2013; MA *et al.*, 2019). This analytical technique revealed a large amount of lignin structures including aryl ether, condensed and uncondensed aromatic and aliphatic carbons.

The aromatic region (aryl) occurred between 153 – 104 ppm, being the mains signals from guaiacyl (G), syringyl (S), and *p*-hydroxyphenyl (H) units. In lignin A, the signal (1) at 147.4 ppm is assigned to the C-5 position of the β-O-4 linkage in the S (syringyl) structural unit. In lignin B, the signal (1) at 148 ppm is assigned to C-3, and C-4 positions in G (guaiacyl) structural unit. The signal (2) and (3) at 133.5 ppm and 116.4 ppm are assigned to C-1 in S and C-5 in G, respectively, while the strong signal (4) at 106 ppm was assigned to a C-5 and C-6 in G, and a C-2 and C-6 in S. The signals in the region 90 – 60 ppm represented the aliphatic C-O bonds (O – alkyl). In both samples, the signal (5) at 73 ppm can be assigned to Cα and Cβ carbons in the β-O-4' linkage of the lignin structure.

Figure 13: Quantitative ^{13}C NMR spectra for Kraft lignin samples

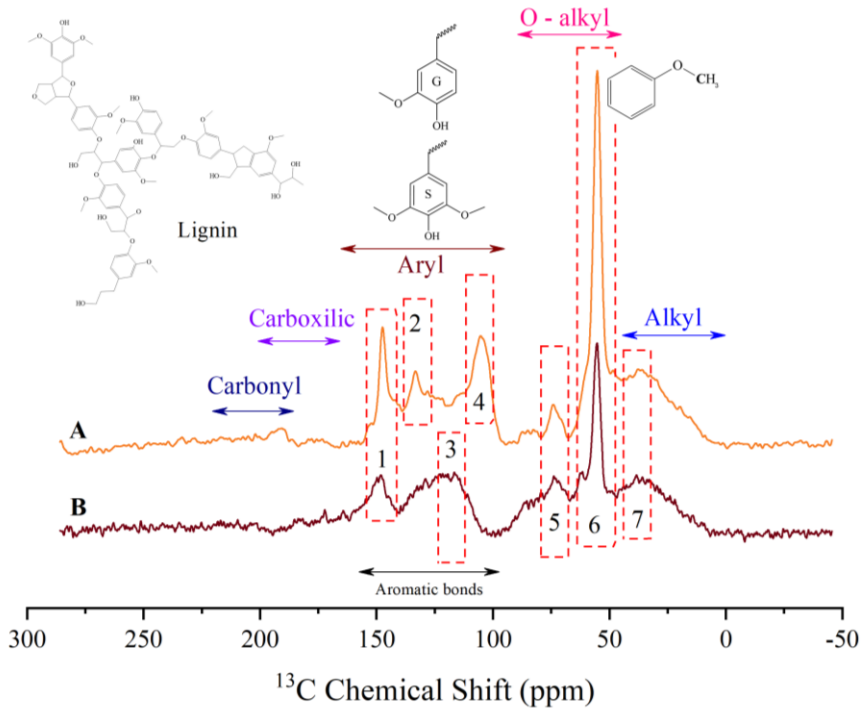

Source: From author.

The signal (6), also in the O – alkyl region, was assigned to a strong peak at 55 ppm belonging to methoxy groups of aromatic units. In particular, this signal was higher in lignin A, and the difference in lignin source can explain it. Usually, lignin derived from hardwood (such as eucalyptus) exhibits higher -OCH_3 content compared to softwoods (such as pinus). The last signal (7) at 38 ppm in the alkyl region represents the aliphatic side chain (C-C bond). None of the samples showed a significant signal from the carbonyl and carboxylic regions. NMR results revealed that both lignin samples have similar structures; however, lignin A exhibited a higher presence of S-units and -COH_3, as evidenced by more intense peaks in the aryl and O-alkyl regions. Conversely, lignin B showed a higher presence of G-units in the same regions (BARDET *et al.*, 2009; BEN; RAGAUSKAS, 2011; HILL; GRIGSBY; HALL, 2013; MELKIOR *et al.*, 2012; NARON *et al.*, 2017; NIMZ *et al.*, 1981; YANG *et al.*, 2016).

3.3.2 Evaluation of thermal decomposition

The thermogravimetry (TGA) and derivative thermogravimetry (DTG) profiles of pyrolysis experiments at different heating rates (5, 10, 15, and 20 °C/min) for both lignin samples are presented in Figure 14. For both lignin samples, the peaks of the DTG curves shifted to higher temperatures as the heating rate increased. This behavior can be attributed to the thermal lag that occurs between the sample temperatures and the controlled environment in TG. The DTG curve's also show a decrease in the peak intensity as the heating rate increases. As the lower heating rate is associated with a longer thermal degradation time, one can see higher mass loss within the same temperature range. The increase in heating rate resulted in a displacement of the TG and DTG curves positions, resulting in a shift towards higher temperatures and a decrease in the amplitude of DTG peaks at the beginning of decomposition (SANTANA; CARVALHO; ATAÍDE, 2018).

Figure 14: TG and DTG curves for lignin samples: (A) Lignin A and (B) Lignin B.

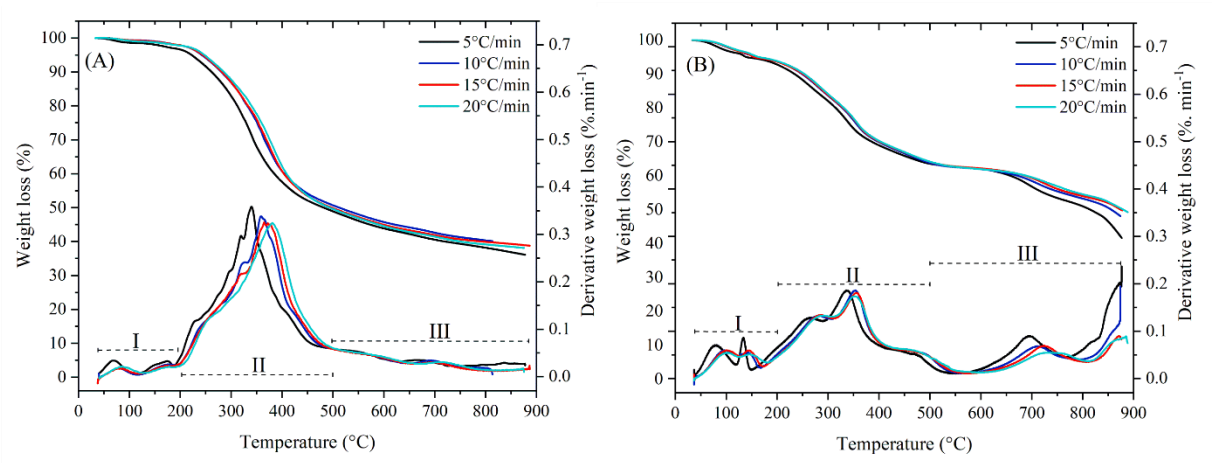

Source: From author.

The lignin thermal pyrolysis can be divided into three stages: the initial one associated with water evaporation (< 200 °C), the primary decomposition (at 200 – 500 °C), and the charring or carbonization stage (> 500 °C). The first phase (I) occurs at temperatures below 200 °C and represents part of the initial stage of the process. Peaks observed before 160 °C correspond to dehydration reactions (through external and internal water removal), resulting in a slight mass decrease. The main peaks observed in the temperature range of 200 – 450 °C occur in the second phase (II), which represents both the continuation of the initial stage and the beginning of the primary decomposition stage with the release of volatile compounds. CO_2 can be released in the temperature ranges of 160 – 270 °C, 270 – 330 °C,

and 330 – 400 °C due to the cleavage and oxidation of ether bonds, carboxylic acid groups, and carbonyl groups. CO starts to be released in the temperature range of 170 – 330 °C and 330 – 400 °C due to the cleavage of ether bonds and C-O side chains, and CH_4 is released in the temperature range of 330 – 400 °C, because of methoxy cleavage. The cleavage of ether bonds and C-O side chains can lead to the generation of smaller lignin fragments, which can undergo repolymerization reactions to form larger or different compounds, as well as promote the formation of char residues (LU; GU. 2022).

In the primary stage (400 – 600 °C), volatile reactions of depolymerization, dehydration, demethoxylation, and fragmentation of the lignin side chain and carbohydrates started to occur. As the temperature increases, the production of phenolic monomers is significantly enhanced due to the increase in lignin conversion. The third phase (III) represents the final part of the primary stage (500 – 600 °C) and the charring stage (600 – 900 °C). During this stage, one can see the following steps: (i) rearrangement of benzene rings in a polycyclic structure, (ii) secondary cracking of volatile aromatic rings, (iii) rearrangement of lignin side chains, (iv) removal of functional groups in char, and (v) carbonization of the char in response to increasing temperature. Moreover, in this stage, pyrolysis releases a significant amount of CO between 500 – 800 °C due to the conversion of remaining oxygenated groups present in the residue (COLLARD; BLIN, 2014; LU; GU, 2022).

As can be seen in Table 3, an increase in the heating rate resulted in a slight decrease in the weight loss for both samples. The first heating rate (5 °C/min) exhibited higher weight loss in both the initial and final stages when compared to the other heating rates. Specifically, it can be observed that as the heating rate increased, the production of biochar decreased. Between 10 and 20 °C/min, the weight loss remained constant, indicating that the heating rate influenced the DTG curve. These results suggest that as the heating rate increases, the reactions occur at higher temperatures. Such temperature changes can influence the yield and composition of the pyrolysis products. This behavior can be seen, for example, in lignin A where the main peaks occurred at the second phase and were shifted towards higher temperatures, causing a slight increase in the weight loss. Despite the similar behavior in the second phase, lignin B had the most relevant displacement in phases I and III.

DTG curves of lignin samples indicate the occurrence of high peaks between 300-400°C. At this temperature range, a majority of the C-C bonds within and between the alkyl chains become unstable and react. These reactions release phenolic compounds such as p-creosol, guaiacol, and syringol, which contain methyl groups. Moreover, there is a rupture in

the linkages between the aromatic rings, which is responsible for the highest rate of lignin decomposition (360 – 400 °C) and the maximum phenol production. Compared to lignin B, lignin A exhibits fewer peaks in the first phase, indicating a lower occurrence of dehydration reactions. In addition, lignin A has higher peaks in the second phase, suggesting a high repolymerization reaction rate. However, the DTG curves of lignin B exhibit peaks in the third phase, indicating the release of volatile compounds through rearrangement reactions, such as CO and CO_2 (COLLARD; BLIN, 2014).

Table 3: Weight loss (%) in each phase.

Heating Rate (°C/min)	Lignin A			Lignin B		
	Phases					
	I	II	III	I	II	III
5	3.40	47.69	12.79	7.21	29.25	21.89
10	2.31	48.43	10.10	6.30	29.92	15.69
15	2.15	48.02	11.06	6.39	29.46	14.37
20	2.22	48.19	11.50	6.19	29.66	14.17

Source: From author.

Figure 15 shows a comparison between lignin samples at a heating rate of 20 °C/min. At phase one, lignin B (A: 2.22%; B: 6.19%) displayed a higher mass loss, resulting in a prominent peak. This peak is associated with dehydration and depolymerization reactions that generate G-type phenols. In contrast, lignin A lost more mass at phase II (A: 48.19%; B: 29.66%) possibly through depolymerization and repolymerization reactions of methoxyl groups. Moreover, hardwood lignin contains a higher proportion of ether bonds due to the presence of S-units, resulting in lower biochar production rates. However, lignin B has a higher condensation degree due to the G-unit and high carbon-carbon linkages, resulting in higher biochar yield. Therefore, lignin B is more susceptible to the second cracking of aromatic rings and rearrangement reactions in the third phase (A: 11.50%; B: 14.17%). Second cracking explains the higher weight loss compared to lignin A (CHIO; SAIN; QIN, 2019; LU; GU, 2022; YANG *et al.*, 2018).

Figure 15: TG and DTG curves of lignin samples at 20 °C/min

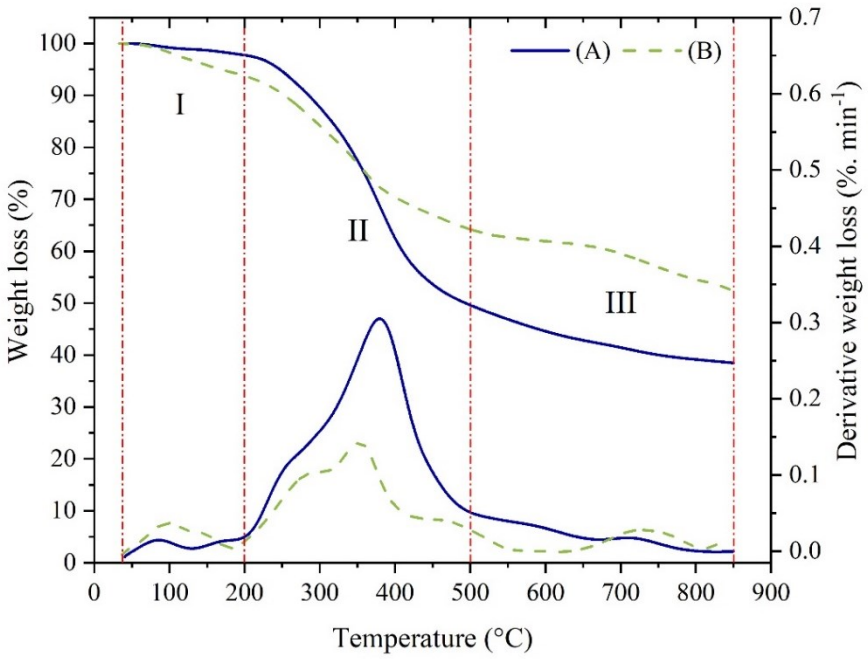

Source: From author.

The deconvolution of DTG curves presented nine peaks during the temperature rise (Figure 16). The first two peaks in both lignins represented the initial stage (< 200 °C), where the weak bonds at the functional groups are cleaved with the melting of lignin to form liquid intermediates. Peak one (A: 86 °C; B: 98 °C) can represent the water evaporation while the second peak (A: 171 °C; B: 143 °C) indicates the start of the ether linkages breakdown caused by the depolymerization reaction that forms the condensed lignin phase with a larger molecular weight (CHEN *et al.*, 2019; CHIO; SAIN; QIN, 2019; LU; GU, 2022). Peaks 3 and 4 between 200–350 °C represent the intermediate depolymerized into monolignols that can be converted to methoxyphenol through the cleavage of C-O and C-C bonds. Peak 3 (A: 247 °C; B: 217 °C) represents the breaking of the most common linkage in lignin (β-O-4) and the reorganization of the chemical groups formed by breaking of the ether bonds, leading to the formation of oxygenated compounds such as CO, CO_2, and H_2O. Peak 4 (A: 313 °C; B: 292 °C) indicates a possible break of the bond between monomer units that provoke the release of phenolic compounds with a structure close to one of the monomer units (e.g. 4-vinylguaiacol) (CHEN *et al.*, 2019).

Figure 16: Deconvolution of DTG curves at a heating rate of 20°C/min: (A) Lignin A and (B) Lignin B

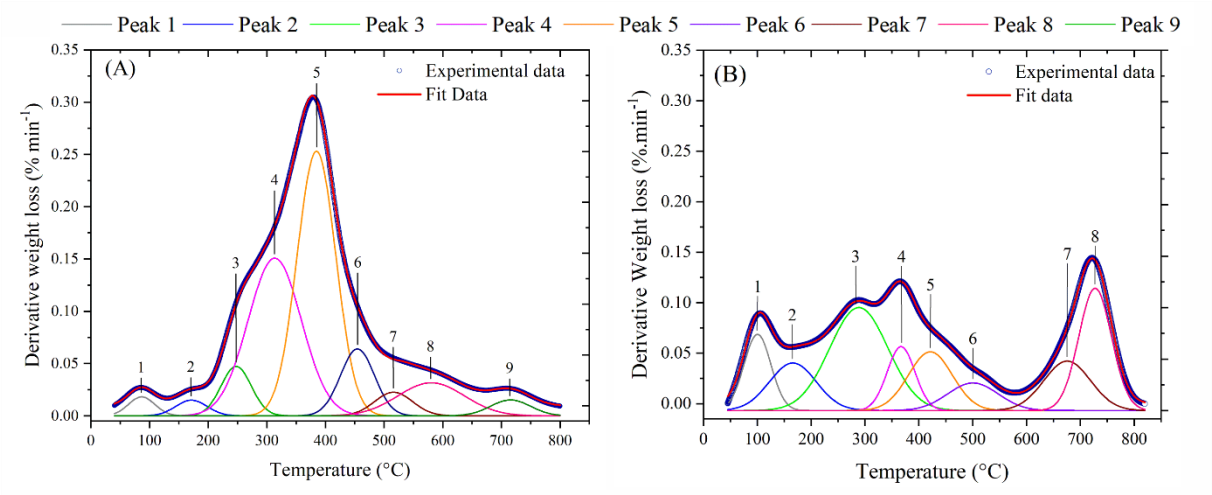

Source: From author.

In lignin A, when the temperature reaches 385 °C at peak 5, the methoxy groups in the ortho position of the hydroxyl group become reactive, and different types of fragmentation reactions result in the substitution of the methoxy group. However, these reactions tend to occur at a lower temperature in lignin B (357 °C), indicating that the bonds in lignin B were easier to cleave compared to lignin A. This can be attributed to the lower presence of ether bonds in lignin B compared to lignin A (COLLARD; BLIN, 2014; WANG *et al.*, 2017).

At peak 6 (A: 455 °C; B: 418 °C), most of the initial bonds between monomer units have broken and severe gasification reactions started. At this stage, the substituent methoxyl groups were cleaved and hydroxyl or methylated groups bonded to the aromatic units, i.e., the major products formed in this stage like syringol can be converted into o-vanillin, guaiacol, and o-quinonemethide, meaning that the maximum yield of phenolic products can be achieved (CHIO; SAIN; QIN, 2019).

The second pyrolysis starts from peaks 7 and 8 in lignin A (516 °C; 579 °C) and at peak 7 in lignin B (488 °C). These peaks can be designated as reactions of demethylation, demethoxylation, and dehydrogenation that convert G-type compounds into catechol-type ones, alkyl-phenols, and aromatics. The presence of peaks 7 and 8 in lignin A can indicate the degradation of S-type units to G-type units, resulting in the formation of other compounds such as methyphenol. Additionally, these peaks can also represent the breakdown of benzene rings and their conversion into non-condensable gases (CHIO; SAIN; QIN, 2019). These peaks can also mean the start of the coke formation by the depolymerization process of the methyl groups. Peak 8 (728 °C) and Peak 9 (715 °C) in lignin B and lignin A, respectively,

represent the coke formation, meaning that these peaks can be related to reconstruction, condensation, and polycondensation of the aromatic-ring structures (LU; GU, 2022).

3.3.3 Pyrolysis runs

3.3.3.1 Effect of reaction temperature on product yield

The yield results at each temperature for the samples of Kraft lignin are depicted in Figure 17. The correlation matrix between the output variables (bio-oil, biochar, and biogas yields) and the input variables (type of lignin and temperature) involved in the thermal pyrolysis process was calculated using the Statistica® software. Correlation matrix is presented in the Table 4.

Figure 17: Lignin Products yield (wt.%)

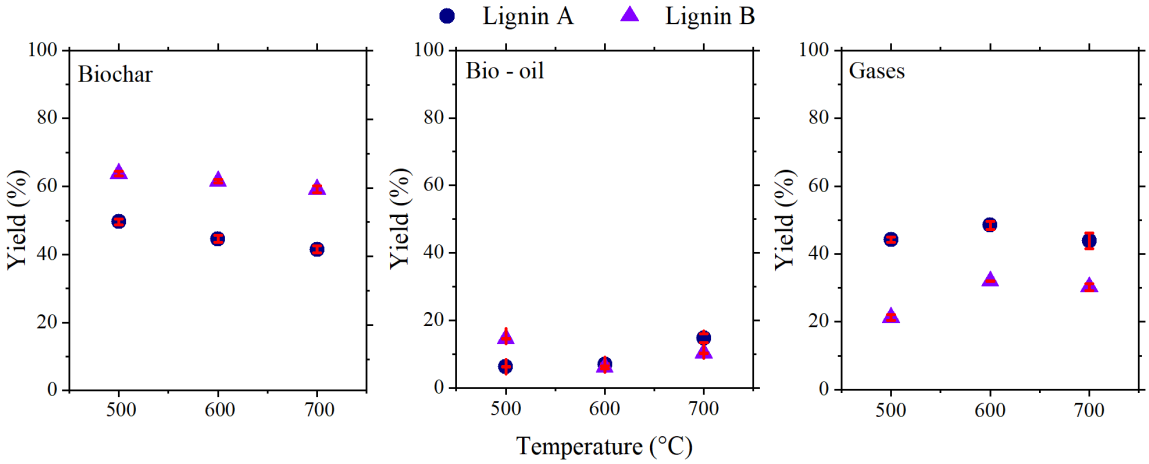

Source: From author.

Table 4: Correlation matrix between the variable involved in the thermal pyrolysis process.

Variables	Temperature	Type of lignin	Bio-oil	Biochar	Gases
Temperature	1.00	0.00	0.30	-0.28	0.14
Type of lignin	0.00	1.00	-0.07	-0.95	0.92
Bio-oil	0.30	-0.07	1.00	-0.06	-0.37
Biochar	-0.28	-0.95	-0.06	1.00	-0.91
Gases	0.14	0.92	-0.37	-0.91	1.00

Source: From author.

Based on the results presented in the correlation matrix (Table 4) and Figure 17, dependence between temperature and the yields of biochar, bio-oil, and gases was weak or

presented non-linear behavior, as indicated by low correlation coefficients (maximum of 0.30). In lignin A, the effect of temperature had little influence on the yield of biochar, as the solid content decreased slightly between 500 and 700 °C (in accordance with the negative correlation coefficient). However, gas yield increased by 4.2 wt.% between 500 and 600 °C, and then decreased again at 700°C. Therefore, the low correlation coefficient (0.14) between gas yield and temperature can also indicate a non-linear dependence between these variables.

At temperatures between 500 and 600 °C, the initial increase in gas yield can be attributed to the thermal degradation and decomposition of lignin into volatile components such as gases. However, secondary cracking reactions (such as recombination, condensation, or polymerization) take place at 700 °C, which can lead to the formation of biochar. These reactions can consume volatile gases, resulting in a decrease in gas yield (COLLARD; BLIN, 2014). Particularly, a high correlation coefficient (-0.91) was computed between biochar and bio-gas yields, corroborating the inverse dependence due secondary reactions.

Regarding the bio-oil, its yield increased by 8.5 wt% with temperature, reaching its highest value at 700 °C (in accordance with the positive correlation coefficient). Particularly, hardwood lignin contains fewer carbon-carbon linkages (5-5, β-1, and β-5) and more ether bonds (β-O-4), while the S-unit is substituted by methoxyl groups. When these bonds break, phenolic compounds are released, which require higher temperatures for degradation (COLLARD; BLIN, 2014; WANG *et al.*, 2017).

In the case of lignin B, the bio-oil yield was the highest at 500 °C and the lowest at the intermediate temperature, followed by a new increase at 700 °C. Particularly, this behavior can be attributed to the lower presence of ether bonds, specifically the β-O-4, α-O-4, and γ-O-4 linkages, which were thermally cleaved at temperatures ranging from 200 to 250 °C, leading to the formation of phenolic products (WANG *et al.*, 2017). At 600 °C, side reactions can consume the precursors for bio-oil or favor the formation of other byproducts, thereby reducing the bio-oil yield. These reactions could involve secondary reactions, cross-linking, or polymerization reactions, which shift the degradation pathways away from bio-oil formation towards biochar and bio-gas formation. However, at 700 °C, the production of bio-oil can increase again as the higher temperature promotes the breakdown of larger molecular fragments and facilitates the release of additional volatile compounds (BEN; RAGAUSKAS, 2011; COLLARD; BLIN, 2014). Therefore, the low correlation coefficient between bio-oil yield and temperature suggests a non-linear dependence between these variables.

Meanwhile, the temperature also influenced the yield of biochar and gases, even though the decrease in biochar is less than 5 wt% and the gases increase by 10.6 wt% only between the first few temperatures, remaining stable at 700 °C. The higher formation of coke happens because the second pyrolysis increases the depolymerization of methyl and methoxy groups (CHIO; SAIN; QIN, 2019).

Figure 17 shows a comparison between the yields of both lignins. It can be observed that lignin B had a higher biochar yield (14-18 wt%), whereas lignin A exhibited a higher gas yield (13-22 wt%), which is attributed to the differences in lignin types. From the analysis of the correlation matrix, biochar yield showed high correlation with the type of lignin. Particularly, biochar yield was higher in lignin B (softwood) than in lignin A (hardwood). Unlike ester bonds, carbon-carbon bonds such as β-1 and β-5 have low reactivity, and the cleavage of these bonds, combining carbon atoms in different aromatic rings from carbon-carbon bonds (such as 5-5), is challenging. As discussed, softwood lignin has a higher density of β-5 and 5-5 bonds compared to hardwood lignin, due to the predominant presence of guaiacyl repeat structures. Therefore, the higher degree of aromatic ring condensation in softwood lignin B contributes to a higher biochar yield compared to hardwood lignin A. The higher density of these bonds also explains the greater thermal stability of softwood lignin compared to hardwood lignin (which has a higher density of β-O-4 ester bonds and a lower density of 5-5 C-C bonds), as can be seen in the results of thermogravimetric analysis (Figure 15). Additionally, methoxyl groups can decompose into radicals that stabilize the larger molecule fragments produced during lignin pyrolysis and prevent their polymerization into biochar. Therefore, the higher content of methoxyl groups in hardwood lignin (A) inhibits the formation of biochar (WANG *et al.*, 2017).

Bio-oil yield was also influenced by the decomposition of -OCH_3 groups, as the conversion of type-S phenols to type-G phenol, monophenol, or catechol can enhance oil production at higher temperatures. As lignin A had higher amounts of –OCH3 groups, the bio-oil yield was higher at 700 °C, while for lignin B, it was higher at 500 °C. In particular, the conversion of methoxy groups is complete at 500 °C, whereas higher temperatures (such as 700 °C) are required for the degradation of stable phenolic moieties (COLLARD; BLIN, 2014; WANG *et al.*, 2017). Lastly, the role of –OCH3 groups also explain the higher yields of biogas in lignin A, corroborating the high correlation coefficient between the bio-gas yield and type of lignin.

3.3.4 Products analysis

In lignin pyrolysis, the pathways for guaiacol formation have been reported in literature, were the compounds undergoes scission of the methoxyl groups at the aromatic ring to produce pyrocathecol, cresol, methypyrocathecol, phenol, methylguaiacol, aromatics and other compounds (LI *et al.*, 2020a; LIU *et al.*, 2018; LU; GU, 2022; MUN; KU; PARK, 2007; SUPRIYANTO *et al.*, 2020). Syringol has also been reported as an intermediate or product of lignin pyrolysis. Therefore, for a better understanding of the formation of products, Figure 18 presents the possible pathways for syringol secondary reactions.

Figure 18: Proposed pyrolysis pathways for syringol.

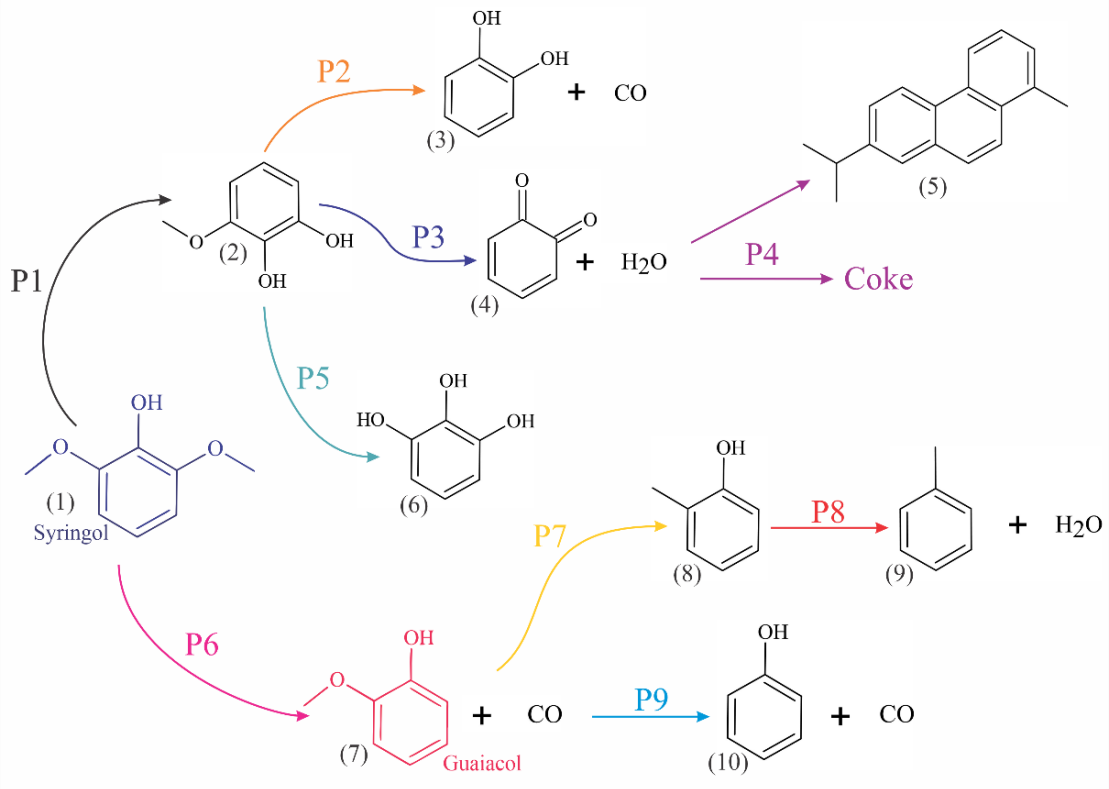

Source: From author.

In the first reaction pathway (**P1**) syringol (1) generate a radical that was converted to a 3-methoxycatechol (2) by hydrogenation reaction that can follow three different pathways such as **P2** where it can undergo dehydration, isomerization, dehydrogenation and decarbonylation to form catechol (3) and CO. Alternatively, 3-methoxycatechol can suffer a demethylation and hydrogenation (**P5**) to form pyrogallol (6). If 3-methoxycatechol (2) reacts through dehydration, isomerization, and hydrogenation (P3), o-quinonemethide (4) can be

formed. This product can be converted into coke by polymerization reaction or can generate polycyclic aromatic hydrocarbons such as retene (5) after condensation reactions **(P4)**. In reaction P6, syringol (1) undergoes O – H bond scission to form radicals that react through isomerization. Then, the radical suffers dehydrogenation to form 2-hydroxy-3-methoxybenzadehyde that reacts through decarbonylation to form guaiacol (7) and CO. Guaiacol also can be produced when a hydrogen coupled to syringol is further dehydrogenated (**P7**) to form a radical that reacts through isomerization and hydrogenation to form methylphenol (8). In addition, that can form toluene (9) can be formed by dehydration of methylphenol (**P8**). Lastly, guaiacol also can form phenol (10) through dehydrogenation followed by decarbonylation **(P9)** (HUANG *et al.*, 2013).

The vapors of pyrolysis possess a significant quantity of carboxylic and carbonyl oxygenates, including acetic acid, carboxylic acid, aldehydes, and ketone. These compounds can be converted by converting two carboxylic acid molecules into ketone, CO_2 and H_2O, a process commonly referred to as ketonization and aldol condensation (Figure 19). Ketones, such as Methyl Isobutyl Ketone, may be generated through a cross-aldol condensation involving two ketones (Acetone) and/or aldehydes (GAMMAN; JACKSON; WIGZELL, 2010; RAHMAN; LIU; CAI, 2018; WANG *et al.*, 2017)

Figure 19: Possible scheme of the chemical reactions for Methyl Isobutyl Ketone formation

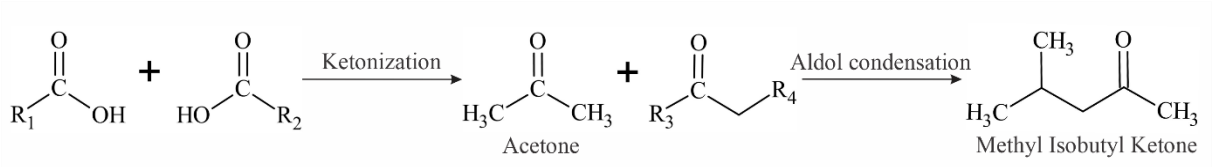

Source: From author.

3.3.4.1 Components distribution on bio-oil

Figure 20 displays the distribution area of compounds in the bio-oil GC-MS analysis, categorized as aromatic hydrocarbons, guaiacol, syringol, ketone (KET), and other oxygenated aromatics (OA). The latter class encompasses compounds that possess a guaiacol or syringol linkage to another hydrocarbon chain or any other aromatic structure with an oxygen linkage. The unidentified (UNK) components refer to the compounds present in the bio-oil that cannot be recognized or identified by the GC-MS analysis. Table 5 presents a

comprehensive list of the identified products, along with the indication of the lignin source of the bio-oil in which they are found.

Figure 20: Distribution of products in bio-oil during lignin pyrolysis runs: (A) Lignin A and (B) Lignin B.

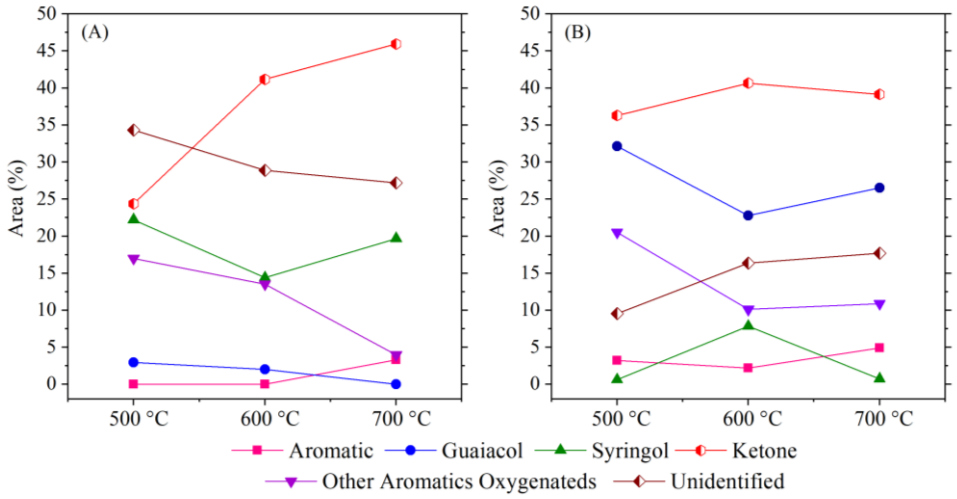

Source: From author

Table 5: Bio-oil components composition

(continues)

Components	Classification
Toluene [a, b]	Aromatic
Retene [b]	
Phenol, 2-methoxy- [a, b]	Guaiacol
Phenol, 2,6-dimethoxy- [a, b]	Syringol
Methyl isobutyl ketone [a, b]	Ketone
1,2-Benzenediol, 3-methoxy- [a]	Other aromatics oxygenated
1,2-Benzenediol, 3-methyl- [a]	
2,3-Dimethoxytoluene [b]	
2-Methoxy-4-vinylphenol [a, b]	
2-Methoxy-5-methylphenol [b]	
3,4-Diethylphenol [b]	
3,4-Dimethoxytoluene [b]	
3-Methoxyacetophenone [b]	
5-tert-Butylpyrogallol [a]	
Apocynin [a]	

Table 5: Bio-oil components composition

(conclusion)

Components	Classification
Benzaldehyde, 4-hydroxy-3,5-dimethoxy- [a]	Other aromatics oxygenated
Benzene, 1,2-dimethoxy- [b]	
Benzene, 4-ethyl-1,2-dimethoxy- [b]	
Creosol [a, b]	
Ethanone, 1-(4-hydroxy-3,5-dimethoxyphenyl) - [a]	
Homovanillic acid [b]	
Mequinol [b]	
p-cresol [b]	
Phenol, 2,3,5,6-tetramethyl- [b]	
Phenol, 2,3,5-trimethyl-[b]	
Phenol, 2,3,6-trimethyl- [b]	
Phenol, 2,3-dimethyl- [b]	
Phenol, 2,4,6-trimethyl- [b]	
Phenol, 2,4-dimethyl [b]	
Phenol, 2,6-dimethoxy-4-(2-propenyl) - [a]	
Phenol, 2-ethyl-6-methyl- [b]	
Phenol, 2-methoxy-3-methyl- [a, b]	
Phenol, 2-methyl- [b]	
Phenol, 3,4-dimethoxy-[a]	
Phenol, 3,5-dimethyl [b]	
Phenol, 3-ethyl- [b]	
Phenol, 4-ethyl-2-methoxy- [a, b]	

*a – lignin A: Eucalyptus *spp*; b – lignin B: Pine Tree. Source: From author.

At 500 °C, lignin A does not form aromatics, meaning that at this temperature; most of the reactions involved the first pyrolysis. Between 350–500 °C, multiple reactions such as dealkylation and demethoxylation converted the methoxyphenols directly into monomers, such as guaiacol, syringol, and alkylphenols (CHEN *et al.*, 2019; WANG *et al.*, 2017). At this temperature, the formation of guaiacol and oxygenated aromatics (OA) may involve syringol as an intermediate compound. Additionally, ketone formation can occur through the degradation of various compounds present. These processes suggest that the thermal reactions taking place at 500 °C involve the transformation and breakdown of different components, resulting in the formation of guaiacol, OA, and ketones. At 600 °C, the pyrolysis enters the second stage; however, the formation of aromatics continues to be absent, which may be

attributed to the higher amount of ether bonds present in this type of lignin. As the concentration of ether bonds increases, a higher temperature is required for the reactions to occur (WANG *et al,*, 2017). Guaiacol and oxygenated aromatics (OA) still have syringol as intermediate compound at this stage (600 °C). Additionally, ketone formation can now occur through the decomposition of guaiacol and OA. These processes suggest that, at higher temperature, the reactions involving syringol, as an intermediate, play the main role in the formation of guaiacol and OA. All possible mechanisms are summarized in Figure 21.

Figure 21: Possible mechanism pathways for each temperature in lignin A.

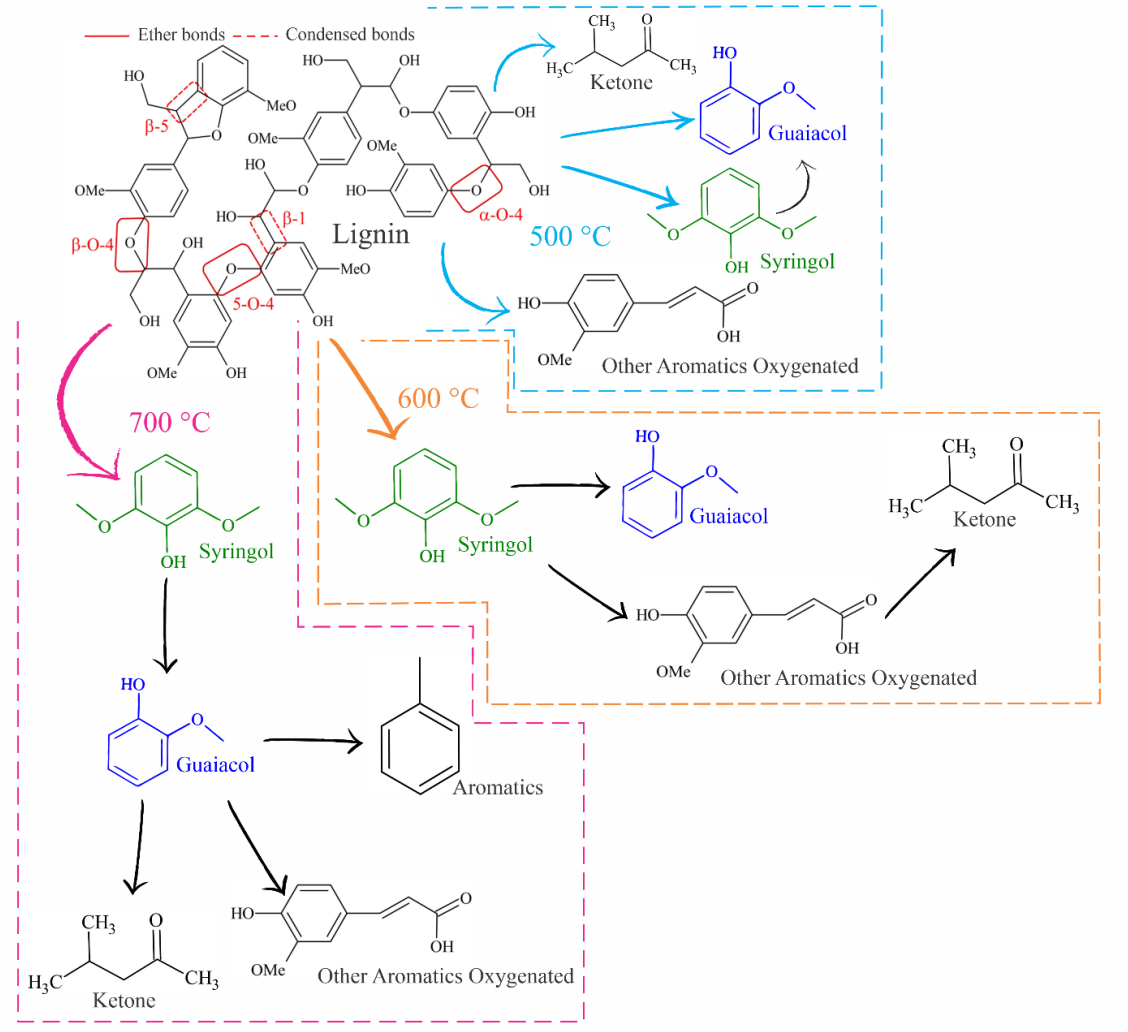

Source: From author

At 700 °C, guaiacol production ceases, and the formation of aromatic hydrocarbons starts. This suggests that guaiacol, produced by syringol as its precursor, becomes the main pathway for the formation of oxygenated aromatics (OA), ketones, and aromatic compounds. Lignin B has more condensed linkages than lignin A, having a higher condensation degree

that contributes to greater char yield and a diverse bio-oil composition (WANG *et al.*, 2017). The possible mechanisms for lignin B are summarized in Figure 22.

Figure 22: Possible mechanism pathways for each temperature in lignin B.

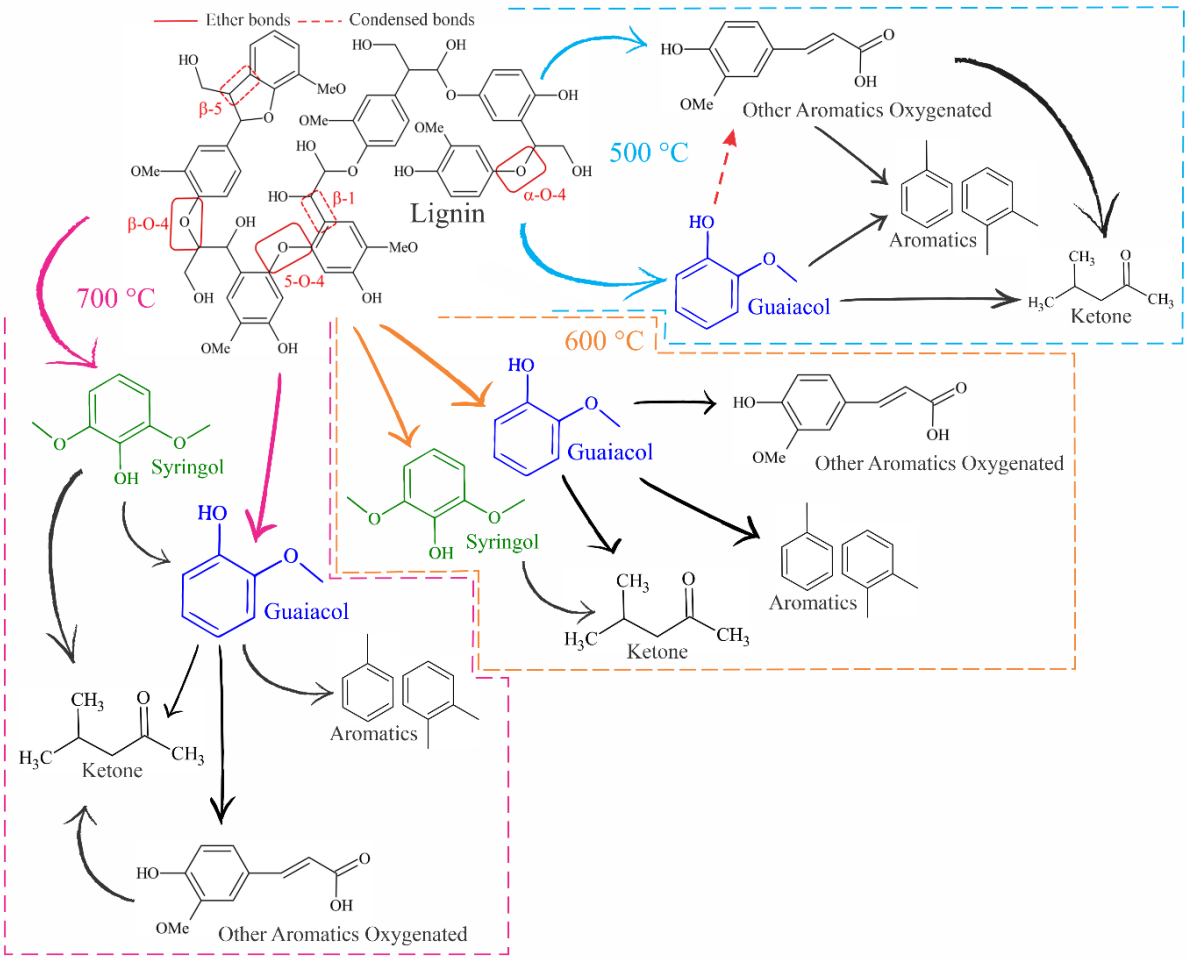

Source: From author

At 500 °C, guaiacol and oxygenated aromatics (OA) serve as the primary pathways for aromatic and ketone formation. Additionally, the OA compounds had guaiacol as precursor. At 600 °C, the conversion of oxygenated aromatics (OA) can result in the formation of aromatics. Specifically, benzene ring can undergo breakdown, releasing non-condensable gases. Additionally, the cleavage of methoxyl groups occurs, while hydroxyl or methylated groups become attached to the aromatic units (CHIO; SAIN; QIN, 2019). Ketone could be mostly produced by syringol and guaiacol degradation. At 700 °C, there is an increase in the concentration of oxygenated aromatics (OA) and guaiacol, along with the formation of aromatics. This suggests that OA and guaiacol were simultaneously produced, while syringol

was consumed. The relationship between guaiacol and syringol indicates that more than one pathway is involved for guaiacol formation at this temperature.

Correlation analysis between the all variables was used to detect possible dependence between the temperature, bio-oil components, and source of Kraft lignin. The values generated on the *Statistica* software are presented as a matrix for all variables (Table 6).

Table 6: Correlation Matrix for all variables.

Variable	Temp	TL[1]	Aromatic	Guaiacol	Syringol	OA	KET	UNK
Temp	1.00	0.00	0.34	-0.09	-0.04	-0.39	0.16	0.02
TL[1]	0.00	1.00	0.36	0.66	-0.61	0.11	0.03	-0.67
Aromatic	0.34	0.36	1.00	0.20	-0.42	-0.06	0.16	-0.51
Guaiacol	-0.09	0.66	0.20	1.00	-0.33	0.52	-0.53	-0.38
Syringol	-0.04	-0.61	-0.42	-0.33	1.00	0.19	-0.57	0.85
OA	-0.39	0.11	-0.06	0.52	0.19	1.00	-0.78	0.07
KET	0.16	0.03	0.16	-0.53	-0.57	-0.78	1.00	-0.47
UNK	0.02	-0.67	-0.51	-0.38	0.85	0.07	-0.47	1.00

[1]Type of Lignin. Source: From author

In Table 7, correlation matrix reveals moderate linear dependence between the amounts of guaiacol and syringol with the source of lignin. This finding aligns with existing literature, as the composition of lignin is directly associated with the specific tree species from which it is derived. As observed in the NMR results, lignin A exhibited a higher presence of S-units and methoxy groups, whereas lignin B demonstrated a higher presence of G-units. These findings support the higher levels of syringol observed in the thermal pyrolysis of lignin A, while lignin B released higher amounts of guaiacol. Regarding the temperature effect, low correlation coefficients were computed, indicating a non-linear dependence between the amounts of guaiacol and syringol and source of lignin. As previously discussed, guaiacol and syringol undergo multiple reactions as the temperature increases.

Likewise, the aromatics content shows correlation with both the lignin source and the temperature. The positive correlation with temperature suggests that increasing the temperature can lead to an increase in aromatic compounds production. Therefore, these results demonstrate that aromatic compounds are predominantly released during the secondary pyrolysis stage (SUPRIYANTO *et al.*, 2020).

The syringol compound presented a weak correlation with aromatics, which, for being indirect, may indicate that the aromatics are produced by the decomposition of syringol. The

presence of guaiacol compounds is also found to be associated with the degradation of syringol, as the breakdown of syringol can result in the formation of guaiacol components. Additionally, there is a direct relationship between guaiacol and oxygenated aromatics, indicating that these compounds are produced simultaneously (WANG *et al.*, 2017). Ketone exhibits a strong and moderate inverse dependence with all oxygenated compounds, suggesting that its formation depends on the degradation of these components.

The unidentified components presented a strong direct dependence on syringol, indicating that lignin degradation with a higher proportion of S-units tend to produce compounds that cannot be identified through the analysis. This behavior has been seen at Figure 20 where lignin A exhibited higher content of unknown components compared to lignin B. However, as the production of aromatics, ketones, and guaiacol increases, the presence of these unknown components tends to decrease.

Similar analyses were also performed by Kraft lignin source, as can be seen in Table 7 and Table 8. Regarding the results of Table 8, one can see that temperature played an interesting role during the pyrolysis of lignin A. In particular, the production of aromatic hydrocarbons had a direct dependence with temperature, which only occurred at the highest temperature. Simultaneously, guaiacol and OA were consumed, indicating that higher temperatures promoted demethylation and demethoxylation reactions. Ketones were also produced with the increase of temperature, due the degradation of oxygenated compounds (guaiacol, syringol and OA) by thermal cracking via dealkylation, deoxygenation and dehydration (MOHAN; PITTMAN; STEELE, 2006; SUPRIYANTO *et al.*, 2020).

Table 7: Lignin A - correlation matrix of bio-oil components.

Variable	Temp	Aromatic	Guaiacol	Syringol	OA	Ketone	UNK
Temp	1.00	0.44	-0.61	-0.08	-0.48	0.29	1.00
Aromatic	0.44	1.00	-0.29	-0.25	-0.26	0.26	0.44
Guaiacol	-0.61	-0.29	1.00	0.44	0.97	-0.79	-0.61
Syringol	-0.08	-0.25	0.44	1.00	0.61	-0.89	-0.08
OA	-0.48	-0.26	0.97	0.61	1.00	-0.90	-0.48
Ketone	0.29	0.26	-0.79	-0.89	-0.90	1.00	0.29
Unidentified	-0.33	-0.48	0.75	0.84	0.85	-0.95	-0.33

Source: From author

Table 8: Lignin B - Correlation Matrix of bio-oil components

Variable	Temp	Aromatic	Guaiacol	Syringol	OA	Ketone	UNK
Temp	1.00	0.28	-0.12	0.01	-0.31	0.04	0.43
Aromatic	0.28	1.00	-0.06	-0.32	0.05	0.06	-0.24
Guaiacol	-0.12	-0.06	1.00	0.18	0.73	-0.95	0.09
Syringol	0.01	-0.32	0.18	1.00	-0.05	-0.45	0.60
OA	-0.31	0.05	0.73	-0.05	1.00	-0.69	-0.48
Ketone	0.04	0.06	-0.95	-0.45	-0.69	1.00	-0.24
Unidentified	0.43	-0.24	0.09	0.60	-0.48	-0.24	1.00

Source: From author

Syringol presented a non-linear dependence on temperature (low correlation coefficient) due to the complex and multiple reactions involved in its formation and degradation. Syringol was favored at 500 °C, and beyond that range, its amounts decreased (as seen at 600 °C) due competing reactions, such as sequential degradation or secondary reactions leading to the formation of other compounds. Secondary pyrolysis reactions of lignin can release syringol. During secondary pyrolysis, as the temperature increases, additional decomposition and rearrangement of the lignin structure occur. This can lead to the formation of various intermediate compounds, including syringol (as seen at 700 °C). These secondary reactions can involve processes such as demethoxylation, demethylation, and further fragmentation of lignin components (LU; GU, 2022; YOGALAKSHMI *et al.*, 2022).

Guaiacol had a direct dependence on syringol and OA in the thermal decomposition of lignin due to their structural similarities and the potential reaction pathways involved. As previously discussed, syringol is an intermediate compound in the degradation process of lignin, leading to the formation of guaiacol. Conversion of syringol into guaiacol occurs through demethoxylation or demethylation reactions. In addition, the decomposition of methoxyl groups can also lead to conversion of syringol into phenols linked to a guaiacol, monophenol or catechol explaining the directed relation of the syringol in the production of guaiacol and OA (KAWAMOTO, 2017; WANG *et al.*, 2017).

In contrast to lignin A, the bio-oil derived from lignin B (as can be seen in Table 8), exhibits a more diverse composition. This is attributed to the higher presence of condensed linkages typically found in softwood. These condensed linkages contribute to an increased quantity of aromatics and ketones, which is evident even at lower temperatures. However, the temperature did not exhibit a higher correlation with the compounds, as most of the linkages are broken down before reaching 450 °C. Therefore, there is only a moderate direct dependence with aromatics and an indirect dependence with OA. This suggests that as the

temperature increases, OA compounds are consumed, potentially for the formation of aromatics and ketones through depolymerization processes. Guaiacol contents were high in this oil, and was directly related to the OA, showing these compounds can have a G-type linkage or were produces by a guaiacyl monomer (CHIO; SAIN; QIN, 2019; SUPRIYANTO *et al.*, 2020).

The formation of ketone compounds during pyrolysis exhibited an indirect relationship with the degradation of OA and guaiacol. This suggests that at 600 °C, guaiacol was consumed and likely contributed to the formation of ketones. The observed correlations implies that the degradation of guaiacol and OA during the pyrolysis process plays a role in the production of ketone compounds. Indeed, at 500 °C and 700 °C, the production of ketones can also be attributed to the degradation of syringol and OA, as indicated by the moderate inverse dependence between these compounds. In this particular type of lignin, the production of aromatics seems primarily associated with the degradation of syringol. This observation can explain why, at 500 °C and 700 °C, the bio-oil contains more aromatic compounds compared to 600 °C, as syringol is almost entirely consumed during the pyrolysis process. As syringol undergoes degradation, it contributes to the formation of various aromatic compounds. This behavior explains the non-linear dependence between syringol contents and temperature.

Previous results regarding the product distribution in bio-oil were also evaluated through Principal Component Analysis (PCA). If experimental fluctuation of bio-oil components is controlled by chromatographic measurements errors, the mechanistic interpretation of pyrolysis based on results of correlation matrix can induce to mistakes (LARENTIS *et al.*, 2003). Particularly, PCA allows evaluating whether experimental fluctuation of components contents in bio-oil is controlled by commons sources of errors. PCA was performed in software STATISTICA with the experimental data of bio-oil products distribution in different temperatures. PCA results for pyrolysis of lignin A are presented in Table 9.

Table 9: Principal directions of fluctuation and vector coefficients of factor (eigenvector) with original direction of variable fluctuation for bio-oil components of Lignin A.

	Temperature			
	500 °C		700°C	
Component	Factor 1	Factor 2	Factor 1	Factor 2
Aromatics	**-**	-	-0.50	**-0.86**
Guaiacol	**0.99**	0.001	-	-
Syringol	**0.99**	0.157	**0.99**	-0.14
Oxygenated Aromatics	**0.99**	-0.070	**0.93**	-0.35
Ketones	**-0.99**	-0.030	**-0.98**	0.19
Unidentified	**0.99**	-0.125	**0.97**	0.24
Eigenvalue	4.95	0.04	4.00	0.99
Explained Variance (%)	99.0	1.0	80.0	0.20

Numbers in bold denote eigenvector coefficients higher than 0.7. Source: From author

Results of PCA for pyrolysis of lignin A indicated that two directions concentrated more than 80% of the total experimental variance in all cases. Therefore, these results supported the hypothesis that few common sources of fluctuation disturb the experimental setup (LARENTIS *et al.*, 2003). For instance, the most important source of fluctuation (as seen in the first direction) is expected to be the unavoidable changes in reaction rates because of fluctuations in the reaction temperature, feed composition, lignin mass, or flow pattern in the reactor bed, while the second direction represents experimental noise. In addition, the most important direction of fluctuation establishes the clear role between the component of bio-oil, and these results corroborated the matrix correlation. In particular, guaiacol, syringol, oxygenated aromatics, and ketones presented high vector coefficients (or scores) to build up the first principal component, and, therefore, are significant products in bio-oil at 500°C. At 500°C, the vector coefficients of ketones and the other components have opposite signals, corroborating the role of secondary pyrolysis of syringol, guaiacol and aromatic oxygenated into ketones. At 700°C, one can see the complete conversion of guaiacol. Particularly, the vector coefficients of ketones and aromatics presented opposite signals to the other components, corroborating the role of secondary pyrolysis of syringol, guaiacol and aromatic oxygenated into ketones and aromatics. PCA results for pyrolysis of lignin B are presented in Table 10.

Table 10: Principal directions of fluctuation and vector coefficients of factors (eigenvectors) with original direction of variable fluctuation for bio-oil components of Lignin B.

	Temperature					
	500 °C		600°C		700°C	
Component	Factor 1	Factor 2	Factor 1	Factor 2	Factor 1	Factor 2
Aromatics	**-0.90**	0.44	**-0.81**	-0.58	-0.16	**-0.98**
Guaiacol	**0.99**	-0.02	**-0.99**	0.15	**0.86**	-0.50
Syringol	0.67	**0.74**	-0.33	**0.94**	**0.99**	0.16
Oxygenated Aromatics	**0.99**	0.00	**-0.97**	-0.22	-0.37	**-0.93**
Ketones	**-0.99**	-0.05	**0.83**	-0.55	**-0.72**	0.69
Unidentified	**-0.99**	0.14	0.23	**0.97**	**0.96**	0.29
Eigenvalue	5.24	0.76	3.44	2.55	3.32	2.67
Explained Variance (%)	87.3	12.7	57.4	42.6	55.4	44.6

Numbers in bold denote eigenvector coefficients higher than 0.7. Source: From author

Regarding the results of PCA for pyrolysis of lignin B, two principal components concentrated more than 80% of the total variance in all cases, indicating again the hypothesis that a few common sources of fluctuation disturb the experimental setup. At 500°C, guaiacol, aromatics, oxygenated aromatics, and ketones presented high vector coefficients (scores) in the first principal component, and, therefore, are significant products in bio-oil. At 500°C, the vector coefficients of ketones and aromatics have opposite signals to other components, corroborating the role of secondary pyrolysis of guaiacol and aromatic oxygenated into ketones and aromatics. Lignin B (softwood) is rich in guaiacyl units, and the results of the first component highlighted the role of guaiacol in the production of aromatic compounds. Syringol presented a high vector coefficient in the second eigenvector, while other components presented moderate and low vector coefficients, indicating that high temperatures are required to syringol decomposition.

At 600°C, aromatics, guaiacol, oxygenated aromatics, and ketones presented again high vector coefficients (scores) in the first eigenvector, indicating similar behavior for the thermal decomposition of lignin B in this temperature. However, only guaiacol, syringol, and ketones presented high scores in the first eigenvector at 700°C, indicating a possible change in the thermal decomposition pathway. In particular, one can see the decomposition of syringol and guaiacol mainly into ketones (high scores) at higher temperatures, while the low score was seen for aromatics and oxygenated aromatics. In the second eigenvector (44.6% of explained variance), high scores can be seen for aromatic and oxygenated aromatics,

highlighting the role of aromatic and oxygenated aromatics of secondary products in bio-oil through the decomposition of syringol.

3.3.4.2 Components distribution on biochar

The FT-IR spectra of the biochar samples are reported in Figure 23, along with the results of the lignin samples spectra. The biochar (BC) spectra from the experiments at 500 °C, 600 °C e 700 °C are similar, although the intensities of the bands changed at each temperature.

Both the lignin and biochar samples exhibited the OH stretching vibration (1) and C-H vibration of alkyl groups (2), although with lower intensity in the biochar samples. The peak remaining between 1650 – 1566 cm^{-1} (3) represents the stretching vibration of the benzene ring skeleton (C=C) from aromatic compounds, while the peaks corresponding to the G and S-units are nearly absent (4) (MA *et al.*, 2019). In the fourth region, most of the C-O bonds disappeared, and the present peak between 1300 and 1000 cm^{-1} could be attributed to a C-C bond or deformation vibrations of C-H and C-O coupled stretching in different structural units. In the last region (5), the intensity of the bonds below 1000 cm^{-1} decreases, while the remaining peaks are attributed to deformation vibrations of C-H bonds in the aromatic rings in both samples. The results suggest that carbon-rich matter was formed and that most of the oxygenated functional groups are present in the bio-oil compounds (BORELLA *et al.*, 2022a, 2022b; MINU; JIBY; KISHORE, 2012).

Figure 23: FT-IR spectra of Kraft lignin samples and their respective pyrolysis biochar: (A) Lignin A; (B) Lignin B.

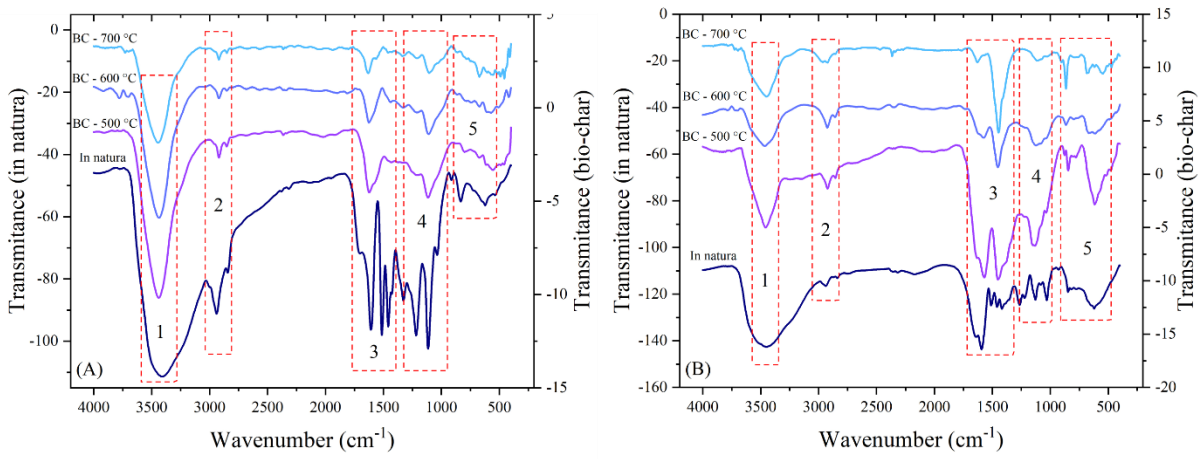

Source: From author

The solid-state (ss) NMR analysis was used to characterize in detail the chemical changes that occurred during the conversion of lignin into biochar.

Figure 24 shows the ^{13}C NMR spectra of three types of biochar from each temperature in comparison to the in natura sample. As the pyrolysis temperature increased, the oxygen-containing functional groups and aliphatic carbon structures gradually decreased, resulting in biochar predominantly composed of aromatic carbon structures. In lignin A, the carbonyl region exhibited a slight signal that could indicate the formation of ketones with the increasing temperature. However, in lignin B, this behavior occurs until 600 °C. As the aryl region increased, the biochar samples became the dominant carbon structure, as indicated by the presence of signals corresponding to aromatic C-C and aromatic C-H bonds. The reduction in O-alkyl groups could be attributed to the breakage of oxygen-containing functional groups through dihydroxylation, decarboxylation, decarbonylation, and dimethoxy reactions. Additionally, the decrease in the alkyl region suggests that aliphatic chains were converted into shorter alkyl components or polycyclic aromatic structural units (BEN; RAGAUSKAS, 2011; HILL; GRIGSBY; HALL, 2013; MA *et al.*, 2019).

Figure 24: ^{13}C NMR analysis of in natura Kraft lignin and pyrolysis biochar.
(A) Lignin A; (B) Lignin B.

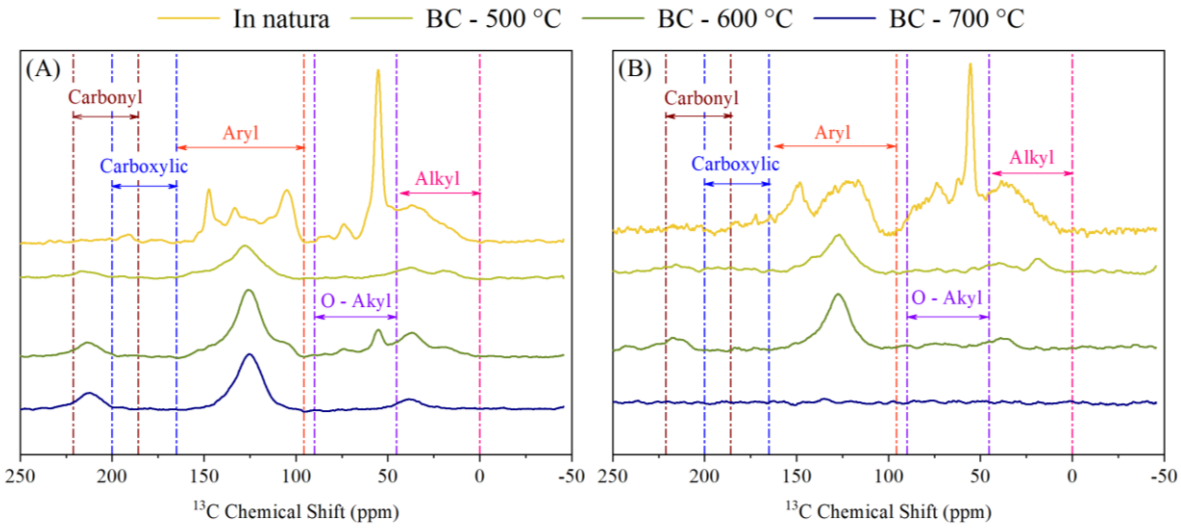

Source: From author

The absence of peaks in the biochar from lignin B at 700 °C is consistent with high-temperature pyrolytic exposure, indicating the formation of fused polyaromatic regimes, such as polyaromatic hydrocarbons (PAHs) like naphthalene. Therefore, quantitation of other functional groups did not occur by low signal-to-noise. In particular, many carbon atom in the

pyrolyzed lignin samples reside close to paramagnetic centers that cause the shielding and rapid relaxation effects that make them difficult to observe (DIEHL *et al.*, 2013).

3.4 CONCLUDING REMARKS

The results of this study indicate that the main constituents of lignin samples were guaiacyl and syringyl, and their decomposition was affected in different ways by pyrolysis. The methoxy content plays a significant role during both primary and secondary pyrolysis. The high -OCH3 content present in lignin A (hardwood) affected the biochar yield and required higher temperatures to produce aromatics in the bio-oil, because S-units exhibit high thermal stability. Therefore, lignin B (softwood) has a higher affinity to the production of aromatics than lignin A due to a higher number of condensable bonds.

The main products of thermal pyrolysis are biochar and gases at evaluated conditions, while bio-oil has a maximum yield of 15%, requiring an upgrade of operational conditions depending on the objective of pyrolysis. Higher temperatures yield bio-oil richer in aromatics in both lignins, and the formation of aromatic compounds followed the pathway of sequential conversion of syringol into guaiacol and then to aromatic compounds. Biochar content also was influenced by the increase in temperature since most oxygenated were transformed into condensable and non-condensable gases.

The present work holds potential usefulness for future studies aiming to produce specific compounds or high-added value products from Kraft lignin. The temperatures studied can be used in the optimization stage of a biorefinery.

CHAPTER 4

Chapter 4 presents the results of catalytic pyrolysis using ZSM-5 from hardwood and softwood Kraft lignin, including catalyst characterization and bio-oil composition.

Graphical Abstract

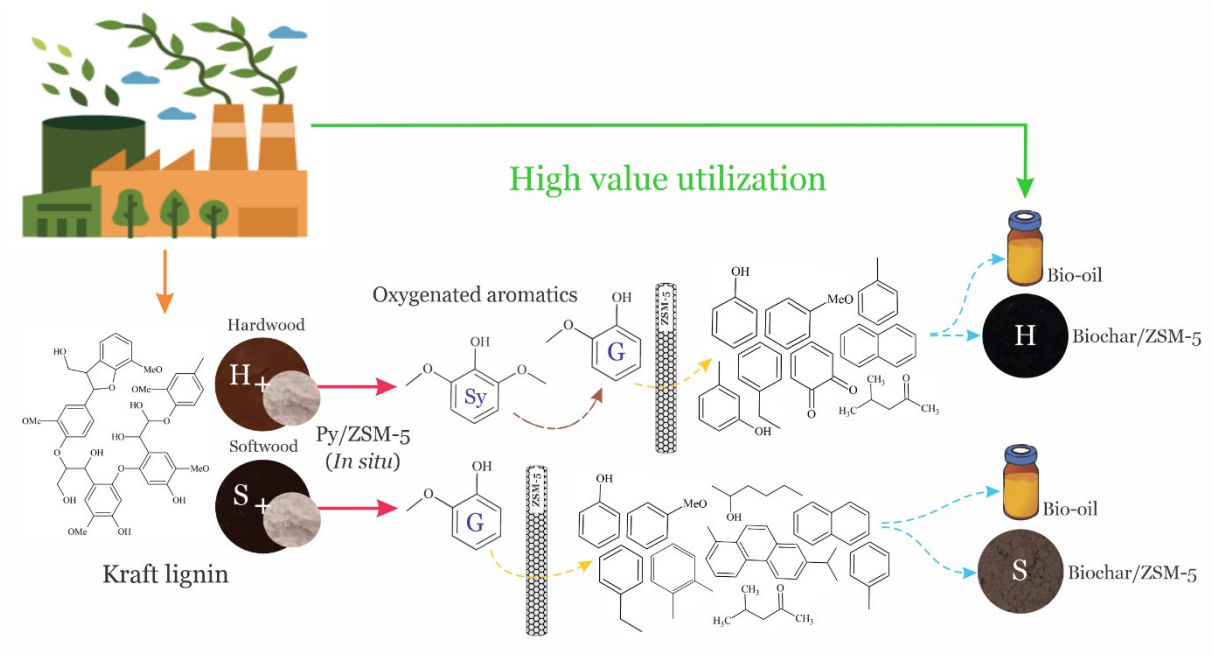

4 ANALYSIS OF THERMAL AND CATALYTIC DEGRADATION BEHAVIOR OF SOFTWOOD AND HARDWOOD KRAFT LIGNINS

Abstract: This research aims to examine the catalytic thermochemical conversion of lignin, which can be used as a promising source of aromatic compounds. Due to its complex structure, the source of lignin can influence the composition of the final products. Therefore, the main objective of this study is to understand how a commercial catalyst (ZSM-5) behaves at pyrolysis of different types of Kraft lignins. Catalyst pore structure and acidity were evaluated through BET and BJH analysis, XRD, and pyridine FT-IR analyses. The preliminary evaluation of catalytic degradation was performed using TGA/DTG coupled with a deconvolution method. In addition, the pyrolysis behavior of two Kraft lignin (*Eucalyptus spp*, Pine Tree) with ZSM-5 catalyst was evaluated using a fixed-bed reactor at different temperatures (500, 600, 700 °C) for a few seconds. An analysis of covariance was performed to assess the degree of functional dependence existing between the different variables in the pyrolysis product yields exhibited by different lignin samples and temperatures in the experiment. The results of catalytic pyrolysis demonstrated that the inclusion of ZSM-5 catalyst has the potential to significantly improve bio-oil yield by approximately 10-25% wt%. The gases released were reduced by 3-14% wt% for lignin A (*Eucalyptus spp*) and 10% wt% for lignin B (Pine Tree). Biochar is directly linked to the source of lignin and is less affected by the catalyst. Although the results have shown that ZSM-5 has the potential to reduce oxygen content in bio-oil composition, lignin source has been identified as the most important variable in non-oxygenated component formation, such as aromatics (BTX). Softwood produces higher amounts of aromatics (31%) and a high variety of components due to guaiacol decomposition, while hardwood bio-oil exhibits an increase in oxygenated products with 4% of aromatics. This is related to the high molar mass monolignol derived from syringyl that is not effectively converted by ZSM-5 due to size exclusion or pore blockage. Therefore, the softwood lignin has a higher affinity towards commercial ZSM-5, while hardwood lignin requires a modified catalyst to convert syringyl units more efficiently. This study highlights the potential of lignin as a renewable resource for energy and chemical applications. The findings offer valuable insights into optimizing conversion processes and catalyst selection for sustainable lignin-based solutions.

Keywords: Kraft lignin; softwood; hardwood; catalytic pyrolysis; ZSM-5.

4.1 INTRODUCTION

Lignocellulosic biorefinery is proving as a viable way to obtain renewable chemicals and energy. Lignin has gained attention as an abundant renewable polymer and the largest natural source of aromatics and high-value chemicals due to its low cost and extensive production in the pulp and paper industry (KUMAR *et al.*, 2019).

The lignin structure is formed by three building blocks (guaiacyl (G), syringyl (S), and p-hydroxyphenyl (H)) connected through ether or carbon-carbon bonds in a cross-linked and three-dimensional structure, which imparts rigidity to these polymers (YOGALAKSHMI *et al.*, 2022). However, the proportions of the monomer units are highly variable and strictly dependent on the lignin species. For instance, lignin from softwood mainly contains guaiacyl units, around 90–95%, while lignin from hardwood usually contains guaiacyl and syringyl units, around 25–50% and 50–75%, respectively. In contrast, lignin from grass typically contains all three units. (CHIO; SAIN; QIN, 2019).

Bio-oil derived from lignin thermal pyrolysis is characterized by high oxygen content, elevated acidity, and increased viscosity, which restrict its use in petrochemical applications. Therefore, the use of catalysts to efficiently remove oxygen from raw materials has garnered considerable attention in the literature. In particular, catalytic pyrolysis has been extensively studied as a method to produce high-energy density fuels with high amounts of aromatic compounds (BI *et al.*, 2018).

Catalytic pyrolysis involves the thermal degradation of biomass into oxygenated compounds, which undergo deoxygenation, cracking, isomerization, aromatization, condensation, and oligomerization reactions on the catalyst surface. The use of catalysts with strong Brønsted acidity induces deep deoxygenation of the produced bio-oil, resulting mainly in mono-aromatics (BTX), naphthalene, and alkyl-phenols (LAZARIDIS *et al.*, 2018a).

Zeolites are a well-known type of catalyst formed by a crystalline aluminosilicate with inner pores and cavities interconnected within channels in a defined architecture. ZSM-5 is an aluminosilicate and pentasil type, consisting of fourteen tetrahedrals combined to form a sub-unit, with eight faces forming a pentagonal. Their channels and pores have a uniform diameter suitable for shape-selective catalysis, and aromatics and olefins formation (HARTANTO *et al.*, 2016; NISHU *et al.*, 2020). Due to their Lewis and Brønsted acid sites, zeolites are well-suited for cracking reactions, as they can catalyze several reactions such as

decarboxylation, decarbonylation, hydrocracking, hydro-deoxygenation, hydrogenation, and polymerization (KIM *et al.*, 2020).

Nishu *et al.*, (2020) and Rahman; Liu; Cai, (2018) studied the effect of shape selectivity of ZSM-5 zeolite to obtain high quality bio-oil. These authors presented the reaction pathway for catalytic pyrolysis over ZSM-5, as illustrated in Figure 25, and concluded that the unique microporous structure of ZSM-5 favors the production of aromatic compounds. However, coke formation on the surface inevitably deactivates the catalyst. This technique enhances bio-oil by converting oxygenates and increasing its energy value. Initially, deoxygenation and cracking reactions release the repeating units of lignin and other compounds, which subsequently undergo various conversion pathways to yield non-oxygenated compounds. These pathways include the hydrocarbon pool mechanism, aromatization, ketonization, and oligomerization, with the specific outcomes influenced by factors such as biomass type, reaction mode, catalyst type, and other operational conditions. (RAHMAN; LIU; CAI, 2018).

Figure 25: Reaction routes for catalytic pyrolysis of lignin over a zeolite catalyst.

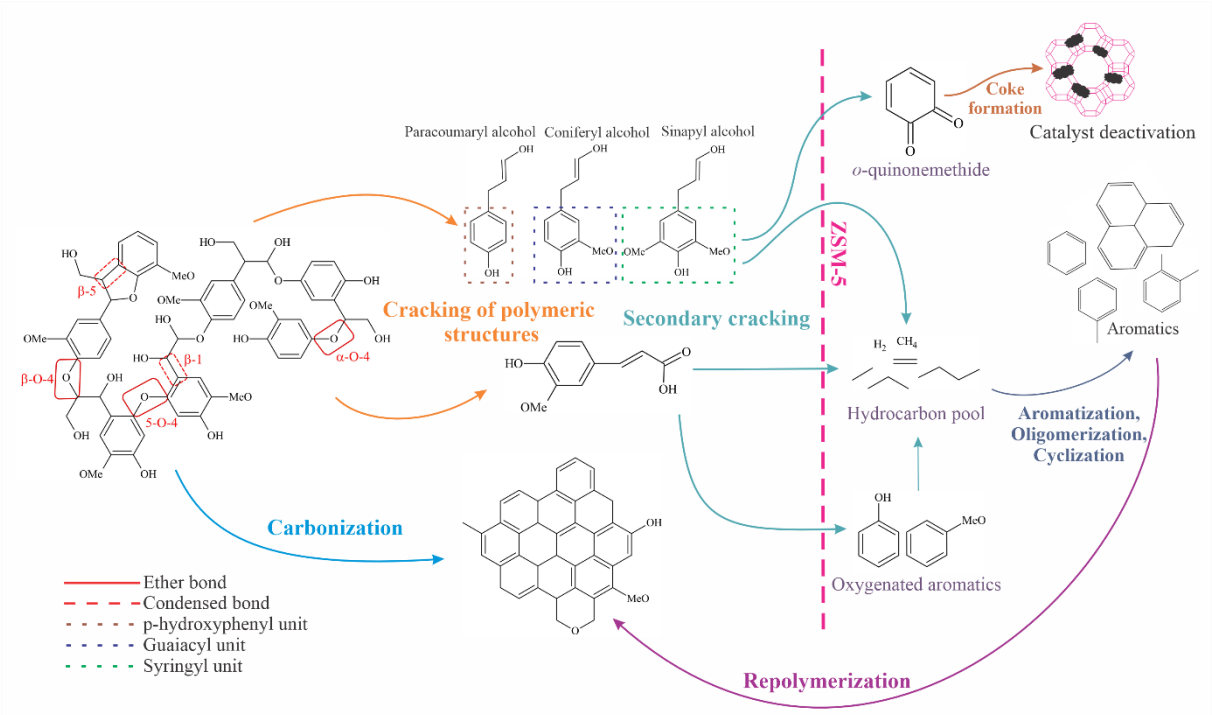

Source: Adapted from Kim *et al.* (2020); Nishu *et al.* (2020), and Yang *et al.* (2020).

The ZSM-5 pore architecture plays a crucial role in catalytic activity to achieve desired products. During catalytic pyrolysis, oxygenated compounds formed, such as syringyl aromatics, cannot diffuse through zeolite micropores, resulting in coke formation on the

surface of ZSM-5. The product shape selectivity, shown in Figure 26, establishes that reaction products of a particular shape and size formed within zeolite pores are unable to diffuse out of the pores due to incompatibilities with pore size. However, the product molecule that is less hindered possesses the capability to diffuse out of zeolite micropores. Conversely, larger-sized products either do not form, diffuse very slowly, or are converted into undesired products. As a result, the pores become blocked, leading to catalyst deactivation (KIM *et al.*, 2015; NISHU *et al.*, 2020; PATTIYA, 2018; RAHMAN; LIU; CAI, 2018).

Figure 26: ZSM-5 product shape selectivity.

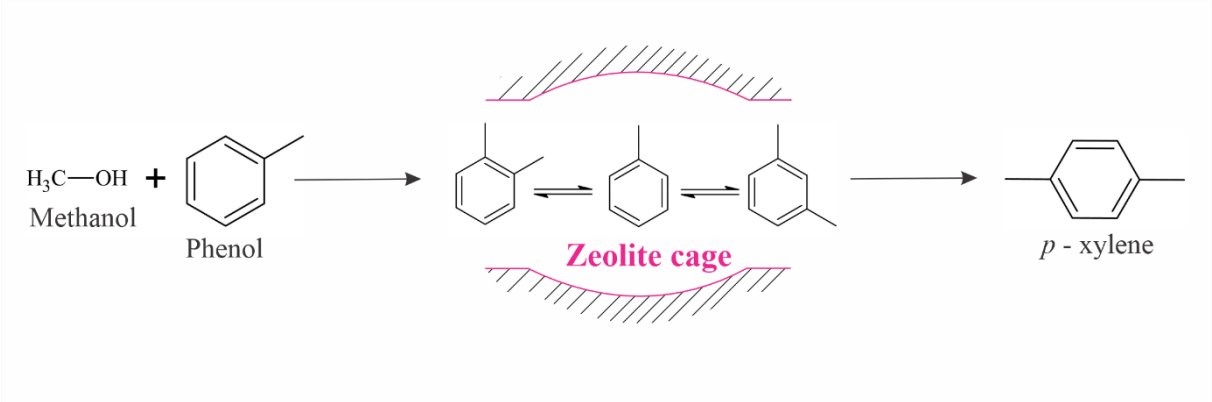

Source: Adapted from Nishu *et al.* (2020).

The zeolite acidity presents an impact in catalytic reactions such as cracking, deoxygenation, oligomerization, and polymerization, through the carbonium ion mechanism forming carbocation intermediate by the active Brønsted acid sites. The acid sites are present on the outer surface of ZSM-5, being responsible for the cracking of larger oxygenate while the conversion of smaller ones into aromatics occurs on the acid sites inside the pores. The acidity plays a crucial role in the formation of aromatic compounds from pyrolytic vapors. Increasing the acidity leads to enhance selectivity towards aromatic compounds, further highlighting the importance of acidity in influencing the product distribution during catalytic reactions (NISHU *et al.*, 2020)

Nonetheless, it is important to note that the application of ZSM-5 to hardwood is limited and still relatively unexplored. As a result, it is crucial to understand the behavior of this catalyst in this specific context to adapt and optimize the process. In this regard, this study aims to evaluate the physical, chemical, and thermal characteristics of two different Kraft lignin samples and characterize the pyrolysis products using ZSM-5 under the same conditions. Additionally, statistical methods such as covariance matrix will be employed to

differentiate the spectral patterns exhibited by the different lignin sources under the catalytic and thermal degradation, contributing to a better understanding of the mechanisms involved in by-products formation and enabling process adaptation.

4.2 MATERIALS AND METHODS

4.2.1 Biomasses and catalysts selection and preparation

The *Eucalyptus spp* lignin (referred to as lignin A) was donated from International Paper and the Pine Tree lignin (referred to as lignin B) (CAS# 8068-05-1, cata# 471003) was purchased from Sigma-Aldrich. These samples can be classified as hardwood (*Eucalyptus spp* lignin) and softwood, respectively. The ZSM-5 powder (SM27) was donated from CENPES/PETROBRÁS. Before use, the catalyst powder was sieved to 300 μm, followed by calcination in an electric furnace at 450 °C for 4 h in air, and then stored in a desiccator (PAYSEPAR *et al.*, 2018).

For catalytic pyrolysis, since the size of ZSM-5 particles was larger than that of lignin, it was necessary to standardize the particle sizes to 300 μm before mixing the lignin with the ZSM-5. The sample for the pyrolysis test was prepared by physically mixing the kraft lignins and the catalyst in a 1:1 proportion until a homogeneous mixture was achieved.

4.2.2 Characterization

Lignin characterization was detailed in the previous chapter. The ZSM-5 structure was characterized by X-ray diffraction (XRD) on a Rigaku-MiniFlex powder diffractometer, using the 2θ range of 10°-70° with a step width of 0.02°. The measurement of the surface area and the porosity of ZSM-5 particles were determined through the nitrogen physisorption isotherms at -195.8 °C, under a critical pressure of 33.5 atm and relative pressures (P/P0) of approximately 0.99. These analyzes were performed on a Quantachrome Instruments - Autosorb-1 surface area analyzer. A sample of approximately 0.1 g of particles was used to perform the analysis. The surface area, diameter, and volume of the pores were obtained from the data treatment through the method of Brunauer, Emmett, and Taller (BET) and Barrett, Joyner e Halenda (BJH).

A pyridine FT-IR method was used to analyze the forces of the ZSM-5 Brønsted and Lewis acid sites, using a small amount of zeolite (0.2 g) that was oven dried at 105 °C for 2h. Then, 50µL of pyridine was added to the catalyst followed by oven-drying at 105 °C for another 2h. Lastly, the catalyst mass was mixed and pressed with potassium bromide powder (KBr) at a ratio of 1:100 to make a disk that was subsequently analyzed by a FT-IR analysis in a Spectrum 100 spectrophotometer (PerkinElmer, USA) in the range between 4000 and 400 cm-1 (PAYSEPAR *et al.*, 2018).

4.2.3 Lignin catalytic decomposition evaluation.

The evaluation of lignin/catalyst (1:1 m/m) pyrolysis was performed using a DTG-60 thermogravimetric analyzer (Shimadzu, Japan) through differential thermogravimetric analysis (DTG/TGA). For each experimental analysis, the initial sample mass (approximately 10 mg) was heated from room temperature to 900°C, using four different heating rates (5, 10, 15, 20 °C/min) under a constant flow rate (100 $mL.min^{-1}$) of high purity nitrogen gas (99.997%) (DA SILVA *et al.*, 2020; SAHOO *et al.*, 2021).

4.2.4 Pyrolysis runs

The experimental procedure was initiated by weighing dehumidified lignin (using a Moisture Analyzer, model MX-50) and calcined ZSM-5 in a 1:1 ratio. The total mass of the sample was 1g. The catalytic pyrolysis and product recovery procedures followed the same patterns as in the previous chapter.

Bio-oil recovery was carried out using two solvents. Specifically, dichloromethane (99.8%, CAS number 75-09-2, Sigma Aldrich, Darmstadt, Germany) was employed to recover bio-oil in both thermal and catalytic pyrolysis experiments. However, dichloromethane proved ineffective in recovering bio-oil during catalytic pyrolysis runs involving lignin B. In these particular runs, bio-oil recovery was achieved using acetone (99.5%, CAS number 67-64-1, Sigma-Aldrich, Darmstadt, Germany). Storage and GC-MS analyses protocols followed the same standards as for thermal pyrolysis.

Analysis of covariance was performed to assess the degree of functional dependence existing between different variables of pyrolysis process, including temperature, lignin type, catalyst use, product yields, and bio-oil composition. Covariance matrices were computed

using the *Statistic* software with the same methodology described at the preview chapter (MIRANDA, 2016).

4.3 RESULTS AND DISCUSSION

4.3.1 Characterization

The XRD patterns of the ZSM-5 (Figure 27a) displayed the characteristic diffraction peaks associated with the Mordenite Framework Inverted (MFI) crystalline structure, specifically at 2θ = 14.74°, 23° and 45°. These peaks are indicative of the typical morphology of MFI crystals, which exhibit a uniform pentagonal prism shape (NISHU *et al.*, 2020; SABARISH; UNNIKRISHNAN, 2019; TREACY; HIGGINS, 1983; WEI *et al.*, 2020; WIDAYAT; ANNISA, 2017).

Figure 27: Zeolite characterization: (a) XRD analysis; (b) BET analysis; (c – d) BJH analysis

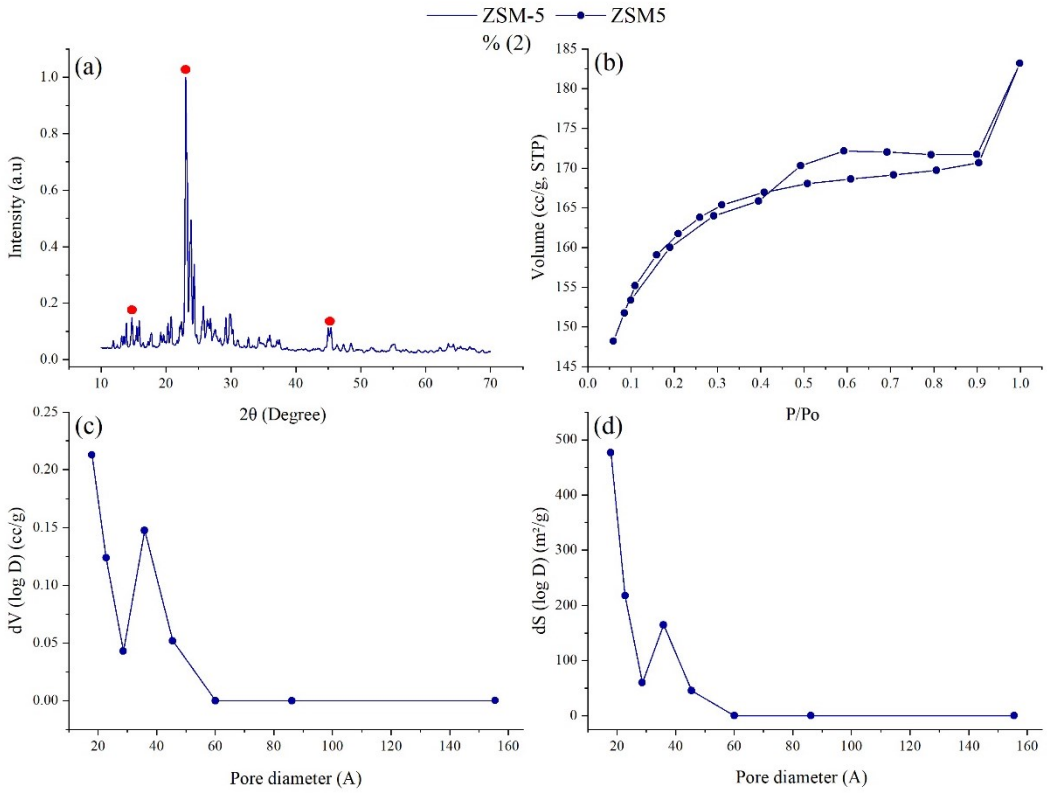

Source: From author

The N_2 adsorption-desorption isotherms and the BJH pore size distribution curve of the ZSM-5 was presented in Figure 27b, 27c, and 27d. Nitrogen physisorption isotherms exhibited the characteristics of a conventional microporous zeolite, as described by the type I isotherm. Therefore, ZSM-5 exhibits a typical behavior of a microporous solid without significant mesoporosity. In addition, ZSM-5 catalyst exhibited a high specific surface area (518 m^2/g), a small pore volume (0.28 cm^3/g), and a pore diameter of 2.194 nm. These results are slightly larger than the sizes reported in the literature (BI *et al.*, 2018; KUMAR *et al.*, 2019; LAZARIDIS *et al.*, 2018a; NOOR *et al.*, 2018; PAYSEPAR *et al.*, 2018; YAO *et al.*, 2018; YU *et al.*, 2012).

The infrared analysis in the presence of pyridine detected three distinct vibrations, as shown in the Figure 28, located at 1650-1620 cm^{-1} for silanol groups (as an acid site of Brønsted), 1548-1545 cm^{-1} for Brønsted acidic sites, and at 1442-1419 cm^{-1} for Lewis acidic sites. These results confirm the acidity of the zeolite. (HARTANTO *et al.*, 2016).

Figure 28: FT-IR analysis for the ZSM-5

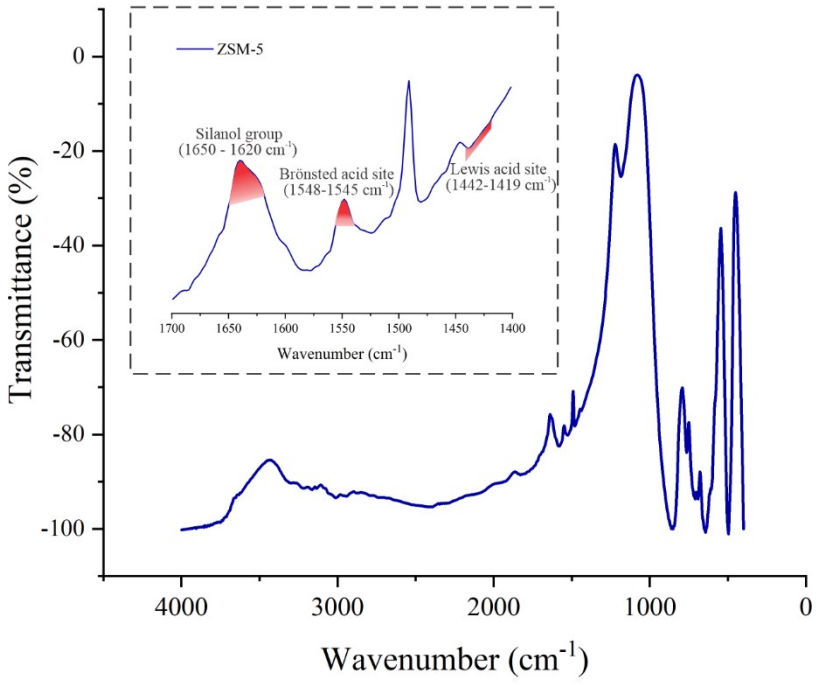

Source: From author

4.3.2 Evaluation of catalytic decomposition

Catalytic upgrading can enhance the reaction occurring in pyrolysis, which include cracking, decarbonization, and decarboxylation. These reactions promote the removal of oxygenated compounds through the release of H_2O and CO_2, reducing molecular weight, and altering chemical structures of the bio-oil. Deoxygenation reactions are intended to control the product distribution towards valuable hydrocarbon compounds. Zeolites are often used in cracking processes, because of their strong Brønsted acidity and a small volume inside the pores, which prevent repolymerization and coke formation reactions inducing a deep-deoxygenation of the liquid product by cracking, dehydration, and adsorption of oxy-compound in the acid site (DICKERSON; SORIA, 2013; LAZARIDIS *et al.*, 2018b; LI *et al.*, 2015). Thermogravimetry analysis enable to evaluate the catalytic degradation of Kraft lignin samples. In Figure 29, the mass loss (TG) and derived mass loss (DTG) for each lignin were presented at different heating rates (5, 10, 15, and 25°C/min) from room temperature to 900 °C.

Figure 29: TG and DTG: (A) Lignin A/ZSM-5, and (B) Lignin B/ZSM-5

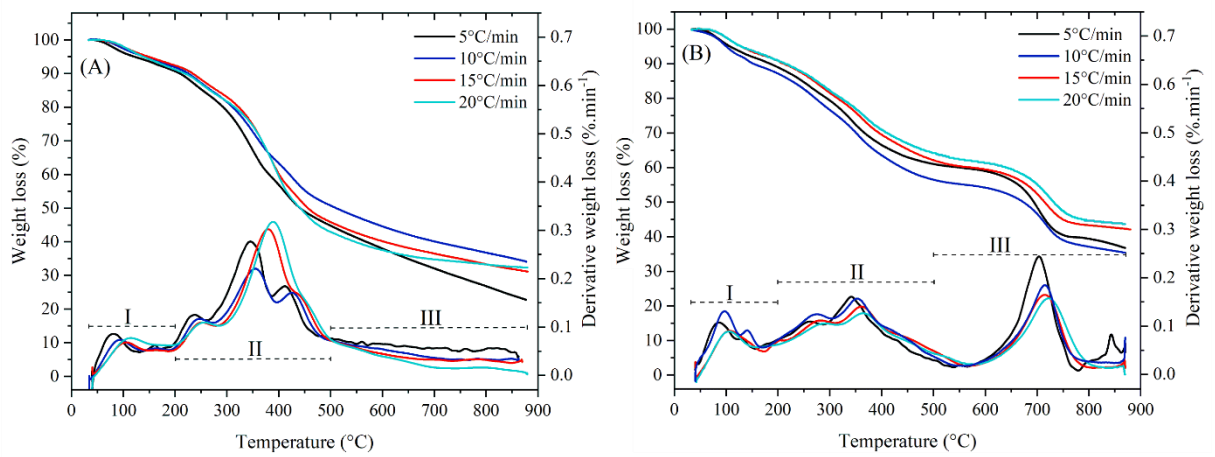

Source: From author

Catalytic pyrolysis was divided into three phases, and the corresponding weight loss of each stage is depicted in Figure 30, comparing both lignins. At the first phase (< 200 °C), the peaks correspond to water evaporation and the initial cleavage of the ether and C-C bonds. Since lignin B has lower amounts of methoxyl groups, its DTG analysis presented a slight increase in the number of peaks and the weight loss was 2 – 4 % higher than lignin A. This difference can be attributed to the repolymerization degree. The second phase, which occurred

between 200 – 500 °C, correspond to the primary decomposition stage. In this stage, both lignin exhibited their highest weight loss among the phases, because of the production of the phenolic monomers. Notably, lignin A exhibited a weight loss of approximately 17 % higher than that of lignin B. This difference can be attributed to the source of lignin, specifically, lignin A, which has a high methoxy group content. Lignins with high methoxy group content, like lignin A, tend to generate less char during decomposition. This is because the methoxyl groups within lignin A can break down into small molecular radical, which serve to stabilize larger molecular fragments and inhibit their transformation into char (WANG *et al.*, 2017). As seen in the last chapter, Lignin B continues to lose more mass in the third phase (500 – 900 °C) due to the charring stage. Weight loss of lignin B was about 5 % higher than lignin A (LU; GU, 2022).

Figure 30: Weight loss (%) between lignins by stages: Lignin A (*Eucalyptus spp*) and Lignin B (Pine Tree)

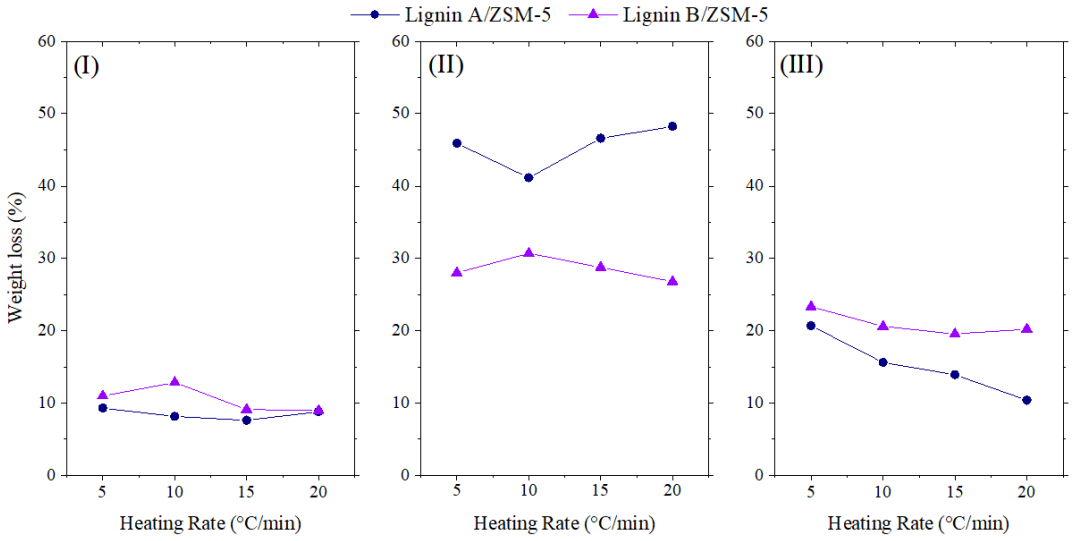

Source: From author

The increase in heating rate played an interesting role in the weight loss of both samples. For example, while the weight loss of lignin A was similar at phase one, lignin B presented an increase in weight loss at 10 °C/min followed by a decrease of weight loss at higher heating rates, and the same behavior was seen in the second phase. However, lignin A presented a decrease of almost 5% in weight loss from 5 °C/min to 10 °C/min followed by an increase in the weight loss at high heating rates, changing the behavior of reaction peaks in DTG. In the final phase, the effect of heating rate in the weight loss was more pronounced in lignin A than lignin B. In case of lignin A, as higher the heating rate, the lower the weight

loss. Conversely, lignin B presented the highest weight loss at 5 °C/min, followed by a plateau at other rates. Therefore, the increase in the heating rate favors the biochar production by decreasing the weight loss between phases with the displacement of repolymerization reactions to higher temperatures.

Since lignin A presented more ether bonds than lignin B, its DTG highest peaks occurred in phase II (300 – 400), through depolymerization and repolymerization reaction of methoxyl groups. Specifically, these reactions involved the cleavage of S-units linkages into G-units or catechol, resulting in the maximum rate of phenol production. It is widely recognized that softwood lignin (such as pine tree) contains a higher concentration of condensed linkages. Therefore, despite the higher mass loss occurs during the second phase, lignin B exhibited its most prominent peaks during phase III. This behavior can be attributed to secondary reactions wherein the G-type units undergo degradation into aromatic compounds or cleavage at benzene rings, with releasing of non-condensable gases. Alternatively, it could indicate the formation of coke through the polycondensation of the aromatic ring structures. (CHIO; SAIN; QIN, 2019; LU; GU, 2022).

4.3.3 Comparison between thermal and catalytic decomposition

For a better understanding of the heating effect in catalytic decomposition, a comparison of the weight loss for both lignin in catalytic and thermal decomposition is illustrated in Figure 31.

Figure 31: Comparison of weight loss by phases between in thermal and catalytic decomposition: (A) Lignin A (*Eucalyptus spp*); (B) Lignin B (Pine Tree)

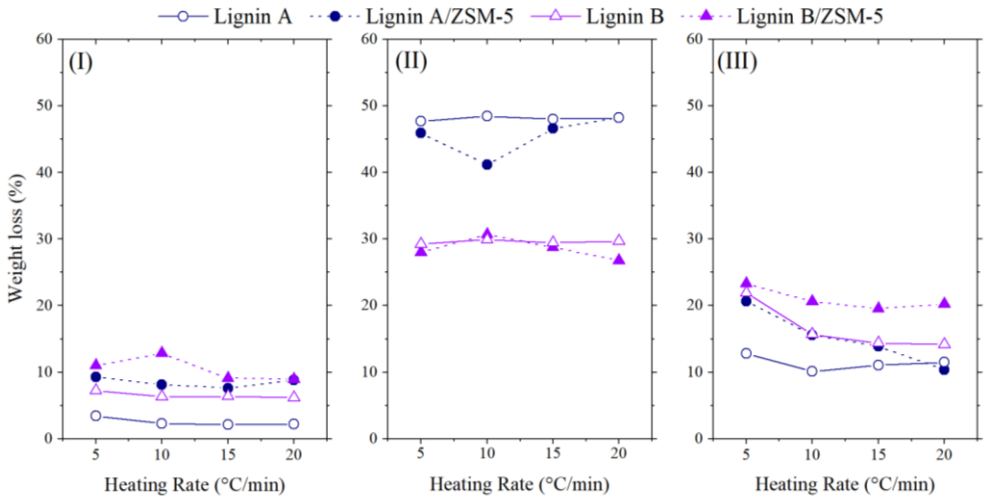

Source: From author

In the first phase (I), the weight loss increased with the presence of catalyst (ZSM-5) for both lignin, indicating that ZSM-5 presented catalytic activity for initial cleavage of the ether and C-C bonds and dehydration reaction. During catalytic decomposition, the weight losses of lignin A and B were 5-6% and 2-6%, respectively, higher than the weight losses observed in thermal reactions. Lignin A and lignin B lost 6% more weight at 20 °C/min and 10 °C/min, respectively, due to the appearance of peaks with higher weight loss at 100 °C, which could represent dehydration reaction and ether linkages degradation (CHIO; SAIN; QIN, 2019).

In the next phase (II), lignin B exhibited a weight loss similar to thermal decomposition, except for a slight reduction in mass loss at 20 °C/min. However, lignin A showed a decrease of weight, mainly at 10 °C/min, indicating that the heating rate affects the catalytic reactions due to selectivity towards the type S-units degradation (CHIO; SAIN; QIN, 2019; WANG *et al.*, 2017).

In the last phase (III), lignin A lost about 2 – 7% more weight than the sample submitted to thermal decomposition. Lignin B presented a decrease in mass (1 to 6%) during this phase, despite exhibiting similar behavior (with the heating rate) when compared to thermal decomposition. This is attributed to the zeolite effect in secondary reactions and char formation (NISHU *et al.*, 2020).

Figure 32 shows a comparison of the TG and DTG curves of thermal and catalytic decomposition at the heating rate of 20°C/min. The TG curve behavior of catalytic decomposition was similar to the thermal curve; however, the presence of the ZSM-5 increased the mass loss in both samples. Lignin A and lignin B presented an average mass loss that was 8% and 6% higher, respectively, when compared to the samples submitted to thermal decomposition. Lignin A exhibited lower weight losses in the first and third phases (8.79% and 10.58%), compared to lignin B (10% and 20.2%). However, lignin B displayed a lower weight loss in the second phase (approximately 27%), while lignin A had an average loss of 48.3%.

Figure 32: TG and DTG at 20°C/min: (A) Lignin A (*Eucalyptus spp*); (B) Lignin B (Pine Tree)

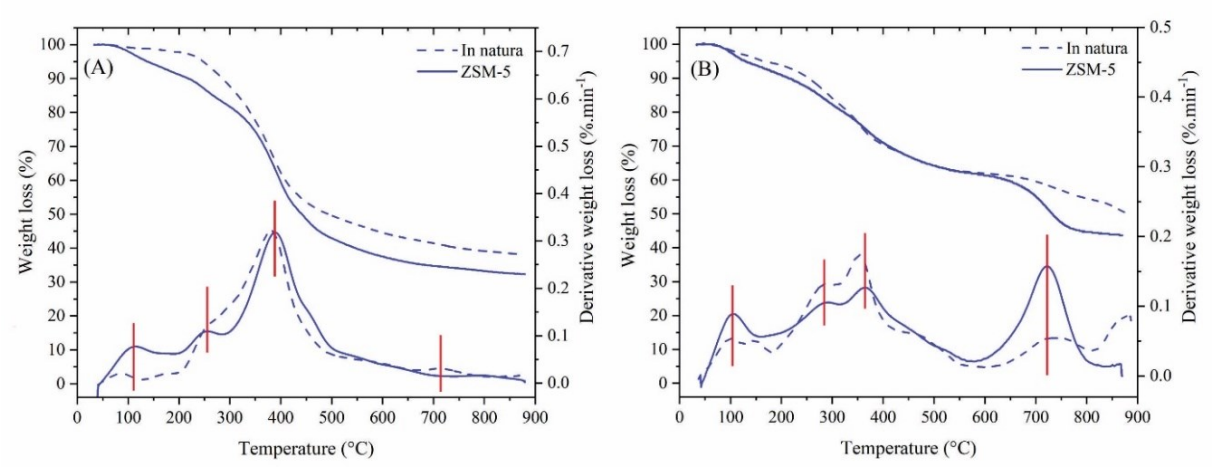

Source: From author

As can be seen in Figure 32, ZSM-5 affected the lignin behavior on DTG curves. For lignin A, ZSM-5 exhibited catalytic activity in dehydration reactions, displaying higher reaction rates, as indicated by the peak of weight loss at 114°C. In the second phase, there is a peak formation at 254.5°C, indicating cleavage of C-O and C-C bonds. The main peak was kept between 300 and 400°C due to methoxy cleavage. However, in the final phase, a slight reduction in peak intensity is observed during the charging stage.

In case of lignin B, the addition of ZSM-5 also affected the degradation behavior. In the first phase, the dehydration peak also increased. However, there is a reduction in peak intensities during the second phase, followed by a notable increase in the peak of charring stage. Therefore, ZSM-5 presented catalytic activity mainly for secondary cracking and rearrangement reactions, resulting in higher release of CO and CO_2 at temperatures exceeding 700 °C. This behavior was seen in the TG analysis, where the sample has an increase of mass loss in the third phase of 14.2% to 20.52% and a decrease in the second phase of 30.37 to 26.75%.

Hence, the addition of ZSM-5 affected primary reactions such as dehydration, rearrangement, and cracking phases, in the case of lignin A. However, ZSM-5 affected the secondary mechanisms and removal of functional groups in char during decomposition of lignin B (DICKERSON; SORIA, 2013; LI *et al.*, 2015; LU; GU, 2022).

4.3.3.1 Catalytic pyrolysis deconvolution

The deconvolution of the DTG curve for the samples submitted to catalytic pyrolysis presented 8 peaks during the temperature rise (Figure 33). In the presence of catalyst, the peaks were shifted towards lower or higher temperatures, followed by changes in their intensity. These changes can be attributed to selectivity of ZSM-5 due to its pore size distribution, which affects the mass transfer of both reactants and products. The well-defined pore structure in ZSM-5 imposes limitations on the transition state of reactants, favoring specific reactions. (NISHU *et al.*, 2020).

Figure 33: Deconvolution of DTG Curves: (A) Lignin A (*Eucalyptus spp*); (B) Lignin B (Pine Tree)

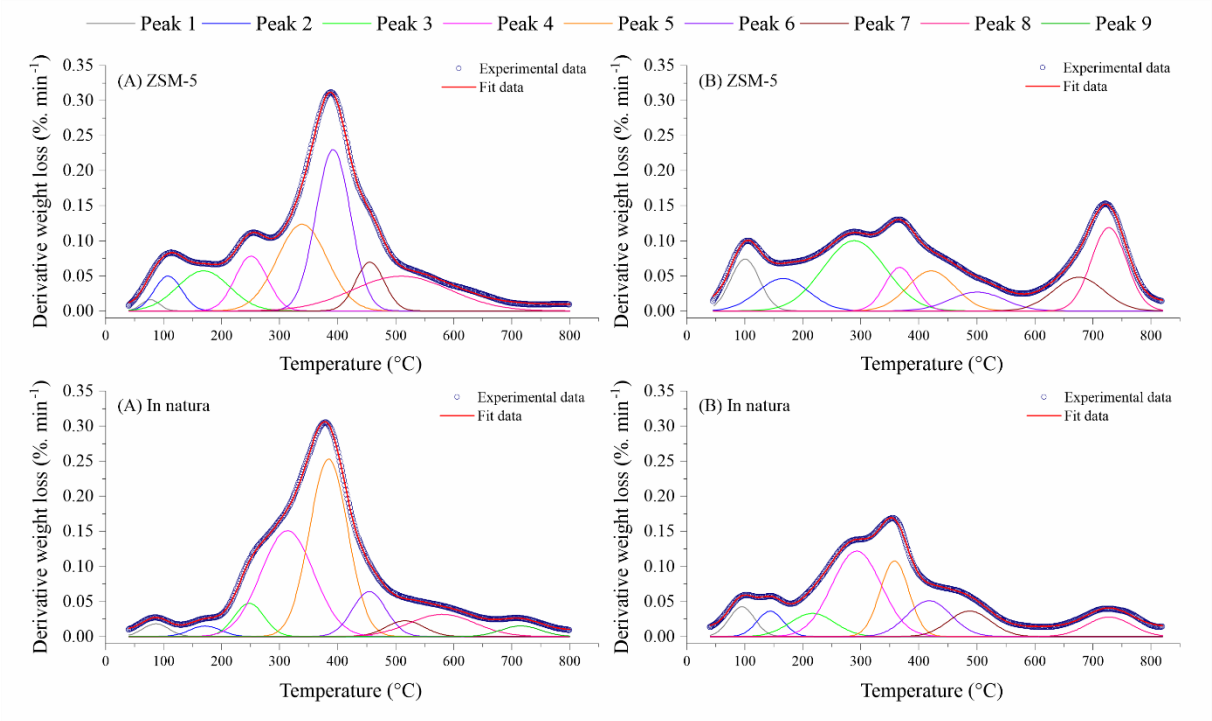

Source: From author

For lignin A/ZSM-5 (AZ), the peaks were shifted to lower temperatures while in lignin B/ZSM-5 (BZ), the peaks were detected in higher temperatures. The initial peak, which corresponds to water evaporation, occurred at temperatures of 78°C for AZ and 99°C for BZ. The subsequent peak was detected at 107°C for AZ and 165°C for BZ and indicates the breakdown of ether linkages through lignin depolymerization. At peak 3 (AZ: 169 °C; BZ: 288 °C) and peak 4 (AZ: 250 °C; BZ: 368 °C), the cleavage of β-O-4 linkages took place, resulting in the conversion of monolignols to guaiacol and syringol units. The higher intensity

of the peaks could be attributed to decarboxylation reaction (which removes -COOH groups as water and CO_2), and the decarbonylation that removes carbonyl groups with CO release. The peak 4 in Lignin B/ZSM-5 can also means the increase of the lignin-derived monomer yield due to hydrogen radical release through lignin depolymerization to stabilize the intermediate or depolymerized fragments (CHEN *et al.*, 2019; CHIO; SAIN; QIN, 2019; LU; GU, 2022).

In lignin A/ZSM-5, the peak (at 339°C) corresponds to conversion of high molar mass compounds into low mass molar products, aromatics, and olefins through processes of fragmentation and re-polymerization. In lignin B/ZSM-5 the peaks 5 and 6 (421 °C; 500 °C) presented a lower intensity, that could be related to gasification reactions, and aromatization reactions which converted olefin and low molecular weight oxygenates (ex: alcohols, aldehydes, esters, ethers) into aromatics, CO_2, CO, and H_2O. These same reactions started to happen in Lignin A/ZSM-5 at peak 6 (392 °C) with a higher intensity due to methoxyl groups cleavage, and formation of phenolic products (CHIO; SAIN; QIN, 2019; RAHMAN; LIU; CAI, 2018).

Peaks 7 and 8 (456 °C, 509 °C) at lignin A/ZSM-5 represents the secondary reactions where G-type compounds were converted by catalytic cracking into aromatics and olefins. In lignin B, ZSM-5 presented catalytic activity for charring process at peaks 7 and 8 (675 °C, 727 °C), characterized by the secondary reactions. These reaction involved the rearranging of char skeleton into a polycyclic aromatic structure while volatile compounds are released due to condensation reactions that can produce toluene and naphthalene (CHIO; SAIN; QIN, 2019; COLLARD; BLIN, 2014; RAHMAN; LIU; CAI, 2018).

4.3.4 Pyrolysis runs

4.3.4.1 Yields of thermal and catalytic pyrolysis

The correlation matrix shown in Table 11 covers all variables associated with catalytic pyrolysis, illustrating the relationships between ZSM-5 and each type of lignin. It is widely recognized that biochar yield is closely linked to the type of lignin used, as well as to the formation of gases during the process (CHIO; SAIN; QIN, 2019; LU; GU, 2022; WANG *et al.*, 2017). Conversely, the catalyst use presented a direct correlation with the production of bio-oil and an inverse correlation with gas formation. This suggests that catalyst use has the

potential to enhance the bio-oil yield with concurrently reduction of release of gases. Biochar also demonstrates an indirect correlation with both bio-oil and gases. This indicates that the formation of bio-oil and gases occurred during the breakdown of biochar.

Table 11: Correlation matrix between all variables involved in the catalytic pyrolysis process.

Variables	Temperature	Type of lignin	Catalyst	Bio-oil	Biochar	Gases
Temperature	1,00	-0,00	0,00	0,27	-0,29	0,08
Type of lignin	-0,00	1,00	0,30	-0,07	0,92	-0,85
Catalyst	0,00	0,30	1,00	0,68	0,13	-0,64
Bio-oil	0,27	-0,07	0,68	1,00	-0,36	-0,41
Biochar	-0,29	0,92	0,13	-0,36	1,00	-0,70
Gases	0,08	-0,85	-0,64	-0,41	-0,70	1,00

Source: From author

Figure 34 shows the comparison between the products of each pyrolysis reaction with the increase of temperature. In catalytic pyrolysis of lignin A, the temperature rise also decrease the biochar yield by 8.2 wt%, while an increase of the gases (4.2 wt%) was seen. However, when compared to thermal pyrolysis, the yield of these components in catalytic reactions decreased between 6 – 7 wt% and 3 – 14 wt% respectively, due to the prevention of high molar mass products formation within the zeolite small pores, which acts as coke precursors (NISHU *et al.*, 2020). While the bio-oil increased between 10 – 25 wt%, presenting the higher yield at 600 °C, a different behavior was seen in thermal pyrolysis. In this case, the higher yield was measured at 700 °C, indicating a possible advancement in the decomposition of methoxyl groups.

In lignin B, the gas yield also decreased with the catalyst addition up to 10 wt%, while the biochar has the same behavior in the lower temperatures, and only suffers a decrease of 4.5 wt% at 700 °C. In catalytic pyrolysis, the bio-oil presented the higher yield at 700 °C with an increase of 11.7 wt% when compared to thermal pyrolysis that had a higher production at 500 °C. These changes can be linked to the ZSM-5 selectivity that affects the secondary decomposition and favors aromatization reaction (CHEN *et al.*, 2019; NISHU *et al.*, 2020).

Figure 34: Comparison between products yields of thermal and catalytic pyrolysis.

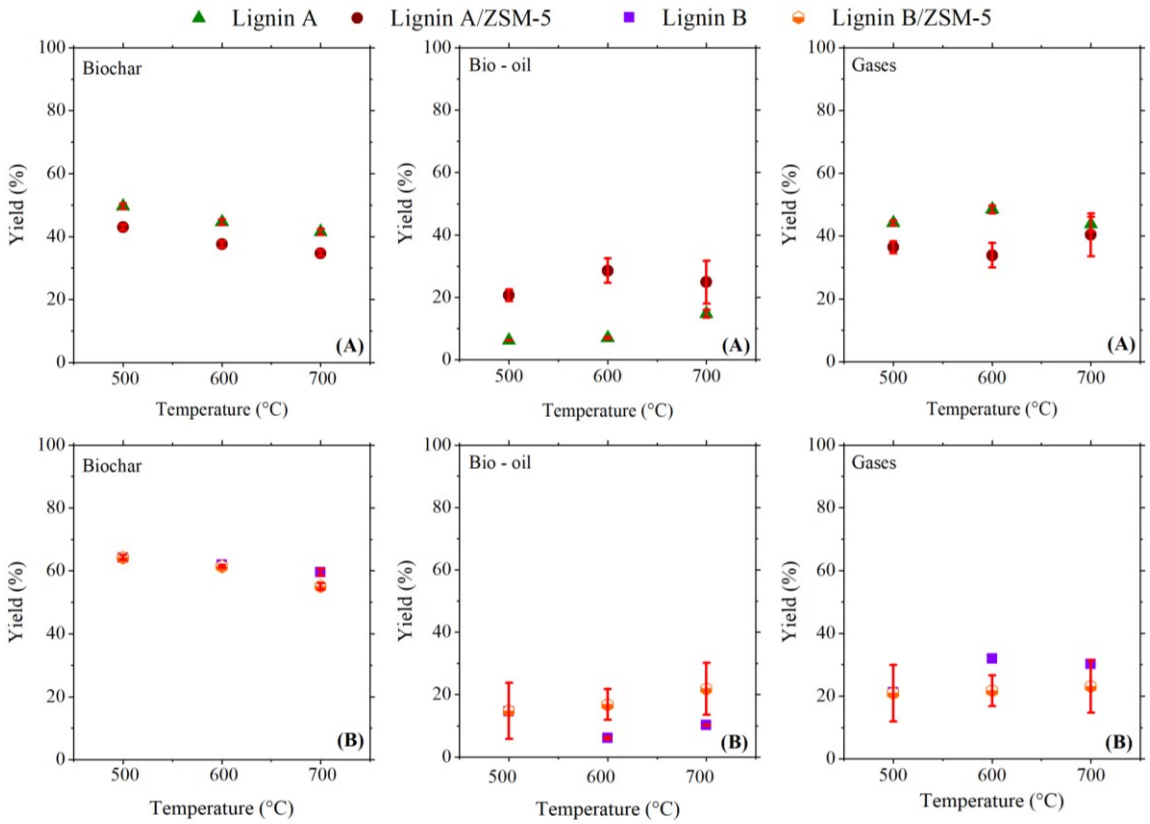

Source: From author

4.3.4.2 Effect of reaction temperature and ZSM-5 for each type of lignin

The zeolite fulfills a dual role in the lignin pyrolysis reaction, which included the well-defined porosity to stabilize intermediates and acid sites to cleave C-O and C-C bonds. The primary products are readily polymerized to produce solid, or stabilized to form low molecular weight aromatics (LI *et al.*, 2015). Regarding the catalytic products yield (Table 12), biochar and bio-gas yields decreased, while the bio-oil yield increased, suggesting that the selectivity of ZSM-5 improves the yield and quality of bio-oil by oxygenated compounds removal through dehydration, decarbonylation, and decarboxylation reactions with simultaneously increase of aromatic species (ILIOPOULOU *et al.*, 2012b; NISHU *et al.*, 2020).

Table 12: Catalytic pyrolysis yields (wt%)

Product	Lignin A/ZSM-5			Lignin B/ZSM-5		
	Temperature					
	500°C	600°C	700°C	500°C	600°C	700°C
Biochar[a]	42.92	37.53	34.72	64.27	61.39	55.06
Bio-oil	20.65	28.58	24.86	14.79	16.83	21.87
Gases[b]	36.43	33.89	40.42	20.93	21.78	23.06

a - Calculated by TGA analysis; b – Calculated by mass balance. Source: From author

Figure 35 shows a comparison between the product yields of catalytic pyrolysis of both lignin. Bio-char yield decreased in both samples when temperature is increased. Lignin B/ZSM-5 exhibited 21 wt% more biochar than lignin A/ZSM-5, primarily due to differences in the lignin types. However, lignin A/ZSM-5 showed a higher yield of bio-oil (2 - 11 wt%) and gases (12 – 17 wt%).

Figure 35: Comparison between product yields with ZSM-5 presence.

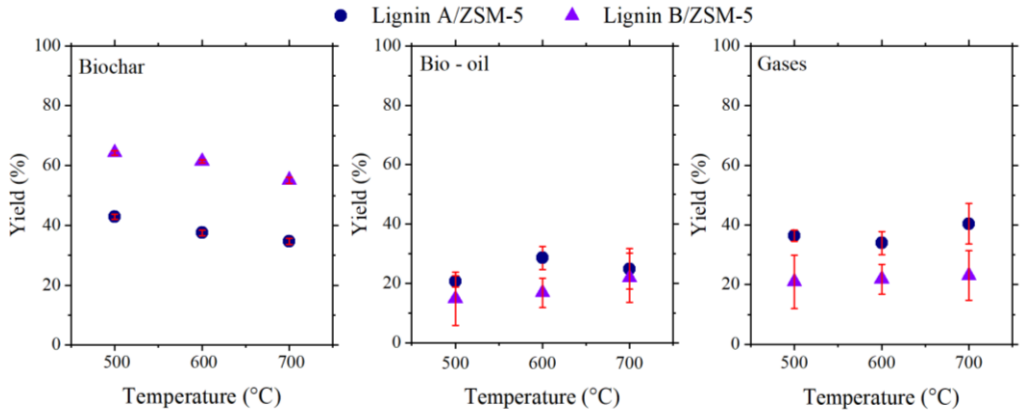

Source: From author.

The correlation matrix for lignin A/ZSM-5 (Table 13) indicated that temperature has an indirect dependence on the production of biochar and a low direct effect in bio-oil and biogas yields. The ZSM-5 affected all products, having an indirect dependence on the biochar and gases, and a high direct dependence on the bio-oil, suggesting that the addition of a catalyst promoted bio-oil production. The matrix also indicated that biochar and biogas yields presented an indirect dependence on bio-oil. Therefore, when the biochar and biogas yields decreased, the amount of bio-oil increased as shown in Figure 35.

Table 13: Lignin A/ZSM-5 - Correlation matrix between the variable involved in the catalytic pyrolysis.

Variables	Temperature	Catalyst	Bio-oil	Biochar	Gases
Temperature	1.00	0.00	0.30	-0.69	0.16
Catalyst	0.00	1.00	0.91	-0.71	-0.87
Bio-oil	0.30	0.91	1.00	-0.87	-0.88
Biochar	-0.69	-0.71	-0.87	1.00	0.52
Gases	0.16	-0.87	-0.88	0.52	1.00

Source: From author

The correlation matrix for lignin B/ZSM-5 (Table 14) indicated high effect of temperature in biochar yield and the indirect dependence means a decrease in the biochar production when temperature increases. Differently from Lignin A, the ZSM-5 did not have the same effect in lignin B, the catalyst only showed a direct and indirect influence on bio-oil and gases. However, the bio-oil showed an indirect dependence on both biochar and gases, suggesting that the ZSM-5 promotes a higher yield of bio-oil while biochar and gases yields decreased. This behavior was shown in Figure 35 , when the highest bio-oil yield was followed by the lowest yields of biochar and biogas.

Table 14: Lignin B/ZSM-5 - Correlation matrix between the variable involved in the catalytic pyrolysis.

Variables	Temperature	Catalyst	Bio-oil	Biochar	Gases
Temperature	1.00	0.00	0.25	-0.90	0.15
Catalyst	0.00	1.00	0.72	-0.26	-0.76
Bio-oil	0.25	0.72	1.00	-0.62	-0.92
Biochar	-0.90	-0.26	-0.62	1.00	0.26
Gases	0.15	-0.76	-0.92	0.26	1.00

Source: From author

4.3.4.3 Bio-oil analysis

The influence of pathways of lignin pyrolysis in bio-oil composition was discussed in the previous chapter. However, guaiacol and syringol followed distinct pathways in catalytic pyrolysis, due to specific channels and pores of ZSM-5. Particularly, ZSM-5 possess uniform pore size distribution improving the shape-selectivity regarding to aromatic compounds (RAHMAN; LIU; CAI, 2018).

Figure 36 illustrates the distribution (%) of compounds in the bio-oil analyzed by GC-MS at different temperatures. The compounds have been categorized into various types, including aromatic hydrocarbons, guaiacol, syringol, oxygenated aliphatic (AlO), hydrocarbons (HC), organosulfur (OS), ketones (KET), other oxygenated aromatics (OA), and unidentified (UNK) compounds that were not identified by the GC-MS analysis. In Table 15, one can see the products detected in bio-oil, with the corresponding lignin used in catalytic pyrolysis.

Figure 36: Distribution of products in bio-oil during catalytic pyrolysis runs: (A) Lignin A; and (B) Lignin B

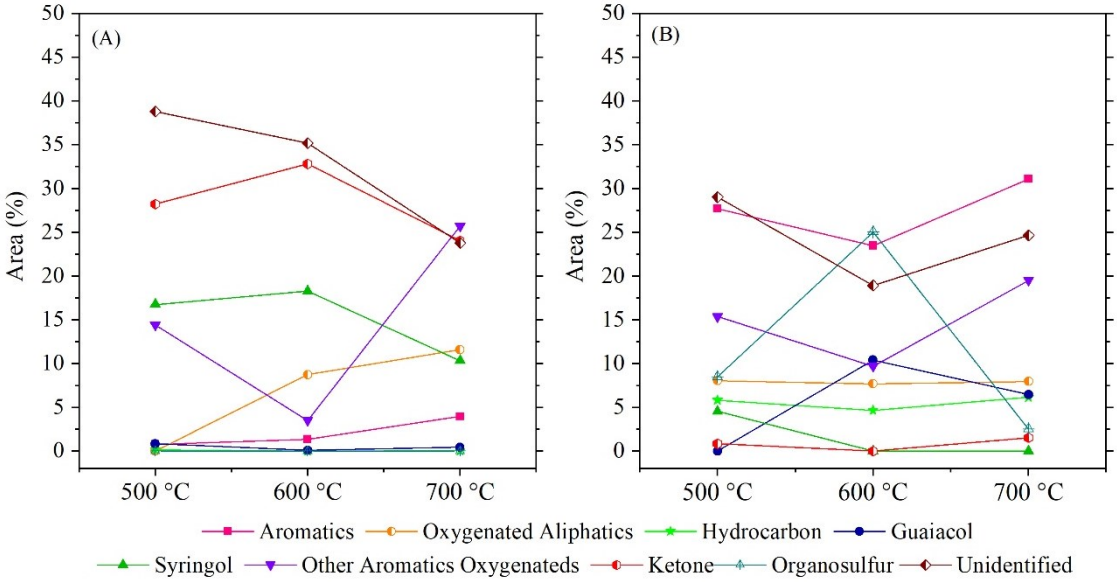

Source: From author

In lignin A, the most abundant known components formed in the bio-oil were ketones due to ketonization reaction involving two carboxylic acid molecules, which are converted into long-chain intermediates, along with the release of CO_2 and H_2O. Following ketones, the next significant compounds were syringol and other oxygenated aromatics (OA), which were produced through dehydration and catalytic cracking processes. The low presence of aromatics, hydrocarbons and guaiacol can be due to difficult cleavage of phenolic ether bonds (CHIO; SAIN; QIN, 2019; RAHMAN; LIU; CAI, 2018).

Table 15: Bio-oil components composition

(continues)

Components	Classification
Benzene, 1,2,3-trimethyl- [b]	Aromatic
Benzene, 1,2,4-trimethyl- [b]	
Benzene, 1-ethyl-2-methyl- [b]	
Benzene, 1-ethyl-4-methyl- [b]	
Ethylbenzene [a, b]	
Mesitylene [b]	
m-xylene [b]	
Naphthalene [b]	
Naphthalene, 1,6-dimethyl- [a]	
Naphthalene, 1-methyl- [a, b]	
Naphthalene, 2,6-dimethyl- [a, b]	
Naphthalene, 2,7-dimethyl- [b]	
Naphthalene, 2-methyl- [a, b]	
Naphthalene, 2-methyl- [b]	
Phenanthrene, 3,6-dimethyl- [b]	
p-xylene [b]	
Retene [b]	
Toluene [a, b]	
Phenol, 2-methoxy- [a, b]	Guaiacol
Phenol, 2,6-dimethoxy- [a, b]	Syringol
Methyl isobutyl ketone [a, b]	Ketone
2-hexanone [b]	
1,3,5-cycloheptatriene [a]	Hydrocarbon
1,3-cyclopentadiene, 5-(1-methylethylidene)- [b]	
Cyclohexane, 1-ethyl-2-methyl-, cis- [b]	
Cyclohexane, propyl- [b]	
Decane [b]	
Nonane [b]	
2-hexanol [a]	Oxygenated Aliphatic
2-pentanol, 4-methyl- [a, b]	
Acetic acid, butyl ester [b]	
Disulfide, dimethyl [b]	Organosulfur
Dimethyl trisulfide [b]	
1,2-benzenediol, 3-methoxy- [a]	Others aromatic oxygenated
2,4-dimethoxytoluene [b]	
3,4-dimethoxytoluene [b]	
5-tert-butylpyrogallol [a]	
Benzene, 1,2-dimethoxy- [b]	
Benzene, 4-ethyl-1,2-dimethoxy- [b]	

Table 15: Bio-oil components composition

(conclusion)

Components	Classification
Creosol [a]	Others aromatic oxygenated
Ethanone, 1-(3,4-dimethoxyphenyl)- [a]	
Ethanone, 1-(4-hydroxy-3,5-dimethoxyphenyl) - [a]	
m - cresol [a, b]	
o - cresol [a, b]	
p - cresol [a]	
Phenol [a]	
Phenol, 2,3-dimethyl- [b]	
Phenol, 2,4,6-trimethyl- [a, b]	
Phenol, 2,4-dimethyl- [a, b]	
Phenol, 2,5-dimethyl- [a, b]	
Phenol, 2,6-dimethoxy-4-(2-propenyl)- [a]	
Phenol, 2,6-dimethyl- [a]	
Phenol, 2-ethyl- [a]	
Phenol, 2-ethyl-4,5-dimethyl- [a]	
Phenol, 2-ethyl-5-methyl- [a]	
Phenol, 2-ethyl-6-methyl- [a]	
Phenol, 3,5-dimethyl- [a, b]	
Phenol, 3-[(trimethylsilyl)oxy]- [a]	
Phenol, 3-methoxy-2-methyl- [a]	
Phenol, 4-ethyl-2-methoxy- [a, b]	
Phenol, 4-ethyl-3-methyl- [a]	
p-vinyguaiacol [a]	

*a – lignin A: *Eucalyptus spp*; b – lignin B: Pine Tree. Source: From author

Aromatic compounds are initially produced at 600°C and its amounts increased with temperature, indicating that aromatization pathway was improved by the zeolite pores. The intermediate oxygenated compounds, such as guaiacol and OA, diffuse and undergo decarboxylation, decarbonylation, and oligomerization reactions within the ZSM-5 pores. These reactions result in the formation of monocyclic and polycyclic aromatic compounds. Oxygenated aliphatic compounds (AlO) were also produced when the temperature increased and can be related with catalyst acidity which influences hydrogen transfer reactions. The acid sites within the zeolite framework enhance the cleavage of C-O and C-C bonds, which likely contributed to AlO production (RAHMAN; LIU; CAI, 2018).

At 700°C, the production of syringol experienced a decline, suggesting that syringol played a crucial role in the generation of aromatics and AlO compounds. Simultaneously, the

OA amounts increased by nearly 30%. This rise might imply that diffusion limitations for larger molecules prompted secondary reactions involving intermediates like o-quinonemethide. These reactions could contribute to the coke formation on the catalyst surface, providing the deactivation of ZSM-5. Studies claimed that lignin with a high presence of S-units cannot be converted by ZSM-5, since S-units have a larger molecular size than the catalyst pore opening (NISHU *et al.*, 2020). All possible mechanisms are summarized in Figure 37.

Figure 37: Possible mechanism pathways for each temperature in lignin A/ZSM-5.

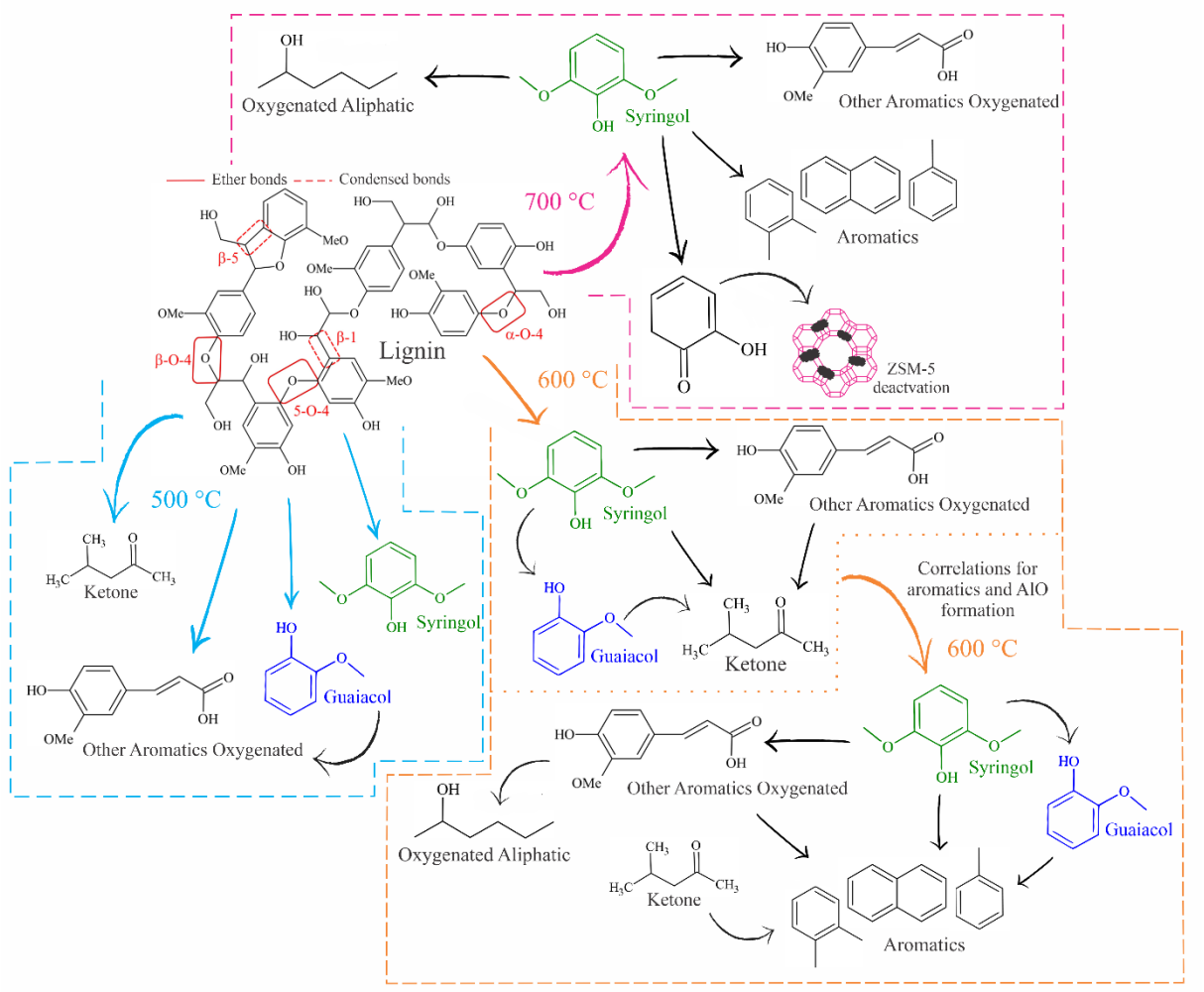

Source: From author

Lignin B showed a greater variety of components with the ZSM-5 presence, which is expected for G-type lignins, that contains more condensable linkages. The lack of guaiacol at 500 °C indicates fragmentation and subsequent re-polymerization of this component to form aromatics, hydrocarbons, AlO and OA. The production of organosulfur could be attributed to the presence of sulfur in the lignin Kraft, and occurs through condensation or

repolymerization reactions, with its production peak at 600 °C (HITA *et al.*, 2018). At 600 °C, syringol was not produced, suggesting that the increase of guaiacol was caused by the degradation of S-units. The decrease of the most components in this temperature occurred because cleavage of the depolymerized linkages requires higher temperatures. In the last temperature, the production of guaiacol decrease by 3.9% leading to a higher production of aromatics and OA. The low ketone presence might be related to the affinity of the ZSM-5 to deoxygenation reactions (RAHMAN; LIU; CAI, 2018). All possible mechanisms are summarized in Figure 38.

Figure 38: Possible mechanism pathways for each temperature in lignin B/ZSM-5.

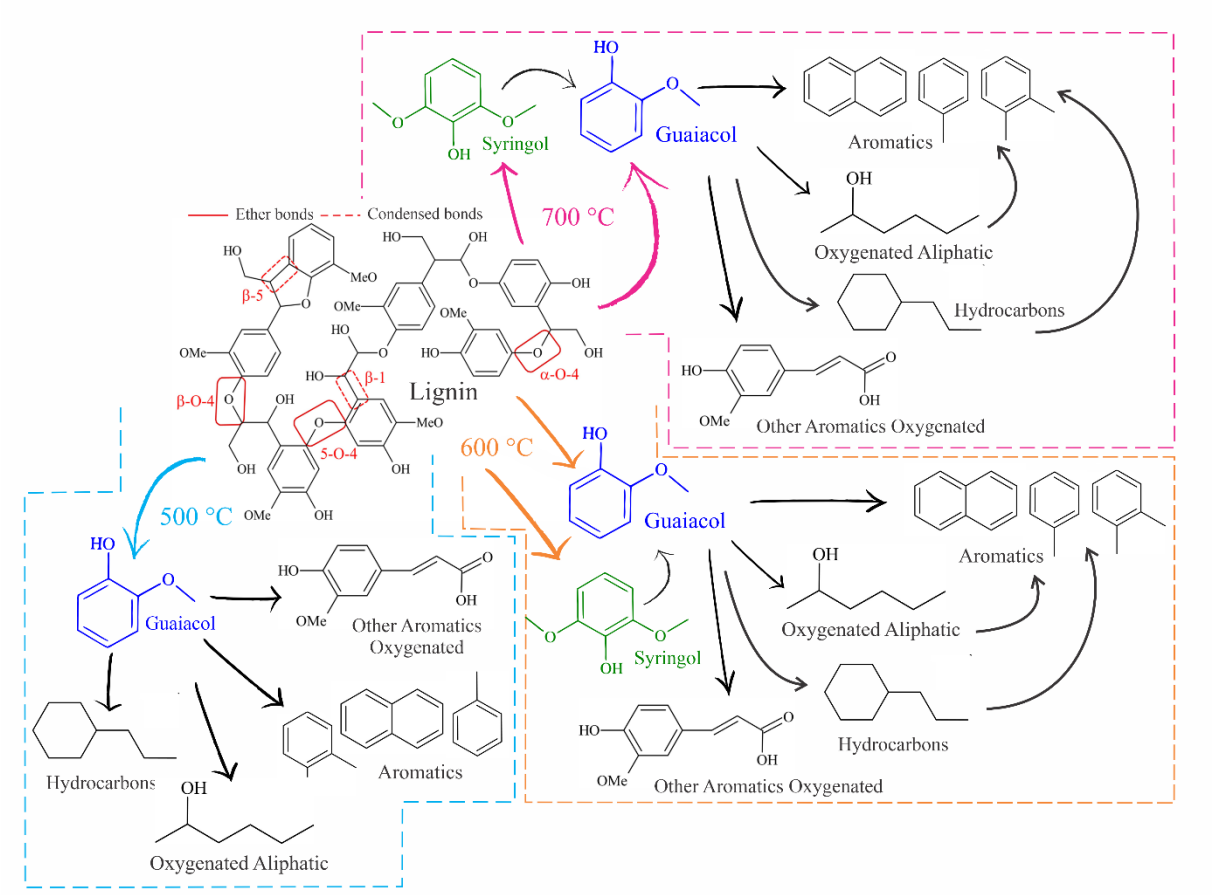

Source: From author

The higher concentration of aromatics in lignin B is associated to selectivity of ZSM-5 to valuable mono-aromatics (BTX) and polyaromatics (naphthalene). These compounds can be formed by Diels-Alder condensation of furan and olefins, or through the hydrocarbon pool mechanism that involves acids, aldehydes, esters, and furans largely converted into aromatics (NISHU *et al.*, 2020; RAHMAN; LIU; CAI, 2018).

Additionally, the interdependence of variables involved in the process was analyzed with the correlation matrixes (as presented in Table 16, Table 17, Table 18), generated by the *Statistica*® software. When the absolute values are close to zero (maximus of 0.25), the correlation degree between variables is low indicating a lack of dependence or a non-linear dependence (MIRANDA, 2016). The plausible scheme for the conversion of oxygenated compounds into aromatics is presented in Figure 39.

Figure 39: A plausible conversion pathway for aromatics hydrocarbons.

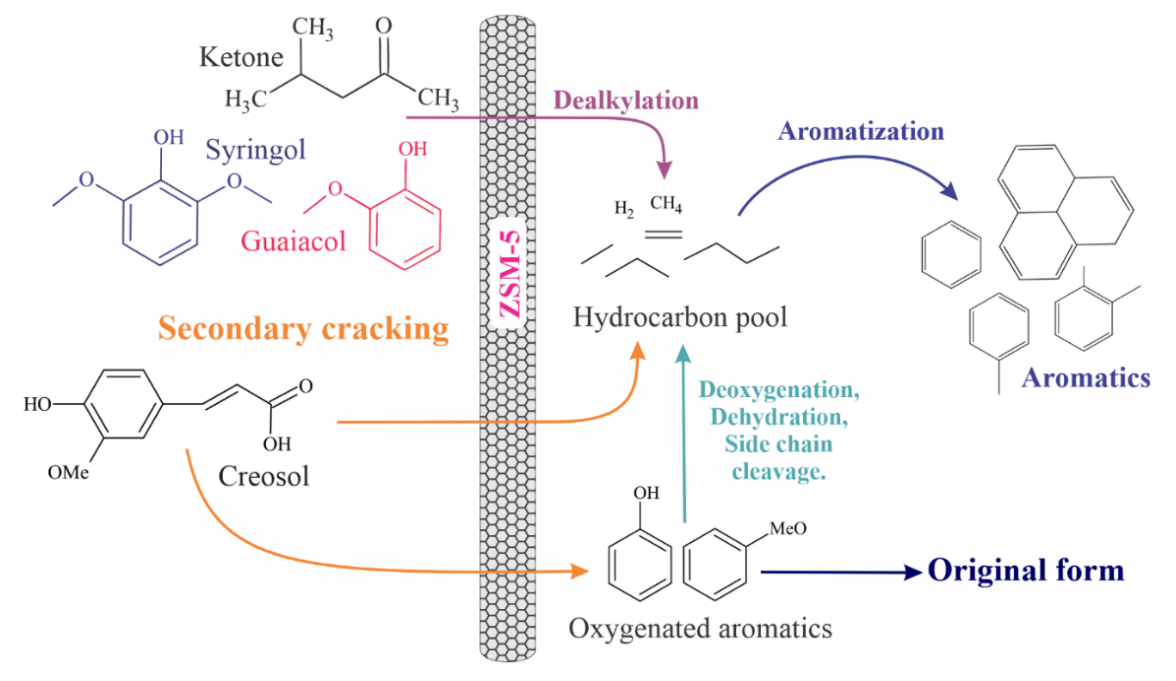

Source: From author

The variables in the Table 16 demonstrated that most of the components present in the bio-oil do not have linear behavior, as can be seen in Figure 36. According to the matrix, the type of lignin (TL) is a decisive factor in the bio-oil distribution composition. The indirect dependence with syringol and ketone shows that a type of lignin has greater affinity on its production, while the low dependence with AlO and OA suggests that both lignins are capable of form these compounds, since their production is favored by the temperature increase. Moreover, the matrix highlighted the correlation between the bio-oil constituents from catalytic pyrolysis, establishing that the formation of one component necessitates the consumption of another. For instance, aromatics, guaiacol, AlO, hydrocarbons (HC), and organosulfur (OS) can be generated through the degradation of syringol and ketone.

From the generated correlation matrix for lignin A/ZSM-5 (Table 17), the increase in KET is attached to the OA by an indirect correlation, caused by the deoxygenation of bio-oil through the degradation of ketones, which involves the conversion of carboxylic and carbonyl oxygenates. In addition, this type of lignin exhibited a high production of UNK products, that are indirectly related to the temperature and aromatics formation. As the matrix suggests, the temperature increase improved the aromatic, AlO, and OA components formation, through guaiacol, syringol, and KET degradation. Therefore, aromatic production might involve an initial deoxygenation reaction, followed by catalytic cracking. This cracking process encompasses the conversion of higher molar mass molecules and dense organic compounds, which originate from fragmentation and re-polymerization during pyrolysis. Next, the hydrocarbon pool eliminates certain compounds, such as acids, aldehydes, esters, and furan, which can ultimately be transformed into aromatics (RAHMAN; LIU; CAI, 2018).

In contrast to lignin A, the components of lignin B/ZSM-5 did not exhibit a strong correlation with temperature. However, the correlation matrix in Table 18 illustrates that guaiacol was formed with the temperature increase, while syringol was consumed. This interdependence indicates that the guaiacol formation at 600 °C and 700 °C was related to the cleavage of syringol, which justified the direct relation between aromatics and syringol since the pathway for their possible formation could come from the degradation of syringol into guaiacol, AlO, and HC. The AlO direct relation with HC and UNK shows that these compounds could be formed simultaneously by OA degradation. The matrix also shows that the KET cleavage could be responsible for the OS formation.

Table 16: Correlation matrix for all variables in the catalytic pyrolysis

Variable	Temp	TL	Aromatics	Guaiacol	Syringol	AlO	HC	OS	OA	KET	UNK
Temp	1.00	-0.08	0.03	0.20	-0.23	0.39	-0.05	-0.17	0.34	0.00	-0.29
TL	-0.08	1.00	0.86	0.57	-0.81	0.02	0.72	0.65	0.01	-0.88	-0.28
Aromatics	0.03	0.86	1.00	0.45	-0.61	-0.15	0.36	0.63	0.24	-0.78	-0.62
Guaiacol	0.20	0.57	0.45	1.00	-0.55	-0.01	0.39	0.62	0.03	-0.53	-0.44
Syringol	-0.23	-0.81	-0.61	-0.55	1.00	-0.35	-0.70	-0.48	0.06	0.61	0.17
AlO	0.39	0.02	-0.15	-0.01	-0.35	1.00	0.29	-0.15	-0.37	0.16	0.06
HC	-0.05	0.72	0.36	0.39	-0.70	0.29	1.00	0.18	-0.10	-0.62	0.17
OS	-0.17	0.65	0.63	0.62	-0.48	-0.15	0.18	1.00	-0.05	-0.60	-0.55
OA	0.34	0.01	0.24	0.03	0.06	-0.37	-0.10	-0.05	1.00	-0.39	-0.44
KET	0.00	-0.88	-0.78	-0.53	0.61	0.16	-0.62	-0.60	-0.39	1.00	0.34
UNK	-0.29	-0.28	-0.62	-0.44	0.17	0.06	0.17	-0.55	-0.44	0.34	1.00

Temp: Temperature; TP: Type of lignin; AlO: Oxygenated Aliphatic; HC: Hydrocarbons; OS: Organosulfur; OA: Others Aromatic oxygenated; KET: Ketone; UNK: Unknown. Source: From author

Table 17: Correlation matrix for Lignin A/ZSM-5

Variable	Temp	Aromatics	Guaiacol	Syringol	AlO	HC	OA	KET	UNK
Temp	1.000	0.654	-0.207	-0.503	0.601	-0.400	0.405	-0.214	-0.751
Aromatics	0.654	1.000	-0.080	-0.242	0.376	-0.158	0.564	-0.339	-0.941
Guaiacol	-0.207	-0.080	1.000	0.133	-0.397	-0.223	0.390	-0.459	0.118
Syringol	-0.503	-0.242	0.133	1.000	-0.527	0.103	0.028	-0.431	0.294
AlO	0.601	0.376	-0.397	-0.527	1.000	-0.492	-0.310	0.413	-0.566
HC	-0.400	-0.158	-0.223	0.103	-0.492	1.000	0.235	-0.131	0.175
OA	0.405	0.564	0.390	0.028	-0.310	0.235	1.000	-0.884	-0.519
KET	-0.214	-0.339	-0.459	-0.431	0.413	-0.131	-0.884	1.000	0.324
UNK	-0.751	-0.941	0.118	0.294	-0.566	0.175	-0.519	0.324	1.000

Source: From author

Table 18: Correlation matrix for Lignin B/ZSM-5

Variable	Temp	Aromatics	Guaiacol	Syringol	AlO	HC	OS	OA	KET	UNK
Temp	1.000	0.127	0.464	-0.548	-0.005	0.036	-0.227	0.257	0.356	-0.104
Aromatics	0.127	1.000	-0.093	0.754	-0.934	-0.756	0.190	0.880	-0.361	-0.801
Guaiacol	0.464	-0.093	1.000	-0.442	0.027	-0.030	0.413	-0.035	-0.277	-0.418
Syringol	-0.548	0.754	-0.442	1.000	-0.750	-0.621	0.207	0.604	-0.446	-0.554
AlO	-0.005	-0.934	0.027	-0.750	1.000	0.918	-0.481	-0.669	0.620	0.815
HC	0.036	-0.756	-0.030	-0.621	0.918	1.000	-0.543	-0.444	0.634	0.644
OS	-0.227	0.190	0.413	0.207	-0.481	-0.543	1.000	-0.200	-0.967	-0.564
OA	0.257	0.880	-0.035	0.604	-0.669	-0.444	-0.200	1.000	0.025	-0.670
KET	0.356	-0.361	-0.277	-0.446	0.620	0.634	-0.967	0.025	1.000	0.667
UNK	-0.104	-0.801	-0.418	-0.554	0.815	0.644	-0.564	-0.670	0.667	1.000

Source: From author

4.3.4.4 Comparison between bio-oil components from thermal and catalytic pyrolysis

As already discussed, catalytic upgrading enhances the bio-oil properties by removing oxygenated compounds as H_2O and CO_2, reducing molecular weight, and altering chemical structure to achieve a desired upgrading effect. ZSM-5 is a promising catalyst because of shape selectivity to obtain hydrocarbons in the range of fossil fuel properties (DICKERSON; SORIA, 2013). For a better understanding of how each type of lignin was affected by ZSM-5, a comparison was made between the same components that appears in the thermal and catalytic pyrolysis, as presented in Figure 40.

Figure 40: Comparison between the main components of thermal and catalytic pyrolysis. (A): Lignin A; (B) Lignin B.

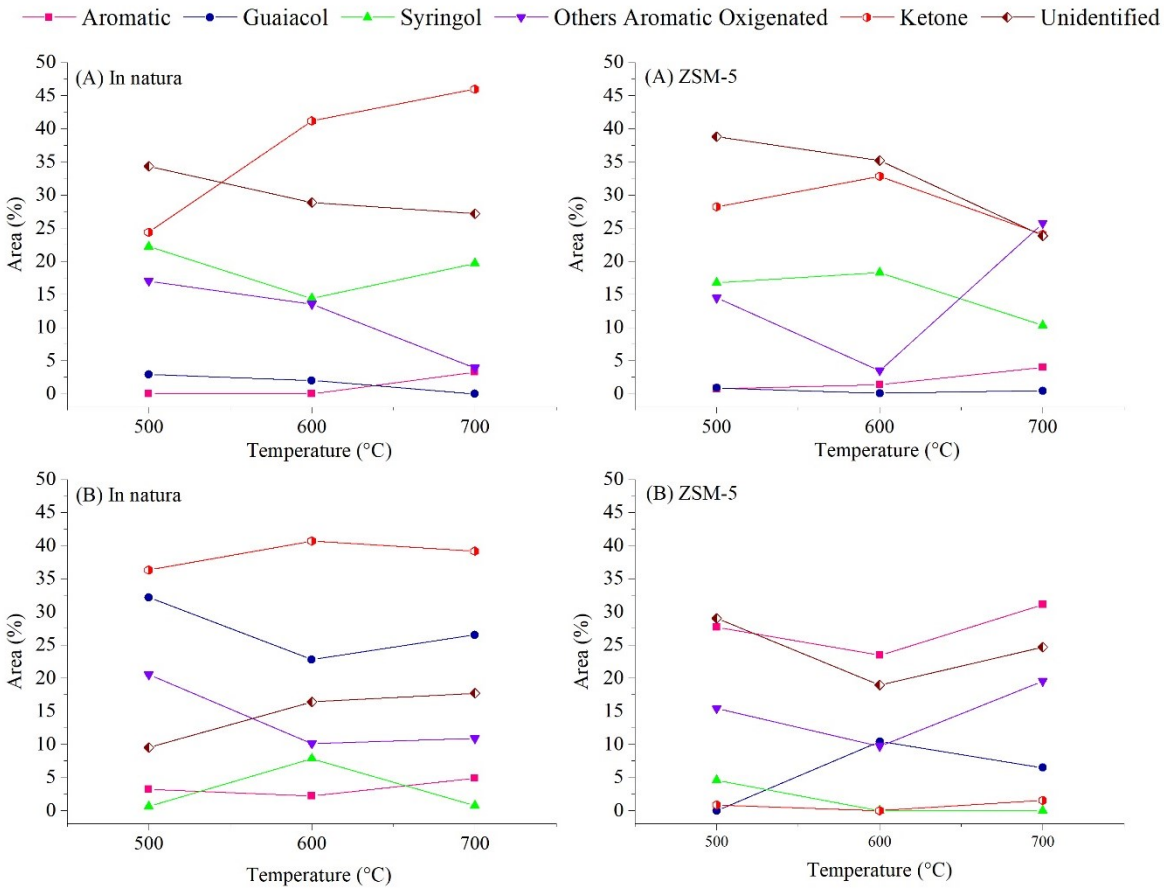

Source: From author

In catalytic pyrolysis of lignin A, guaiacol, syringol, and OA were consumed in low temperatures, with production of KET and UNK. At 600 °C, the syringol production increased, which can indicate the cleaved of OA linkages that have syringyl as repeating unit,

since the OA decreased. Aromatics components started to appear at 600 °C, unlike the thermal pyrolysis, highlighting the ZSM-5 selectivity. The high area of OA at 700 °C of lignin A/ZSM-5 and the decrease of all other compounds can be a result of carbonaceous species formed at the active site in the ZSM-5 that catalytically convert vapor into aromatics species. However, since carbonaceous species comprise a mixture of coke and biochar, coke may form on external acid sites instead of hydrocarbon compounds. This can deactivate the catalyst and prevent the degradation of OA into other components. (NISHU *et al.*, 2020).

Because lignin B possess more condensed units, its affinity to ZSM-5 was stronger, and lead to a wider variety of components. When the main components are compared, one can see that guaiacol was consumed in lower temperature. Therefore, guaiacol also represented a pathway to formation of aromatics in this temperature. In addition, syringol started to appear as well as other components, indicating that the ZSM-5 selectivity allowed the cleave of ether linkages. The guaiacol production at higher temperatures and syringol consumption suggested another route for aromatic formation. Repolymerized products are more resistant to depolymerization, what increase the difficulty of further conversion, explained why guaiacol was not fully consumed, and the high yield of aromatics was at 700 °C (CHIO; SAIN; QIN, 2019). The reason for OA high area at 700 °C can be also related to the catalyst deactivation. It was seen that ZSM-5 fulfill its role in reduction of bio-oil oxygenates compounds, since most of KET was consumed and much of its composition is formed by aromatics hydrocarbons.

For a better understanding of how the components were affected by the catalyst, a correlation matrix was generated by the *Statistica* software and presented in Table 19. According to the matrix, the temperature varied and had a non-linear correlation with the bio-oil components, although the type of lignin and the catalyst presence affected the amounts and selectivity of the products. As suggested by the matrix, the aromatics presented a direct dependence with ZSM-5, HC, OS, and the type of lignin. The indirect correlation between guaiacol, syringol, KET with the majority of bio-oil constituents indicates that the primary route for their formation was through guaiacol, syringol, KET degradation. The correlation matrix also suggests an indirect dependence between KET and OA, which indicates that the formation of OA is related to the deoxygenation reaction of KET components.

Table 19: Correlation matrix for all variables considered in the thermal and catalytic pyrolysis.

Variable	Temp	TL	Catalyst	Aromatics	Guaiacol	Syringol	AlO	HC	OS	OA	KET	UNK
Temp	1.00	-0.04	0.04	0.09	-0.06	-0.10	0.22	-0.01	-0.08	-0.08	0.09	-0.11
TL	-0.04	1.00	-0.10	0.50	0.55	-0.65	-0.06	0.39	0.36	0.06	-0.16	-0.49
Catalyst	0.04	-0.10	1.00	0.47	-0.39	-0.07	0.69	0.43	0.38	0.09	-0.38	0.26
Aromatics	0.09	0.50	0.47	1.00	-0.07	-0.36	0.23	0.48	0.68	0.16	-0.40	-0.32
Guaiacol	-0.06	0.55	-0.39	-0.07	1.00	-0.28	-0.27	-0.10	-0.04	0.33	-0.29	-0.39
Syringol	-0.10	-0.65	-0.07	-0.36	-0.28	1.00	-0.17	-0.34	-0.24	0.14	-0.28	0.54
AlO	0.22	-0.06	0.69	0.23	-0.27	-0.17	1.00	0.48	0.16	-0.11	-0.22	0.21
HC	-0.01	0.39	0.43	0.48	-0.10	-0.34	0.48	1.00	0.31	-0.02	-0.37	0.22
OS	-0.08	0.36	0.38	0.68	-0.04	-0.24	0.16	0.31	1.00	0.00	-0.35	-0.25
OA	-0.08	0.06	0.09	0.16	0.33	0.14	-0.11	-0.02	0.00	1.00	-0.63	-0.14
KET	0.09	-0.16	-0.38	-0.40	-0.29	-0.28	-0.22	-0.37	-0.35	-0.63	1.00	-0.28
UNK	-0.11	-0.49	0.26	-0.32	-0.39	0.54	0.21	0.22	-0.25	-0.14	-0.28	1.00

Source: From author

ZSM-5 is known by its potential in reduction of oxygen content. Figure 41 exhibit a comparation between thermal and catalytic bio-oil composition, considering all known oxygenated and non-oxygenated compounds. Lignin A presented a decrease of oxygenated compounds in 500 and 600°C with an increase at 700°C, while non-oxygenated increased an average of 3 % with increase of temperature. Lignin B lost a greater amount of oxygen, an average of 52 % with the temperature increase, forming about 41.6 % of non-oxygenated compounds. Therefore, the catalyst has a higher affinity to softwood lignins, such as Lignin B, than hardwood lignins.

Figure 41: Comparison of oxygen reduction in the presence of ZSM-5 catalyst.

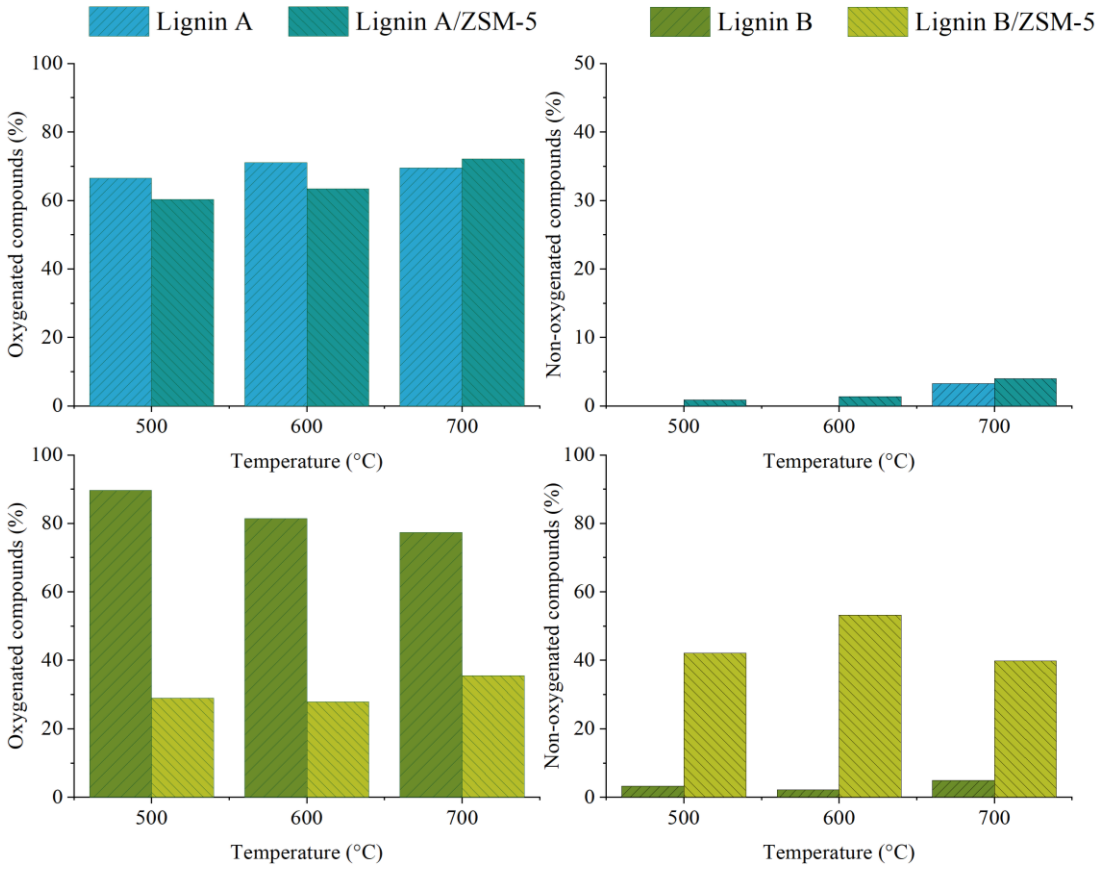

Source: From author

4.4 CONCLUDING REMARKS

This study aimed to understand the ZSM-5 effects on the selectivity of phenolics and aromatics production in the bio-oil of two different kraft lignin types. By comparing the detailed characterization of hardwood and softwood lignin used in the thermal pyrolysis tests with the catalytic tests, the possible pathways for products formation, bio-oil composition, and affinity of each lignin with the ZSM-5 were evaluated. The catalyst effect on both samples was related to a decrease in biochar and gas production, while the bio-oil increased. However, the behavior of bio-oil composition was quite different for both lignin, given that lignin B demonstrated a greater diversity in the composition with a much higher aromatics yield than lignin A.

The type of lignin was the main factor that accounted for the diversity of components, as lignin A had a high -OCH_3 content resulting from S-unit linkages. Particularly, the conversion of high chain size molecules was hindered because the molecular size is higher than the pore opening of ZSM-5, as well as can possibly cause the catalyst deactivation. In this sense, the use of hardwood lignin to produce aromatics compounds requires the improvement of deoxygenation reactions. In this case, functionalization of zeolite, with treatments that improve their acidity and porosity characteristics is a potential way. In future studies, this research may be useful to produce specific compounds or high-added values from kraft lignin. The study about the effects of ZSM-5 in different types of lignins can help the understanding of pyrolysis product pathways and be used to optimize the biorefinery industry.

.

CHAPTER 5

This chapter presents the main conclusion obtained from this research, as well as suggestions for future works.

.

5 CONCLUSIONS

The main repeating units of the lignin samples were guaiacyl and syringyl, and their thermal degradation followed different pathways through the pyrolysis process. The methoxy group content, particularly in hardwood lignin (lignin A), plays a significant role in both primary and secondary pyrolysis. The high -OCH_3 content affects the biochar yield and requires higher temperatures to produce aromatics in the bio-oil. Conversely, softwood lignin (lignin B) has a higher affinity to produce aromatics due to a higher density of condensable bonds.

The primary outputs of thermal pyrolysis are gases (21 – 49 wt.%) and biochar (41 – 65 wt.%) while the bio-oil presented a yield of 6 – 15% wt%. Higher temperatures allowed for the production of bio-oil with aromatics presence in the pyrolysis of both Kraft lignin samples. Softwood lignin produced an average of 14% and 2% more oxygenated and non-oxygenated compounds, respectively, than hardwood lignin. With the assistance of the correlation matrices, a mechanism for aromatics compound formation by syringol decomposition was established. Temperature also affected the biochar content since most oxygenated compounds are converted into condensable and non-condensable gases.

The study also focused on the effects of ZSM-5 on the selectivity of phenolics and aromatics production in the bio-oil derived from two sources of Kraft lignin. Comparing the characterization and yields results of by-products from thermal and catalytic pyrolysis of hardwood and softwood lignin, the catalyst decreased biochar (34 – 65 wt.%) and gases (20 – 41 wt.%) production while increasing the bio-oil yield (14 – 29 wt.%). Moreover, there are differences in the oil composition between lignin A and lignin B, with lignin B demonstrating a greater diversity and higher aromatics yield by 25,4%. Regarding the bio-oil composition, the oxygenated compounds decreased by only 3.7% in bio-oil derived from lignin A, while the non-oxygenated compounds increased by 1%. Regarding bio-oil derived from lignin B, the oxygenated compounds decreased by about 52%, while the non-oxygenated compounds increased by 41.6%.

The source of lignin is a significant factor, which affects the diversity of components in bio-oil. The high -OCH_3 group content in lignin A hindered the conversion of high molar mass components due to their larger molecular size than the pore opening of ZSM-5. This could potentially cause the catalyst deactivation by pore entrapping. To produce aromatic compounds from hardwood lignin, it is required to enhance the deoxygenation reactions of

ZSM-5 by modifying the zeolite to improve its acidity and porosity characteristics. Another strategy requires the use of a reducing agent, such as hydrogen, in hydrocracking processes. Additionally, studies focused on catalyst deactivation and its reuse are also required to ensure the economic viability of pyrolysis processes. In this context, the use of sequential cracking reactors for thermal and catalytic reactions is an interesting strategy.

This research has potential usefulness for future studies aiming to produce specific compounds or high-added value products from Kraft lignin. It can help in understanding the pathways of pyrolysis products and the effects of ZSM-5 on different sources of lignin, as well as providing insights into possible catalyst modification.

REFERENCES

ADAMS, R. P. **IDENTIFICATION OF ESSENTIAL OIL COMPONENTS BY GAS CHROMATOGRAPHY/ MASS SPECTROMETRY, ed. 4.1**. *[S. l.: s. n.]*.

ASTM. E1131-08: Standard Test Method for Compositional Analysis by Thermogravimetry. **ASTM International**, p. 1–6, 2014. Disponível em: https://doi.org/https://doi.org/10.1520/E1131

ASTM. D5373-08: Standard test methods for instrumental determination of carbon, hydrogen, and nitrogen in laboratory samples of coal and coke. **ASTM International**, p. 4, 2016 a. Disponível em: https://doi.org/https://doi.org/10.1520/D5373-16

ASTM. D2702-05: Standard Practice for Rubber Chemicals — Determination of Infrared Absorption Characteristics. **ASTM International**, p. 4, 2016 b. Disponível em: https://doi.org/https://doi.org/10.1520/D2702-05R16

BARDET, M.; GERBAUD, G.; GIFFARD, M.; DOAN, C.; HEDIGER, S.; PAPE, L. Le. 13C high-resolution solid-state NMR for structural elucidation of archaeological woods. **Progress in Nuclear Magnetic Resonance Spectroscopy**, v. 55, n. 3, p. 199–214, 2009. Disponível em: https://doi.org/10.1016/j.pnmrs.2009.02.001

BASU, P. **Biomass Gasification, Pyrolysis and Torrefaction: Practical Design and Theory**. Second ed. *[S. l.]*: Elsevier, 2013.

BEN, H.; RAGAUSKAS, A. J. NMR characterization of pyrolysis oils from kraft lignin. **Energy and Fuels**, v. 25, n. 5, p. 2322–2332, 2011. Disponível em: https://doi.org/10.1021/ef2001162

BI, Y.; LEI, X.; XU, G.; CHEN, H.; HU, J. Catalytic fast pyrolysis of kraft lignin over hierarchical HZSM-5 and Hβ zeolites. **Catalysts**, v. 8, n. 2, 2018. Disponível em: https://doi.org/10.3390/catal8020082

BIZZO, H. R.; BARBOZA, E. G.; SANTOS, M. C. S.; GAMA, P. E. A set of electronic sheets for the identification and quantification of constituents of essential oils. **Quimica Nova**, v. 43, n. 1, p. 98–105, 2020. Disponível em: https://doi.org/10.21577/0100-4042.20170458

BORELLA, M.; CASAZZA, A. A.; GARBARINO, G.; RIANI, P.; BUSCA, G. Conversion of Lignin to Chemical Intermediates: a Study of Pyrolysis of Kraft Lignin. **Chemical Engineering Transactions**, v. 92, n. January, p. 631–636, 2022 a. Disponível em: https://doi.org/10.3303/CET2292106

BORELLA, M.; CASAZZA, A. A.; GARBARINO, G.; RIANI, P.; BUSCA, G. A Study of the Pyrolysis Products of Kraft Lignin. **Energies**, v. 15, n. 3, 2022 b. Disponível em: https://doi.org/10.3390/en15030991

BRIDGWATER, A. V. Review of fast pyrolysis of biomass and product upgrading. **Biomass and Bioenergy**, v. 38, p. 68–94, 2012. Disponível em: https://doi.org/10.1016/j.biombioe.2011.01.048

BRIDGWATER, A. V.; CZERNIK, S.; PISKORZ, J. An Overview of Fast Pyrolysis. **Progress in Thermochemical Biomass Conversion**, v. 30, p. 977–997, 2008. Disponível em: https://doi.org/10.1002/9780470694954.ch80

CHAKAR, F. S.; RAGAUSKAS, A. J. Review of current and future softwood kraft lignin process chemistry. *In*: 2004, **Industrial Crops and Products**. *[S. l.: s. n.]* p. 131–

141.Disponível em: https://doi.org/10.1016/j.indcrop.2004.04.016

CHEN, X.; CHE, Q.; LI, S.; LIU, Z.; YANG, H.; CHEN, Y.; WANG, X.; SHAO, J.; CHEN, H. Recent developments in lignocellulosic biomass catalytic fast pyrolysis : Strategies for the optimization of bio-oil quality and yield. **Fuel Processing Technology**, v. 196, n. August, p. 106180, 2019. Disponível em: https://doi.org/10.1016/j.fuproc.2019.106180

CHIO, C.; SAIN, M.; QIN, W. **Lignin utilization: A review of lignin depolymerization from various aspects**. *[S. l.]*: Elsevier Ltd, 2019. Disponível em: https://doi.org/10.1016/j.rser.2019.03.008

CHOI, H. S.; MEIER, D. Fast pyrolysis of Kraft lignin - Vapor cracking over various fixed-bed catalysts. **Journal of Analytical and Applied Pyrolysis**, v. 100, p. 207–212, 2013. Disponível em: https://doi.org/10.1016/j.jaap.2012.12.025

COLLARD, F. X.; BLIN, J. **A review on pyrolysis of biomass constituents: Mechanisms and composition of the products obtained from the conversion of cellulose, hemicelluloses and lignin**. *[S. l.]*: Elsevier Ltd, 2014. Disponível em: https://doi.org/10.1016/j.rser.2014.06.013

CUI, J.; CHEN, R.; LEI, L.; HOU, Y. Green wood pulping processes with high pulp yield and lignin recovery yield by deep eutectic solvent and its aqueous solutions. **Biomass Conversion and Biorefinery**, n. 0123456789, 2022. Disponível em: https://doi.org/10.1007/s13399-022-03498-7

DA SILVA, J. C. G.; PEREIRA, J. L. C.; ANDERSEN, S. L. F.; MOREIRA, R. de F. P. M.; JOSÉ, H. J. Torrefaction of ponkan peel waste in tubular fixed-bed reactor: In-depth bioenergetic evaluation of torrefaction products. **Energy**, v. 210, 2020. Disponível em: https://doi.org/10.1016/j.energy.2020.118569

DEMUNER, I. F.; COLODETTE, J. L.; DEMUNER, A. J.; JARDIM, C. M. Biorefinery review: Wide-reaching products through kraft lignin. **BioResources**, v. 14, n. 3, p. 7543–7581, 2019. Disponível em: https://doi.org/10.15376/biores.14.3.demuner

DICKERSON, T.; SORIA, J. Catalytic fast pyrolysis: A review. **Energies**, v. 6, n. 1, p. 514–538, 2013. Disponível em: https://doi.org/10.3390/en6010514

DIEHL, B. G.; BROWN, N. R.; FRANTZ, C. W.; LUMADUE, M. R.; CANNON, F. Effects of pyrolysis temperature on the chemical composition of refined softwood and hardwood lignins. **Carbon**, v. 60, p. 531–537, 2013. Disponível em: https://doi.org/10.1016/j.carbon.2013.04.087

DOS SANTOS, J. G. F. J. **Monitoramento e controle dos tamanhos de partículas em polimerizações em suspensão do MMA usando NIRS**. 2012. *[s. l.]*, 2012.

EUGENIO, M. E.; IBARRA, D.; MARTÍN-SAMPEDRO, R.; ESPINOSA, E.; BASCÓN, I.; RODRÍGUEZ, A. Alternative Raw Materials for Pulp and Paper Production in the Concept of a Lignocellulosic Biorefinery. **Cellulose**, 2019. Disponível em: https://doi.org/10.5772/intechopen.90041

FARAG, S.; MUDRABOYINA, B. P.; JESSOP, P. G.; CHAOUKI, J. Biomass and Bioenergy Impact of the heating mechanism on the yield and composition of bio-oil from pyrolysis of kraft lignin. **Biomass and Bioenergy**, p. 1–10, 2016. Disponível em: https://doi.org/10.1016/j.biombioe.2016.07.005

FODIL CHERIF, M.; TRACHE, D.; BROSSE, N.; BENALIOUCHE, F.; TARCHOUN, A. F. Comparison of the Physicochemical Properties and Thermal Stability of

Organosolv and Kraft Lignins from Hardwood and Softwood Biomass for Their Potential Valorization. **Waste and Biomass Valorization**, v. 11, n. 12, p. 6541–6553, 2020. Disponível em: https://doi.org/10.1007/s12649-020-00955-0

FRENCH, R.; CZERNIK, S. Catalytic pyrolysis of biomass for biofuels production. **Fuel Processing Technology**, v. 91, n. 1, p. 25–32, 2010. Disponível em: https://doi.org/10.1016/j.fuproc.2009.08.011

GAMMAN, J. J.; JACKSON, S. D.; WIGZELL, F. A. Synthesis of methyl isobutyl ketone over Pd/MgO/SiO2. **Industrial and Engineering Chemistry Research**, v. 49, n. 18, p. 8439–8443, 2010. Disponível em: https://doi.org/10.1021/ie100770e

GELLERSTEDT, G. **Softwood kraft lignin: Raw material for the future**. *[S. l.]*: Elsevier, 2015. Disponível em: https://doi.org/10.1016/j.indcrop.2015.09.040

HARTANTO, D.; YUAN, L. S.; MUTIA SARI, S.; SUGIARSO, D.; KRIS MURWARNI, I.; ERSAM, T.; PRASETYOKO, D.; NUR, H. The use of the combination of ftir, Pyridine adsorption, 27Al and 29Si MAS NMR to determine the Brönsted and lewis acidic sites. **Jurnal Teknologi**, v. 78, n. 6, p. 223–228, 2016. Disponível em: https://doi.org/10.11113/jt.v78.8821

HÁZ, A.; JABLONSKÝ, M.; ŠURINA, I.; KAČÍK, F.; BUBENÍKOVÁ, T.; ĎURKOVIČ, J. Chemical composition and thermal behavior of kraft lignins. **Forests**, v. 10, n. 6, p. 1–12, 2019. Disponível em: https://doi.org/10.3390/f10060483

HEITNER, C.; DIMMEL, D.; SCHMIDT, J. A. **Lignin and lignans : advances in chemistry**. *[S. l.]*: CRC Press, Taylor & Francis, 2010.

HERNÁNDEZ, M. A.; ABBASPOURRAD, A.; PETRANOVSKII, V.; ROJAS, F.; PORTILLO, R.; SALGADO, M. A.; HERNÁNDEZ, G.; VELAZCO, M. de los A.; AYALA, E.; QUIROZ, K. F. Estimation of Nanoporosity of ZSM-5 Zeolites as Hierarchical Materials. **Zeolites and Their Applications**, 2018. Disponível em: https://doi.org/10.5772/intechopen.73624

HILL, S. J.; GRIGSBY, W. J.; HALL, P. W. Chemical and cellulose crystallite changes in Pinus radiata during torrefaction. **Biomass and Bioenergy**, v. 56, p. 92–98, 2013. Disponível em: https://doi.org/10.1016/j.biombioe.2013.04.025

HITA, I.; DEUSS, P. J.; BONURA, G.; FRUSTERI, F.; HEERES, H. J. Biobased chemicals from the catalytic depolymerization of Kraft lignin using supported noble metal-based catalysts. **Fuel Processing Technology**, v. 179, p. 143–153, 2018. Disponível em: https://doi.org/10.1016/j.fuproc.2018.06.018

HUANG, J. B.; LIU, C.; REN, L. R.; TONG, H.; LI, W. M.; WU, D. Studies on pyrolysis mechanism of syringol as lignin model compound by quantum chemistry. **Ranliao Huaxue Xuebao/Journal of Fuel Chemistry and Technology**, v. 41, n. 6, p. 657–666, 2013. Disponível em: https://doi.org/10.1016/s1872-5813(13)60031-6

ILIOPOULOU, E. F.; STEFANIDIS, S. D.; KALOGIANNIS, K. G.; DELIMITIS, A.; LAPPAS, A. A.; TRIANTAFYLLIDIS, K. S. Applied Catalysis B : Environmental Catalytic upgrading of biomass pyrolysis vapors using transition metal-modified ZSM-5 zeolite. **"Applied Catalysis B, Environmental"**, v. 127, p. 281–290, 2012 a. Disponível em: https://doi.org/10.1016/j.apcatb.2012.08.030

ILIOPOULOU, E. F.; STEFANIDIS, S. D.; KALOGIANNIS, K. G.; DELIMITIS, A.; LAPPAS, A. A.; TRIANTAFYLLIDIS, K. S. Catalytic upgrading of biomass pyrolysis vapors using transition metal-modified ZSM-5 zeolite. **Applied Catalysis B:**

Environmental, v. 127, p. 281–290, 2012 b. Disponível em: https://doi.org/10.1016/J.APCATB.2012.08.030

JABLONSKY, M.; BOTKOVA, M.; ADAMOVSKA, J. Prediction of methoxyl groups content in lignin based on ultimate analysis. **Cellulose Chemistry and Technology**, v. 49, n. 2, p. 165–168, 2015.

JAHIRUL, M. I.; RASUL, M. G.; CHOWDHURY, A. A.; ASHWATH, N. Biofuels production through biomass pyrolysis- A technological review. **Energies**, v. 5, n. 12, p. 4952–5001, 2012. Disponível em: https://doi.org/10.3390/en5124952

JIANG, G.; NOWAKOWSKI, D. J.; BRIDGWATER, A. V. A systematic study of the kinetics of lignin pyrolysis. **Thermochimica Acta**, v. 498, n. 1–2, p. 61–66, 2010 a. Disponível em: https://doi.org/10.1016/j.tca.2009.10.003

JIANG, G.; NOWAKOWSKI, D. J.; BRIDGWATER, A. V. Effect of the temperature on the composition of lignin pyrolysis products. **Energy and Fuels**, v. 24, n. 8, p. 4470–4475, 2010 b. Disponível em: https://doi.org/10.1021/ef100363c

KABIR, G.; HAMEED, B. H. Recent progress on catalytic pyrolysis of lignocellulosic biomass to high-grade bio-oil and bio-chemicals. **Renewable and Sustainable Energy Reviews**, v. 70, n. January, p. 945–967, 2017. Disponível em: https://doi.org/10.1016/j.rser.2016.12.001

KANG, S.; ASMELASH, E. Bioenergy , the undervalued pillar of the clean energy transition. **Smart Energy International**, n. December, p. 1–6, 2021. Disponível em: https://www.smart-energy.com/features-analysis/bioenergy-the-undervalued-pillar-of-the-clean-energy-transition/

KAWAMOTO, H. **Lignin pyrolysis reactions**. *[S. l.]*: Springer Tokyo, 2017. Disponível em: https://doi.org/10.1007/s10086-016-1606-z

KIM, J. Y.; LEE, J. H.; PARK, J.; KIM, J. K.; AN, D.; SONG, I. K.; CHOI, J. W. Catalytic pyrolysis of lignin over HZSM-5 catalysts: Effect of various parameters on the production of aromatic hydrocarbon. **Journal of Analytical and Applied Pyrolysis**, v. 114, p. 273–280, 2015. Disponível em: https://doi.org/10.1016/j.jaap.2015.06.007

KIM, J. Y.; MOON, J.; LEE, J. H.; JIN, X.; CHOI, J. W. Conversion of phenol intermediates into aromatic hydrocarbons over various zeolites during lignin pyrolysis. **Fuel**, v. 279, n. February, p. 118484, 2020. Disponível em: https://doi.org/10.1016/j.fuel.2020.118484

KUMAR, A.; KUMAR, A.; KUMAR, J.; BHASKAR, T. Catalytic pyrolysis of soda lignin over zeolites using pyrolysis gas chromatography-mass spectrometry. **Bioresource Technology**, v. 291, 2019. Disponível em: https://doi.org/10.1016/j.biortech.2019.121822

KUMAR, V. **PYROLYSIS AND GASIFICATION OF LIGNIN AND EFFECT OF ALKALI ADDITION**. *[S. l.: s. n.]*.

KUTHI, F. A. A.; NORZALI, N. R. ‘Adawiyah; BADRI, K. H. Sifat terma mikrokristal selulosa daripada biojisim tandan kosong sawit. **Malaysian Journal of Analytical Sciences**, v. 20, n. 5, p. 1112–1122, 2016. Disponível em: https://doi.org/10.17576/mjas-2016-2005-17

LARENTIS, A. L.; BENTES, A. M. P.; DE RESENDE, N. S.; SALIM, V. M. M.; PINTO, J. C. Analysis of experimental errors in catalytic tests for production of synthesis gas. **Applied Catalysis A: General**, v. 242, n. 2, p. 365–379, 2003. Disponível em:

https://doi.org/10.1016/S0926-860X(02)00525-2

LAZARIDIS, P. A.; FOTOPOULOS, A. P.; KARAKOULIA, S. A.; TRIANTAFYLLIDIS, K. S. Catalytic fast pyrolysis of kraft lignin with conventional, mesoporous and nanosized ZSM-5 zeolite for the production of alkyl-phenols and aromatics. **Frontiers in Chemistry**, v. 6, 2018 a. Disponível em: https://doi.org/10.3389/fchem.2018.00295

LAZARIDIS, P. A.; FOTOPOULOS, A. P.; KARAKOULIA, S. A.; TRIANTAFYLLIDIS, K. S. Supplementary Material - Catalytic fast pyrolysis of kraft lignin with conventional, mesoporous and nanosized ZSM-5 zeolite for the production of alkyl-phenols and aromatics. **Frontiers in Chemistry**, v. 6, n. JUL, p. 1–4, 2018 b. Disponível em: https://doi.org/10.3389/fchem.2018.00295

LEE, H.; KIM, Y. M.; JUNG, K. Bin; JAE, J.; JUNG, S. C.; JEON, J. K.; PARK, Y. K. Catalytic hydrodeoxygenation of Geodae-Uksae pyrolysis oil over Ni/desilicated HZSM-5. **Journal of Cleaner Production**, v. 174, p. 763–770, 2018. Disponível em: https://doi.org/10.1016/j.jclepro.2017.10.315

LEE, H. W.; CHA, J. S.; PARK, Y. K. Catalytic co-pyrolysis of kraft lignin with refuse-derived fuels using ni-loaded ZSM-5 type catalysts. **Catalysts**, v. 8, n. 11, 2018. Disponível em: https://doi.org/10.3390/catal8110506

LI, B.; LV, W.; ZHANG, Q.; WANG, T.; MA, L. Pyrolysis and catalytic pyrolysis of industrial lignins by TG-FTIR: Kinetics and products. **Journal of Analytical and Applied Pyrolysis**, v. 108, p. 295–300, 2014. Disponível em: https://doi.org/10.1016/j.jaap.2014.04.002

LI, C.; ZHAO, X.; WANG, A.; HUBER, G. W.; ZHANG, T. **Catalytic Transformation of Lignin for the Production of Chemicals and Fuels**. *[S. l.]*: American Chemical Society, 2015. Disponível em: https://doi.org/10.1021/acs.chemrev.5b00155

LI, G.; LUO, Z.; WANG, W.; CEN, J. A Study of the Mechanisms of Guaiacol Pyrolysis Based on Free Radicals Detection Technology. 2020 a.

LI, X.; SU, L.; WANG, Y.; YU, Y.; WANG, C.; LI, X.; WANG, Z. Catalytic fast pyrolysis of Kraft lignin with HZSM-5 zeolite for producing aromatic hydrocarbons. **Frontiers of Environmental Science and Engineering in China**, v. 6, n. 3, p. 295–303, 2012. Disponível em: https://doi.org/10.1007/s11783-012-0410-2

LI, Y.; XING, B.; DING, Y.; HAN, X.; WANG, S. A critical review of the production and advanced utilization of biochar via selective pyrolysis of lignocellulosic biomass. **Bioresource Technology**, v. 312, n. March, p. 123614, 2020 b. Disponível em: https://doi.org/10.1016/j.biortech.2020.123614

LIU, C.; YE, L.; YUAN, W.; ZHANG, Y.; ZOU, J.; YANG, J.; WANG, Y.; QI, F.; ZHOU, Z. Investigation on pyrolysis mechanism of guaiacol as lignin model compound at atmospheric pressure. **Fuel**, v. 232, n. January, p. 632–638, 2018. Disponível em: https://doi.org/10.1016/j.fuel.2018.05.162

LU, X.; GU, X. **A review on lignin pyrolysis: pyrolytic behavior, mechanism, and relevant upgrading for improving process efficiency**. *[S. l.]*: BioMed Central, 2022. v. 15. *E-book*. Disponível em: https://doi.org/10.1186/s13068-022-02203-0

LUNA, F. J.; SCHUCHARDT, U. Modificação de Zeólitas para uso de catálise. v. 24, n. 6, p. 885–892, 2001. Disponível em: https://doi.org/https://doi.org/10.1590/S0100-40422001000600027

MA, Z.; YANG, Y.; WU, Y.; XU, J.; PENG, H.; LIU, X.; ZHANG, W.; WANG, S. In-depth comparison of the physicochemical characteristics of bio-char derived from biomass pseudo components: Hemicellulose, cellulose, and lignin. **Journal of Analytical and Applied Pyrolysis**, v. 140, n. December 2018, p. 195–204, 2019. Disponível em: https://doi.org/10.1016/j.jaap.2019.03.015

MAŁACHOWSKA, E.; DUBOWIK, M.; BORUSZEWSKI, P.; ŁOJEWSKA, J.; PRZYBYSZ, P. Influence of lignin content in cellulose pulp on paper durability. **Scientific Reports**, v. 10, n. 1, p. 1–12, 2020. Disponível em: https://doi.org/10.1038/s41598-020-77101-2

MANTE, O. D.; AGBLEVOR, F. A.; OYAMA, S. T.; MCCLUNG, R. The influence of recycling non-condensable gases in the fractional catalytic pyrolysis of biomass. **Bioresource Technology**, v. 111, p. 482–490, 2012. Disponível em: https://doi.org/10.1016/j.biortech.2012.02.015

MELKIOR, T.; JACOB, S.; GERBAUD, G.; HEDIGER, S.; LE PAPE, L.; BONNEFOIS, L.; BARDET, M. NMR analysis of the transformation of wood constituents by torrefaction. **Fuel**, v. 92, n. 1, p. 271–280, 2012. Disponível em: https://doi.org/10.1016/j.fuel.2011.06.042

MINU, K.; JIBY, K. K.; KISHORE, V. V. N. Isolation and purification of lignin and silica from the black liquor generated during the production of bioethanol from rice straw. **Biomass and Bioenergy**, v. 39, p. 210–217, 2012. Disponível em: https://doi.org/10.1016/j.biombioe.2012.01.007

MIRANDA, D. M. V. de. Degradação Térmica E Catalítica Dos Polímeros Poli(Acrilonitrila-Co-Butadieno-Co-Estireno) (Abs) E Poliestireno De Alto Impacto (Hips) Oriundos De Resíduos Eletroeletrônicos. p. 1–194, 2016.

MOHAN, D.; PITTMAN, C. U.; STEELE, P. H. **Pyrolysis of wood/biomass for bio-oil: A critical review**. *[S. l.: s. n.]* Disponível em: https://doi.org/10.1021/ef0502397

MONICA EK, GÖRAN GELLERSTEDT, G. H. **Pulp and Paper Chemistry and Technology Volume 2**. *[S. l.: s. n.]*. v. 22.

MUMBACH, G. D.; ALVES, J. L. F.; DA SILVA, J. C. G.; DE SENA, R. F.; MARANGONI, C.; MACHADO, R. A. F.; BOLZAN, A. Thermal investigation of plastic solid waste pyrolysis via the deconvolution technique using the asymmetric double sigmoidal function: Determination of the kinetic triplet, thermodynamic parameters, thermal lifetime and pyrolytic oil composition for clean. **Energy Conversion and Management**, v. 200, 2019. Disponível em: https://doi.org/10.1016/j.enconman.2019.112031

MUN, S. P.; KU, C. S.; PARK, S. B. Physicochemical characterization of pyrolyzates produced from carbonization of lignocellulosic biomass in a batch-type mechanical kiln. **Journal of Industrial and Engineering Chemistry**, v. 13, n. 1, p. 127–132, 2007.

NALI, E. C.; RIBEIRO, L. B. N. M.; HORA, A. B. Biorrefinaria integrada à indústria de celulose no Brasil: oportunidade ou necessidade? **Papel e Celulose**, v. 43, p. 257–294, 2016. Disponível em: http://web.bndes.gov.br/bib/jspui/handle/1408/9578

NARON, D. R.; COLLARD, F. X.; TYHODA, L.; GÖRGENS, J. F. Characterisation of lignins from different sources by appropriate analytical methods: Introducing thermogravimetric analysis-thermal desorption-gas chromatography–mass spectroscopy. **Industrial Crops and Products**, v. 101, p. 61–74, 2017. Disponível em:

https://doi.org/10.1016/j.indcrop.2017.02.041

NIAOUNAKIS, M. **Building and Construction Applications**. *[S. l.: s. n.]*. Disponível em: https://doi.org/10.1016/b978-0-323-35399-1.00010-7

NIMZ, H.; ROBERT, D.; FAIX, O.; NEMR, M. Carbon-13 NMR Spectra of Lignins, 8 *. **Holzforschung**, v. 35, n. 1, p. 16–26, 1981.

NISHU; LIU, R.; RAHMAN, M. M.; SARKER, M.; CHAI, M.; LI, C.; CAI, J. A review on the catalytic pyrolysis of biomass for the bio-oil production with ZSM-5: Focus on structure. **Fuel Processing Technology**, v. 199, p. 106301, 2020. Disponível em: https://doi.org/10.1016/J.FUPROC.2019.106301

NOOR, P.; KHANMOHAMMADI, M.; ROOZBEHANI, B.; YARIPOUR, F.; BAGHERI GARMARUDI, A. Introduction of table sugar as a soft second template in ZSM-5 nanocatalyst and its effect on product distribution and catalyst lifetime in methanol to gasoline conversion. **Journal of Energy Chemistry**, v. 27, n. 2, p. 582–590, 2018. Disponível em: https://doi.org/10.1016/J.JECHEM.2017.10.031

OHRA-AHO, T.; LINNEKOSKI, J. Catalytic pyrolysis of lignin by using analytical pyrolysis-GC-MS. **Journal of Analytical and Applied Pyrolysis**, v. 113, p. 186–192, 2015. Disponível em: https://doi.org/10.1016/j.jaap.2014.12.012

OLIVEIRA, J. De; CRUZ, T. A.; PEREIRA, I. D. O.; IENCZAK, J. L.; PERALTA, R. A.; LÁZARO-MARTÍNEZ, J. M.; JOSÉ, H. J.; RODRÍGUEZ-CASTELLÓN, E.; MOREIRA, R. de F. P. M. Journal of Analytical and Applied Pyrolysis Mechanistic insights and kinetics of torrefaction of pine wood biomasses using solid-state NMR. v. 172, n. February, 2023. Disponível em: https://doi.org/10.1016/j.jaap.2023.106019

PACIONI, T. R. GASEIFICAÇÃO DE BIOCHARS DE BAGAÇO DE MAÇÃ E DE BORRA DE CAFÉ COM CO2: ESTUDO CINÉTICO. p. 1–109, 2006.

PANDEY, M. P.; KIM, C. S. Lignin Depolymerization and Conversion: A Review of Thermochemical Methods. **Chemical Engineering and Technology**, v. 34, n. 1, p. 29–41, 2011. Disponível em: https://doi.org/10.1002/ceat.201000270

PATTIYA, A. **Catalytic pyrolysis**. *[S. l.]*: Elsevier Ltd., 2018. *E-book*. Disponível em: https://doi.org/10.1016/B978-0-08-101029-7.00002-3

PAYSEPAR, H.; RAO, K. T. V.; YUAN, Z.; SHUI, H.; XU, C. (Charles). Improving activity of ZSM-5 zeolite catalyst for the production of monomeric aromatics/phenolics from hydrolysis lignin via catalytic fast pyrolysis. **Applied Catalysis A: General**, v. 563, p. 154–162, 2018. Disponível em: https://doi.org/10.1016/j.apcata.2018.07.003

RAGAUSKAS, A. J. *et al.* **Lignin valorization: Improving lignin processing in the biorefinery**. *[S. l.]*: American Association for the Advancement of Science, 2014. Disponível em: https://doi.org/10.1126/science.1246843

RAHMAN, M. M.; LIU, R.; CAI, J. Catalytic fast pyrolysis of biomass over zeolites for high quality bio-oil – A review. **Fuel Processing Technology**, v. 180, n. June, p. 32–46, 2018. Disponível em: https://doi.org/10.1016/j.fuproc.2018.08.002

SABARISH, R.; UNNIKRISHNAN, G. Synthesis, characterization and evaluations of micro/mesoporous ZSM-5 zeolite using starch as bio template. **SN Applied Sciences**, v. 1, n. 9, p. 1–13, 2019. Disponível em: https://doi.org/10.1007/s42452-019-1036-9

SAHOO, A.; KUMAR, S.; KUMAR, J.; BHASKAR, T. A detailed assessment of pyrolysis kinetics of invasive lignocellulosic biomasses (Prosopis juliflora and Lantana

camara) by thermogravimetric analysis. **Bioresource Technology**, v. 319, 2021. Disponível em: https://doi.org/10.1016/j.biortech.2020.124060

SALIBA, E. O. S.; RODRIGUEZ, N. M.; MORAIS, S. A. L.; VELOSO, D. P. Ligninas – Métodos De Obtenção E Caracterização Química Lignins – Isolation Methods and Chemical Characterization. **Ciência Rural**, v. 31, n. 5, p. 917–928, 2001.

SANTANA, J. A.; CARVALHO, W. S.; ATAÍDE, C. H. Catalytic effect of ZSM-5 zeolite and HY-340 niobic acid on the pyrolysis of industrial kraft lignins. **Industrial Crops and Products**, v. 111, p. 126–132, 2018. Disponível em: https://doi.org/10.1016/j.indcrop.2017.10.023

SANTANA JÚNIOR, J. A. **EFEITO CATALÍTICO DE ZEÓLITA ZSM-5 E ÁCIDO NIÓBICO HY-340 NA PIRÓLISE E HIDROPIRÓLISE DE LIGNINAS KRAFT INDUSTRIAIS**. *[S. l.: s. n.]*.

SANTANA JUNIOR, J. A.; MENEZES, A. L.; ATAÍDE, C. H. Catalytic upgrading of fast hydropyrolysis vapors from industrial Kraft lignins using ZSM-5 zeolite and HY-340 niobic acid. **Journal of Analytical and Applied Pyrolysis**, v. 144, 2019. Disponível em: https://doi.org/10.1016/j.jaap.2019.104720

SCHAWAAB, M.; PINTO, J. C. **Análise de Dados Experimentais I: Fundamentos de Estatística e Estimação de Parâmetros**. *[S. l.: s. n.]*.

SETTER, C.; SANCHEZ COSTA, K. L.; PIRES DE OLIVEIRA, T. J.; FARINASSI MENDES, R. The effects of kraft lignin on the physicomechanical quality of briquettes produced with sugarcane bagasse and on the characteristics of the bio-oil obtained via slow pyrolysis. **Fuel Processing Technology**, v. 210, n. August, p. 106561, 2020. Disponível em: https://doi.org/10.1016/j.fuproc.2020.106561

SIMMONS, B. A.; LOQUE, D.; RALPH, J. Advances in modifying lignin for enhanced biofuel production. n. March, 2010. Disponível em: https://doi.org/10.1016/j.pbi.2010.03.001

SUPRIYANTO; USINO, D. O.; YLITERVO, P.; DOU, J.; SIPPONEN, M. H.; RICHARDS, T. Identifying the primary reactions and products of fast pyrolysis of alkali lignin. **Journal of Analytical and Applied Pyrolysis**, v. 151, n. June, 2020. Disponível em: https://doi.org/10.1016/j.jaap.2020.104917

TOMANI, P. E. R. THE LIGNOBOOST PROCESS. v. 44, n. October 2005, p. 53–58, 2010.

TREACY, M. M. .; HIGGINS, J. . Collection of simulated XRD powder patterns for zeolites. **Elsevier**, v. 4, n. 9, p. 1063–1069, 1983.

VICTOR, P. A. **COMPÓSITOS POLIMÉRICOS OBTIDOS PELA COMBINAÇÃO DE ESTIRENO E LIGNINA**. 2014. *[s. l.]*, 2014.

VIEIRA, R. A. M. **MONITORAMENTO E CONTROLE EM-LINHA DE REACAO DE POLIMERTZACAO EM EMULSAO**. 2000. *[s. l.]*, 2000.

WAN, S.; WANG, Y. A review on ex situ catalytic fast pyrolysis of biomass. **Frontiers of Chemical Science and Engineering**, v. 8, n. 3, p. 280–294, 2014. Disponível em: https://doi.org/10.1007/s11705-014-1436-8

WANG, S.; DAI, G.; YANG, H.; LUO, Z. Lignocellulosic biomass pyrolysis mechanism: A state-of-the-art review. **Progress in Energy and Combustion Science**, v. 62, p. 33–86, 2017. Disponível em: https://doi.org/10.1016/j.pecs.2017.05.004

WEI, Q.; ZHANG, P.; LIU, X.; HUANG, W.; FAN, X.; YAN, Y.; ZHANG, R.; WANG, L.; ZHOU, Y. Synthesis of Ni-Modified ZSM-5 Zeolites and Their Catalytic Performance in n-Octane Hydroconversion. **Frontiers in Chemistry**, v. 8, n. December, p. 1–8, 2020. Disponível em: https://doi.org/10.3389/fchem.2020.586445

WIDAYAT, W.; ANNISA, A. N. Synthesis and Characterization of ZSM-5 Catalyst at Different Temperatures. **IOP Conference Series: Materials Science and Engineering**, v. 214, n. 1, 2017. Disponível em: https://doi.org/10.1088/1757-899X/214/1/012032

YANG, H.; NORINAGA, K.; LI, J.; ZHU, W.; WANG, H. Effects of HZSM-5 on volatile products obtained from the fast pyrolysis of lignin and model compounds. **Fuel Processing Technology**, v. 181, p. 207–214, 2018. Disponível em: https://doi.org/10.1016/j.fuproc.2018.09.022

YANG, H.; XIE, Y.; ZHENG, X.; PU, Y.; HUANG, F.; MENG, X.; WU, W. Bioresource Technology Comparative study of lignin characteristics from wheat straw obtained by soda-AQ and kraft pretreatment and effect on the following enzymatic hydrolysis process. **BIORESOURCE TECHNOLOGY**, v. 207, p. 361–369, 2016. Disponível em: https://doi.org/10.1016/j.biortech.2016.01.123

YANG, J.; WANG, X.; SHEN, B.; HU, Z.; XU, L.; YANG, S. Lignin from energy plant (Arundo donax): Pyrolysis kinetics, mechanism and pathway evaluation. **Renewable Energy**, v. 161, p. 963–971, 2020. Disponível em: https://doi.org/10.1016/j.renene.2020.08.024

YAO, D.; YANG, H.; CHEN, H.; WILLIAMS, P. T. Investigation of nickel-impregnated zeolite catalysts for hydrogen/syngas production from the catalytic reforming of waste polyethylene. **Applied Catalysis B: Environmental**, v. 227, p. 477–487, 2018. Disponível em: https://doi.org/10.1016/j.apcatb.2018.01.050

YOGALAKSHMI, K. N.; POORNIMA, D. T.; SIVASHANMUGAM, P.; KAVITHA, S.; YUKESH KANNAH, R.; SUNITA, V.; ADISHKUMAR, S.; KUMAR, G.; RAJESH, B. J. Lignocellulosic biomass-based pyrolysis: A comprehensive review. **Chemosphere**, v. 286, n. P2, p. 131824, 2022. Disponível em: https://doi.org/10.1016/j.chemosphere.2021.131824

YU, Y.; LI, X.; SU, L.; ZHANG, Y.; WANG, Y.; ZHANG, H. The role of shape selectivity in catalytic fast pyrolysis of lignin with zeolite catalysts. **Applied Catalysis A: General**, v. 447–448, p. 115–123, 2012. Disponível em: https://doi.org/10.1016/j.apcata.2012.09.012

ZAKHAROV, A. G.; VORONOVA, M. I.; SUROV, O. V.; RUBLEVA, N. V.; AFINEEZSKII, A. V. Synthesis and Properties of Composites of Nanocrystalline Cellulose with Poly(ethylene terephthalate). **Russian Journal of Applied Chemistry**, v. 94, n. 2, p. 202–209, 2021. Disponível em: https://doi.org/10.1134/S1070427221020099

ZAKZESKI, J.; BRUIJNINCX, P. C. A.; JONGERIUS, A. L.; WECKHUYSEN, B. M. The catalytic valorization of lignin for the production of renewable chemicals. **Chemical Reviews**, v. 110, n. 6, p. 3552–3599, 2010. Disponível em: https://doi.org/10.1021/cr900354u

ZHANG, H.; CHENG, Y. T.; VISPUTE, T. P.; XIAO, R.; HUBER, G. W. Catalytic conversion of biomass-derived feedstocks into olefins and aromatics with ZSM-5: The hydrogen to carbon effective ratio. **Energy and Environmental Science**, v. 4, n. 6, p. 2297–2307, 2011. Disponível em: https://doi.org/10.1039/c1ee01230d

ZHANG, M.; RESENDE, F. L. P.; MOUTSOGLOU, A.; RAYNIE, D. E. Pyrolysis

of lignin extracted from prairie cordgrass, aspen, and Kraft lignin by Py-GC/MS and TGA/FTIR. **Journal of Analytical and Applied Pyrolysis**, v. 98, p. 65–71, 2012. Disponível em: https://doi.org/10.1016/j.jaap.2012.05.009

ZHOU, S.; GARCIA-PEREZ, M.; PECHA, B.; KERSTEN, S. R. A.; MCDONALD, A. G.; WESTERHOF, R. J. M. Effect of the fast pyrolysis temperature on the primary and secondary products of lignin. **Energy and Fuels**, v. 27, n. 10, p. 5867–5877, 2013 a. Disponível em: https://doi.org/10.1021/ef4001677

ZHOU, S.; GARCIA-PEREZ, M.; PECHA, B.; MCDONALD, A. G.; KERSTEN, S. R. A.; WESTERHOF, R. J. M. Secondary vapor phase reactions of lignin-derived oligomers obtained by fast pyrolysis of pine wood. **Energy and Fuels**, v. 27, n. 3, p. 1428–1438, 2013 b. Disponível em: https://doi.org/10.1021/ef3019832

ZHU, W.; WESTMAN, G.; THELIANDER, H. Journal of Wood Chemistry and Investigation and Characterization of Lignin Precipitation in the LignoBoost Process Investigation and Characterization of Lignin Precipitation in the LignoBoost Process. n. October 2014, p. 37–41, 2014. Disponível em: https://doi.org/10.1080/02773813.2013.838267

APPENDIX A - PRINCIPAL COMPONENT ANALYSIS (PCA)

Principal Component Analysis (PCA) is widely recognized as a powerful technique for reducing multidimensional data into a smaller number of variables. PCA simplifies complex original data sets by transforming the information into a new, more straightforward representation (FODIL CHERIF *et al.*, 2020). In a simple way, the PCA technique involves manipulating data from matrices X and Y to represent them in a compact form, based on elements that produce the greatest variations in the sets. To put it differently, when n original variables are combined linearly, they produce n principal components. These components are not only orthogonal but are also arranged in descending order of variability (DOS SANTOS, 2012). This linear combination is known as the first principal component or factor. The same procedure is applied to the remaining unmodeled variations to obtain the second principal component. This process continues until a satisfactory degree of modeling is achieved. It is important to note that higher-order components represent smaller magnitudes of spectral variation, taking care to avoid overfitting (VIEIRA, 2000).

This method provides a possibility to reduce the samples dimensionality of the representative points. Although the statistical information in the n original variables is the same as that of the n principal components, usually more than 90% of this information can be found in only 2 or 3 of the first principal components. Therefore, a graph of principal component 1 versus principal component 2, for instance, often provides a statistically significant window for observing points from n-dimensional space (DOS SANTOS, 2012).

According to Ferreira (2015), mathematically, the principal component analysis starts with exploratory analysis of the experimental data matrix, represented as $\boldsymbol{X}$, as seen in the equation below. This technique is used to simplify complex data sets and identify patterns or relationships between variables. By reducing the dimensionality of the data, it becomes easier to interpret and visualize.

$$\boldsymbol{X} = \begin{bmatrix} \vec{x}_1^T \\ \vdots \\ \vec{x}_{NX}^T \end{bmatrix} = \begin{bmatrix} x_{11} & \cdots & x_{1NX} \\ \vdots & \ddots & \vdots \\ x_{N1} & \cdots & x_{NNX} \end{bmatrix} \tag{11}$$

According to Equation 1, $\vec{x}_i, i = 1 \ldots NX$ is a vector of NX experimental variables in a system. In the case of evaluating the composition of pyrolysis bio-oil experiments, NX represents the number of component classes obtained from GC-MS analysis (aromatics,

oxygenated aromatics, hydrocarbons, etc.). If experiments are replicated, there are N experimental measurements for each of the NX variables. The sample means ($\bar{x}_i, i = 1 \dots NX$) of NX variables can be represented in vector form, as shown in the following equation:

$$\bar{\boldsymbol{x}}^{\boldsymbol{T}} = [\bar{x}_1 \quad \dots \quad \bar{x}_{NX}] \tag{12}$$

In addition to sample means, the sample variances ($\sigma_{i,i}^2$) and sample covariances ($\sigma_{i,j}^2$) can be represented in the form of the data covariance matrix ($\boldsymbol{V_X}$), as shown in Equation 13:

$$\boldsymbol{V_X} = \begin{bmatrix} \sigma_{11}^2 & \dots & \sigma_{1,NX}^2 \\ \vdots & \ddots & \vdots \\ \sigma_{NX,1}^2 & \cdots & \sigma_{NX,NX}^2 \end{bmatrix} = \frac{1}{N-1} \boldsymbol{X_{cm}^T X_{cm}} \tag{13}$$

Where:

$$\boldsymbol{X_{cm}} = \begin{bmatrix} x_{11} - \bar{x}_1 & \dots & x_{1NX} - \bar{x}_{NX} \\ \vdots & \ddots & \vdots \\ x_{N1} - \bar{x}_1 & \cdots & x_{NNX} - \bar{x}_{NX} \end{bmatrix} \tag{14}$$

The data covariance matrix provides valuable information about the process, demonstrating that relevant process information may not depend on a single variable, but rather on how different variables change about each other. Decomposing the data covariance matrix into its eigenvalues and eigenvectors through principal component analysis is a useful tool for identifying patterns and reducing data dimensionality. Finding the eigenvalues ($\lambda_i, i = 1 \dots NX$) and eigenvectors ($\vec{d}_i, i = 1 \dots NX$) is a central aspect of PCA. Through matrix decomposition, the data covariance matrix can be represented as follows:

$$\boldsymbol{V_X} = \boldsymbol{D\Lambda D^T} \tag{15}$$

Where:

$$\boldsymbol{\Lambda} = \begin{bmatrix} \lambda_1 & \dots & 0 \\ \vdots & \ddots & \vdots \\ 0 & \cdots & \lambda_{NX} \end{bmatrix} \tag{16}$$

$$\mathbf{D} = \begin{bmatrix} \vec{d}_1 & \dots & \vec{d}_{NX} \end{bmatrix}; \vec{d}_i = [d_{i1} \quad \dots \quad d_{iNX}]^T, i = 1 \dots NX \tag{17}$$

The matrix of eigenvalues of the data covariance matrix ($\boldsymbol{V_X}$), represented by $\boldsymbol{\Lambda}$, is a diagonal matrix in which the eigenvalues are arranged in ascending order. On the other hand, the matrix $\boldsymbol{D}$ is a matrix whose columns are made up of the eigenvectors of $\boldsymbol{V_X}$. The main objective of PCA is to reduce the dimensionality of the experimental data space (which has dimension NX) by projecting the data onto a transformed space. The coordinates in the

transformed space are orthogonal to each other, due to the special characteristics of the data covariance matrix V_X. It is possible to demonstrate that the eigenvectors of $\boldsymbol{V_X}$ are orthogonal to each other. The coordinates in the transformed space are called principal directions ($\vec{z}_i, i = 1 \dots NX$) and can be obtained from the following variable transformation:

$$\vec{z}_i = \boldsymbol{D^T}\vec{x}_i, i = 1 \dots NX \tag{18}$$

Equation 15 establishes that the experimental variables can be represented as linear combinations in the new coordinate system (principal directions or factors). In matrix form, Equation 18 can be rewritten as:

$$\boldsymbol{Z} = \begin{bmatrix} z_{11} & \dots & z_{1NX} \\ \vdots & \ddots & \vdots \\ z_{N1} & \cdots & z_{NNX} \end{bmatrix} = \begin{bmatrix} x_{11} & \dots & x_{1NX} \\ \vdots & \ddots & \vdots \\ x_{N1} & \cdots & x_{NNX} \end{bmatrix} \begin{bmatrix} \vec{d}_1 & \dots & \vec{d}_{NX} \end{bmatrix} \tag{19}$$

It shows that covariance matrix of the data projected onto the principal directions (V_Z) is equal to the matrix of eigenvalues of $\boldsymbol{V_X}$, that is:

$$\mathbf{V_Z} = \begin{bmatrix} \lambda_1 & \dots & 0 \\ \vdots & \ddots & \vdots \\ 0 & \cdots & \lambda_{NX} \end{bmatrix} \tag{20}$$

Therefore, the eigenvalues of $\boldsymbol{V_X}$ have a special meaning and represent the variability of the original data projected onto the new coordinate system (principal directions). Thus, the higher the eigenvalue associated with a principal direction, the better the quality of the data projection in that direction. Moreover, the sum of the eigenvalues represents the total variability of the data, allowing us to define the % of explained variance in a certain principal direction:

$$\%\boldsymbol{Var_i} = \frac{\lambda_i}{\sum_i^{NX} \lambda_i}, i = 1 \dots NX \tag{21}$$

In particular, the dimensionality reduction occurs because only a few eigenvalues of the covariance matrix have significant values so that the experimental data of dimension NX can be represented in one or two factors (principal directions), associated with the highest percentages of explained variance. Typically, one or two principal directions represent 95% of the cumulative variance, so that the other directions can be discarded. These directions represent experimental noise. The eigenvectors ($\vec{d}_i, i = 1 \dots NX$) are also called loadings and allow to establish the functional relationships between the experimental variables in the

transformed space. Geometrically, these concepts can be illustrated in the following Figure 42:

Figure 42*:* Geometric representation of PCA

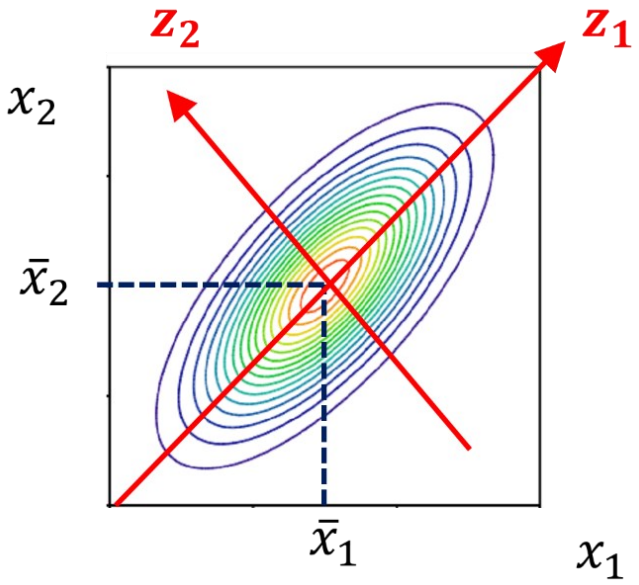

Source: From author

To simplify matters, Figure 42 illustrates the geometric representation of PCA when only two experimental variables are involved. It observed that the two variables represent functional dependence between each other in the original two-dimensional space. In the transformed space (represented by the coordinates z_1 e z_2), it can be noted that the quality of the data projection along z_1 is better than z_2. Therefore, the direction z_1 is associated with the highest eigenvalue (λ_1), while the direction z_2 is associated with the lowest eigenvalue (λ_2). The eigenvectors (or loadings) associated with the direction z_1 allow to establish the functional relationship between x_1 e x_2 in the transformed space. These concepts can be extended to evaluate the typical compositions of bio-oil in pyrolysis experiments and obtain valuable information about the occurring reactions.